Efficiency of degrading packed bed bioreactors.

MSc (Chemical Engineering) DISSERTATION

Prepared by

Anthin John Botes (827590)

Submitted to

School of Chemical and Metallurgical Engineering, Faculty of Engineering and the Built Environment, University of the Witwatersrand, Johannesburg, South Africa

Supervisor: Prof C. Sheridan

Co-Supervisor: Prof C. James

May, 2016

DECLARATION

I Anthin John Botes as a postgraduate student registered for an MSc (Chemical engineering) at the University of the Witwatersrand declare the following:

- I am aware that plagiarism is the use of someone else's work without their permission and or without acknowledging the original source.
- I am aware plagiarism is wrong.
- I confirm that this written work is my own work except where I have stated otherwise.
- I have followed the required conventions in referencing the thoughts and ideas of others.
- I understand that the University of the Witwatersrand may take disciplinary action against me if there is a belief that this is not my own unaided work or if I have failed to acknowledge the ideas or writing of others.

Signature  ……...

Date 2016/05/04

SUMMARY

In South Africa, the need for water treatment is increasing, especially in the mining sector. As active water treatment technologies are expensive, the mining sector has an increasing need for passive water treatment technology, with low maintenance and operating costs, yet efficient water treatment ability. Literature on passive water treatment suggests that these systems only offer a narrow range of treatment capabilities. Therefore, hybrid water treatment systems could be a solution to low-cost water treatment in South Africa. The Degrading Packed Bed Reactor (DPBR) is one of the units comprising the hybrid treatment group. The DPBR's main action is to convert sulfates into sulfides and alkalinity. In practice, the main drawback of the DPBR is clogging. Clogging lessens the amount of Acid Mine Drainage (AMD) that comes into contact with Sulfur Reducing Bacteria (SRB) in the DPBR, thereby reducing the efficiency of the bioreactor.

In this study, six small-scale DPBRs were constructed. Each was classified according to its unique organic source (manure, straw, vegetable food processing waste, wood shavings, chicken litter and a combined sample with layers of all the carbon sources). Synthetic AMD was fed through the six bioreactors for a period of three months. From the small-scale DPBRs, the permeability, sulfate, iron and pH of the exit samples were measured.

On average, the carbon sources removed 50 % of the sulfates and 98 % of the iron from the fed AMD. The different carbon sources showed no significant difference between each other in terms their sulfate and iron removal. The range between the best performing carbon source and the poorest performing carbon source, in terms of sulfate removal, was 17%. For iron removal, the range between the best and poorest performing carbon sources was only 2%. It was found that the permeability of the carbon sources played a larger role in the efficiency of the DPBR than the type of carbon source used.

Manure is highly effective in terms of pH improvement, sulfate and iron removal. However, this is at the expense of permeability, as its packing clogs very rapidly. Compost and straw have excellent permeabilities which do not change significantly over long timeframes. This is, however, at the expense of the remedial ability of the packing materials. The combined reactor, in every instance, offers a good compromise between these different behaviours.

ACKNOWLEDGEMENTS

I wish to express my appreciation to the following organisations and persons who made this dissertation possible:

- Professor Craig Sheridan for his excellent supervision;
- Professor Chris James for his help in formulating an interesting topic;
- The libraries at the University of Witwatersrand and Golder Associates for help in obtaining literature;
- The Golder Associates Research Laboratory for help with the analysis of samples;
- My family for their unfailing support; and most importantly
- Roxanne for all her invaluable assistance.

LIST OF FIGURES

LIST OF TABLES

1. INTRODUCTION

The world is in a water crisis ("Water Quotes and Facts," 1999).

Water is a necessity in all aspects of life; in recent decades, the world's water use has significantly increased, resulting in water availability becoming scarce. More than eighty of the world's countries are currently experiencing water shortages and the cost of water infrastructure has significantly increased. Simultaneously, the quality of water has drastically decreased due to pollution and waste contamination from cities, industry and agriculture. Globally, more than one billion people lack safe water.

Alocation of the world's water usage is shown in Figure 1,(Heimbuch, 2010).

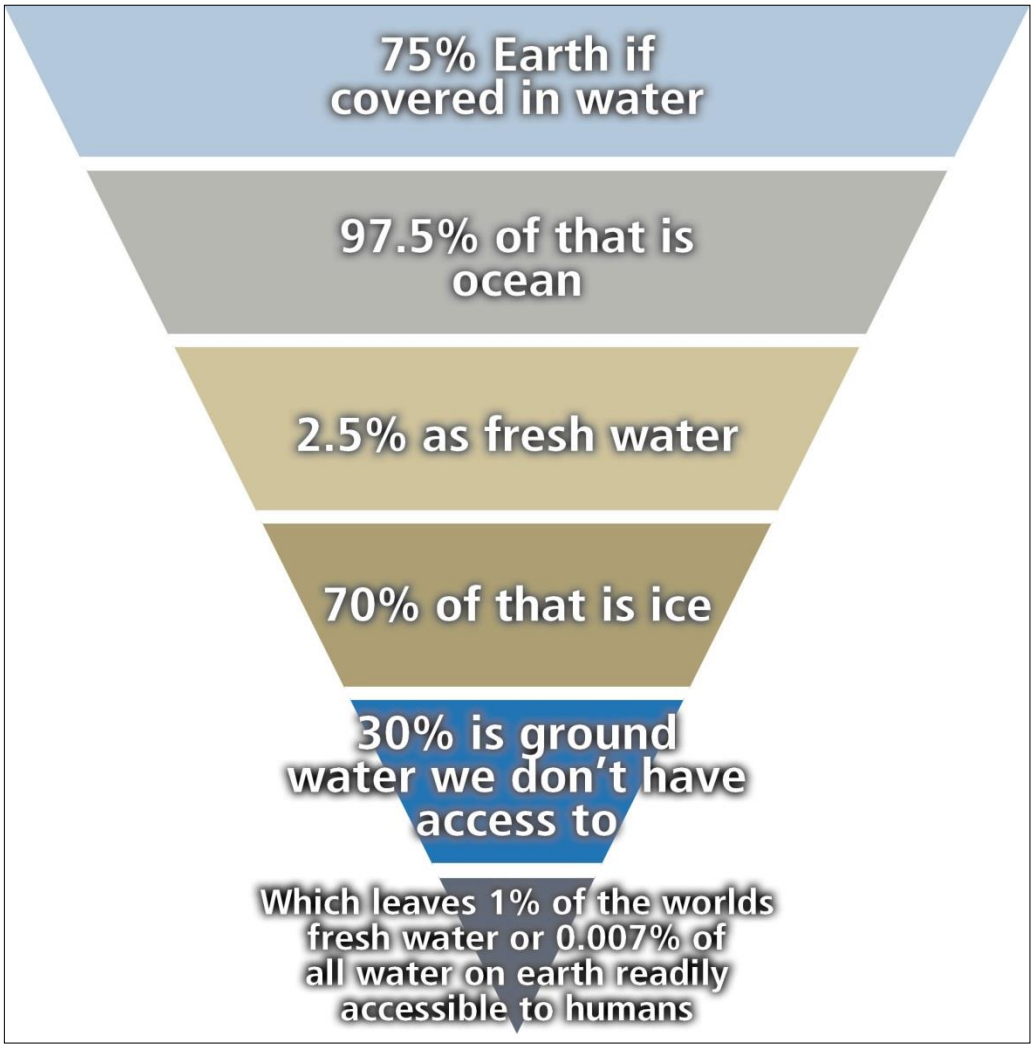

Figure 1: Worlds water usage (Heimbuch, 2010)

The world's population is constantly growing ("2013 World Population Data Sheets," 2013). With this increase in population, the need for natural resources is ever growing. With only a small amount of accessible water, society cannot afford to pollute the already dwindling supply of fresh water. Nonetheless, the benefits of certain economic activities outweigh their downsides in polluting water. In order to address the shortage of fresh water supply, humans have started treating water.

The first evidence of basic water treatment dates back to 4000BC, the main aim of which was the treatment of odor and taste (*25 Years of Safe Drinking Water Act: History and Trends*, 1999). Early Greek literature spoke about a number of treatment options such as filtration, sunlight exposure, boiling and straining (Baker, 1981). Chemicals such as alum were used by the ancient Egyptians as far back as 1500BC to help remove suspended particles from water. Filtration of water first came about in the 1700s. In the 1800s, slow sand filtration was common practice across Europe in the treatment of water. Also during this time, the first evidence of non-visible drinking water contaminants was extensively researched (*25 Years of Safe Drinking Water Act: History and Trends*, 1999). Since then, large strides in water treatment have been made worldwide but most treatments are far from optimized.

Globally, water treatment is a huge industry. Freedomina, (2015) explains that the world demand in water treatment products was estimated at 35 billion dollars in 2014. This number is expected to increase at 7.4% compound annual growth until 2020. Africa and Asia are predicted to have the most aggressive market gains during this time. Despite the vigorous market growth, however, hundreds of millions of people will still be left without safe drinking water (Freedomina, 2015).

The African continent is extremely water stressed (UNEP, 2002). At least thirteen countries are severely water stressed and this number is expected to double by the year 2025 (UNEP, 2002). One of the reasons that Africa is so water stressed, is the fact that Africa only has 9% of the global freshwater resources, despite having 15% of the global population (UNEP, 2010). This makes Africa the second driest continent in the world, before Australia. Fortunately, Africa does have nodes of water surplus (more than 750mm precipitation and 250mm runoff); these include but are not limited to the Lesotho Highlands, Angolan Plateau, Albertine Rift, Kenyan Highlands, Ethiopian Highlands, Jos Plateau and Fauta Djallon (UNEP, 2010).

The nodes of water surplus can be seen in Figure 2.

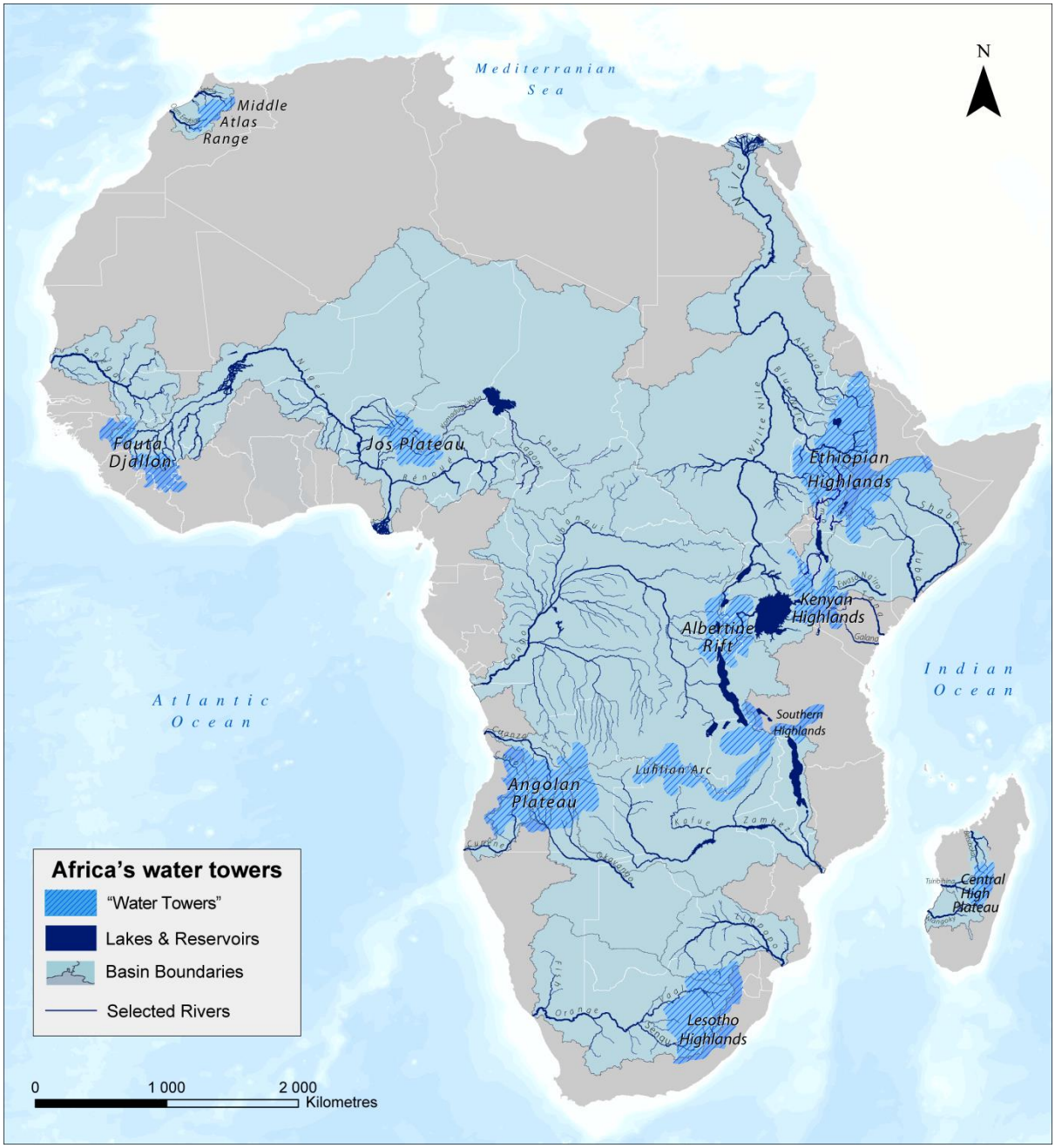

Figure 2: Water surplus nodes (UNEP, 2010)

Despite having water surplus nodes, Africa still suffers from a lack of water interconnectivity. That is, Africa lacks the infrastructure to spread water across catchments to points of water scarcity (UNEP, 2002). For this reason, Africa has started purifying water as a means to re-use and protect the small amount of existing water supply.

The world average rainfall is 860mm per year. South Africa is classified as a semi-arid country which is water stressed and has an average rainfall of about 450mm per year. Major problems South Africa faces when it comes to water availability are listed below (*Overview of the South African Water Sector*, n.d.):

- South Africa has low stream flow volumes in most of its major rivers;
- High levels of evaporation;
- Uneven distribution and seasonality of rainfall (43% of the rain falls on 13% of the land);
- South Africa is drought prone; and
- The large economic, urban and industrial developments in South Africa are not situated near the major water sources.

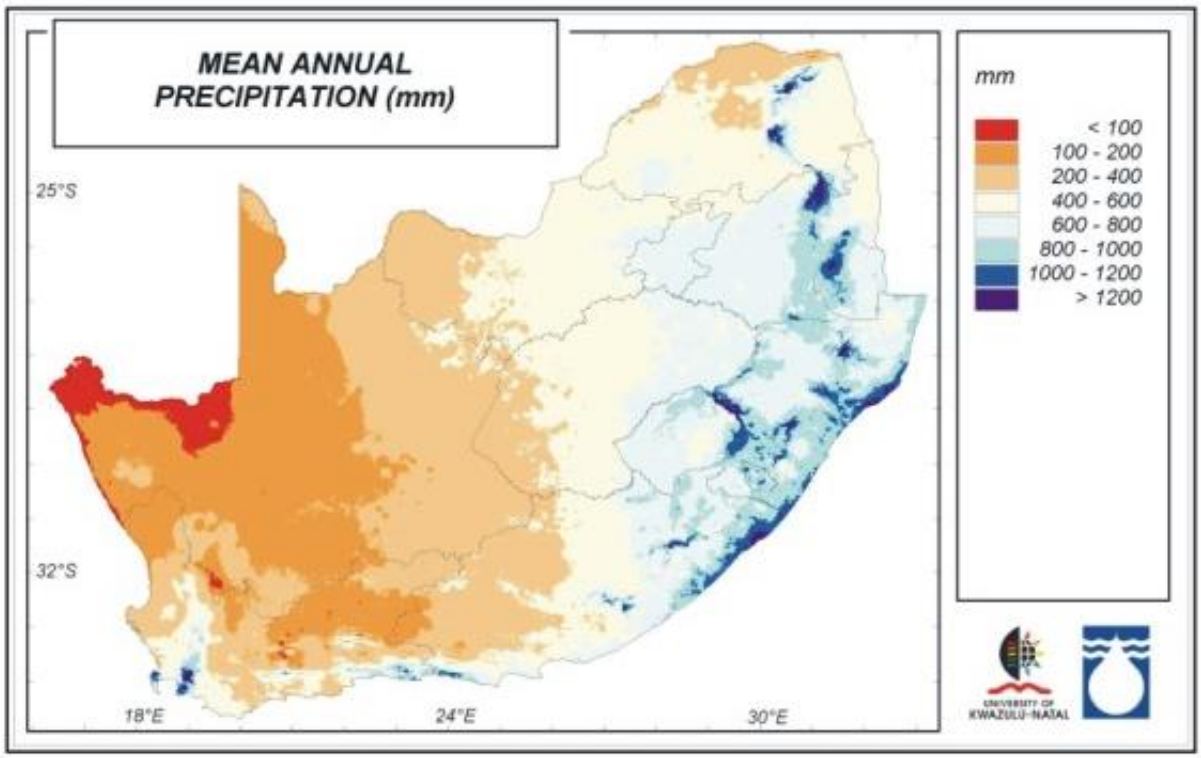

Figure 3: Mean annual precipitation in South Africa (Lynch, 2004)

South Africa's natural water supply is low and graphically mismatched because the areas of high population density do not correspond with regions of high rainfall (*National Water Resource Strategy 2*, 2013). This mismatch causes strain on the decreasing supply of available water in the country. With a shortage of clean water supply, it becomes imperative to utilize

the available water where it will be of most value to society and the economy. It is therefore exceptionally important to treat any polluted water to discharge standards.

The main economic sectors that make use of South Africa's water supply, along with the percentages used, are as follows and are depicted in Figure 4: (*National Water Resource Strategy 2*, 2013)

- Agriculture 60%;
- Municipal/ domestic 27%;
- Industrial 3%;
- Power generation 2%;
- Livestock watering and nature conservation 2.5%;
- Afforestation 3%; and
- Mining sectors 2.5%.

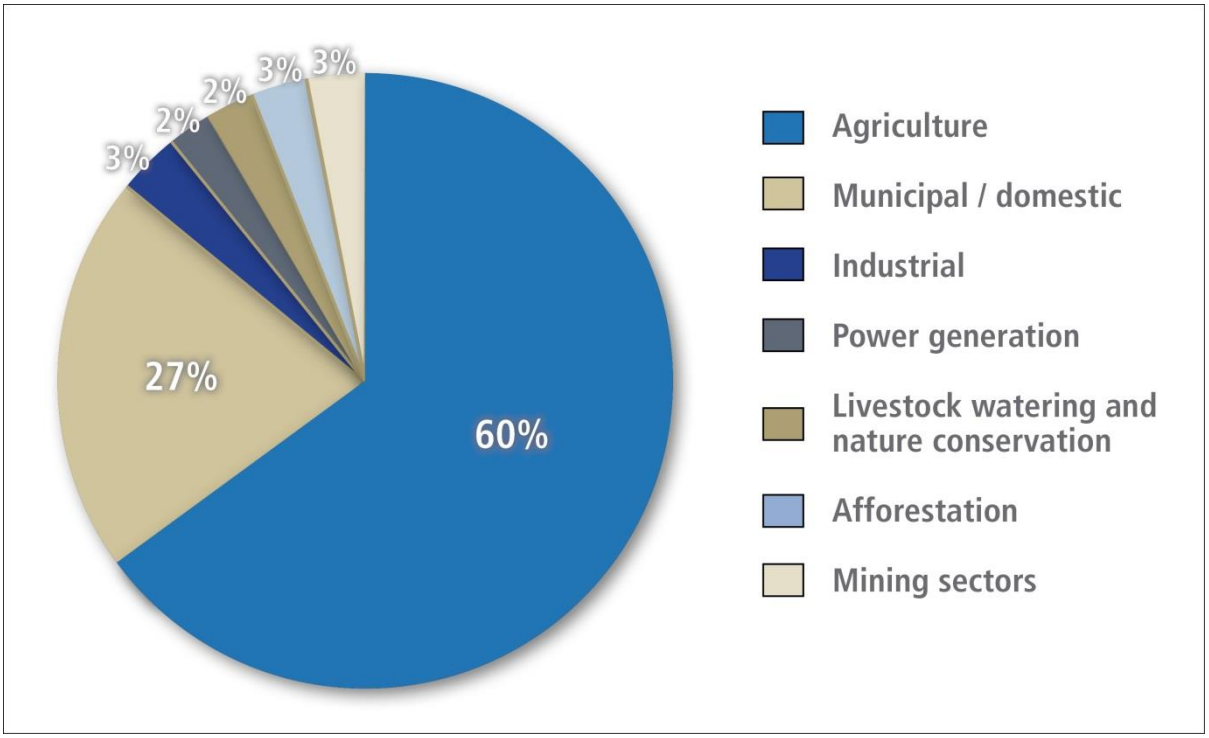

Figure 4: Water usage in economic sectors in South Africa (*National Water Resource Strategy 2*, 2013)

The subsurface of South Africa possesses some of the world's richest mineral deposits; therefore the mining sector in South Africa is suitably large. The Chamber of Mines published that the mining sector subsidizes 8.8% directly and 10% indirectly of the Gross Domestic Product (GDP) of South Africa (*Government Communication and Information System*, 2011).

Mining creates numerous career opportunities and attracts large amounts of foreign investment in the country. Since mining plays an important role in South Africa's GDP, care must be taken to balance this sector's water supply and demand, as well as the treatment thereof.

There are numerous rich ore deposits around South Africa. Some of the key mining areas are the Witwatersrand Goldfields, Waterburg coal fields, Highveld coal fields (Witbank and Mpumalanga) and the Bushveld platinum complex (CSIR, 2010).

Most of the rich ore deposits are shown in Figure 5.

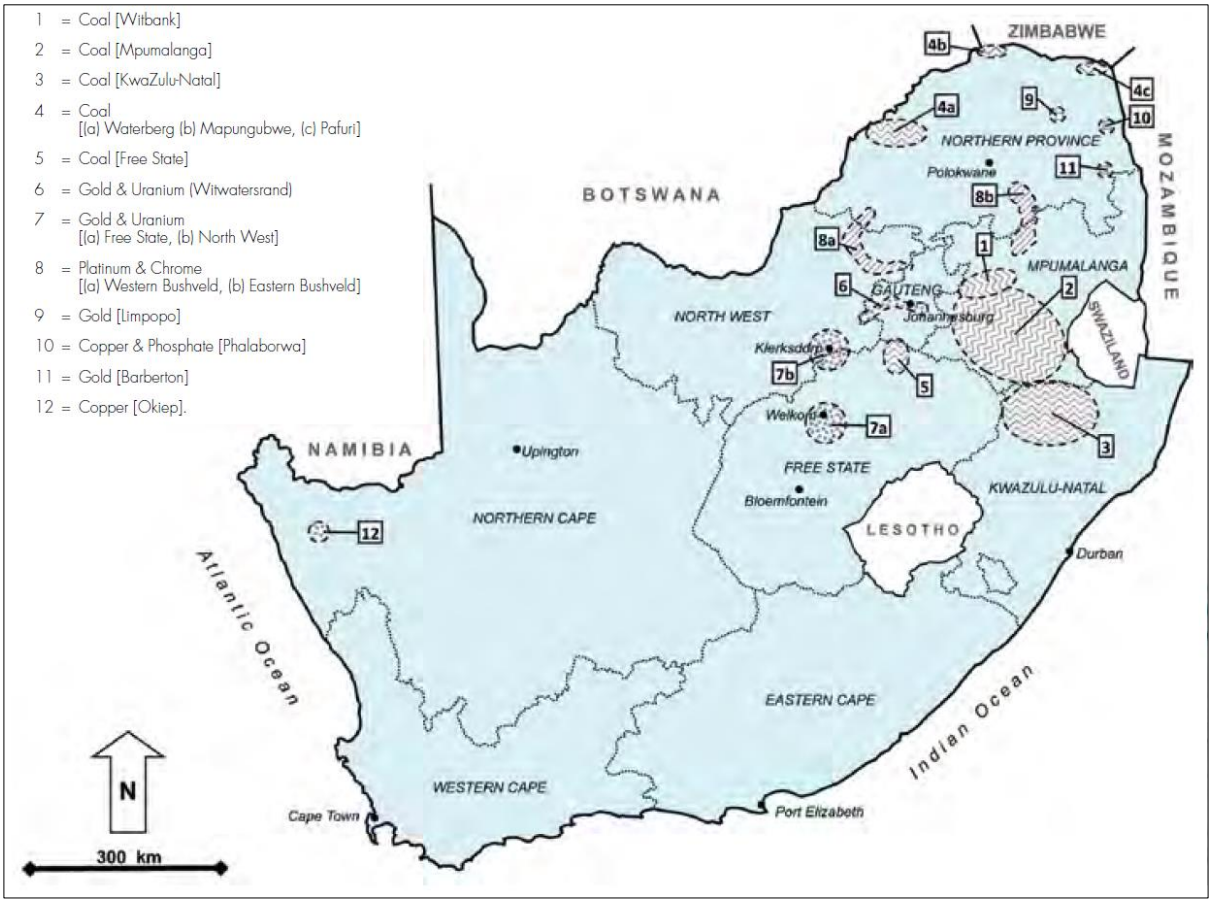

Figure 5: Mining areas in South Africa (Hobbs & Kennedy, 2010)

In the mining process, sizeable quantities of water are utilized, stored and diverted. Water thus frequently comes into contact with the mining process. Under certain circumstances (short-term or long-term), water reacts with its environment, thus becoming contaminated and/or polluted. Mining houses treat polluted water to certain standards before the water is reintroduced into the environment.

There is a need to treat polluted mine water, along with legislation compelling mining houses to treat mine water pollution under the *National Water Act of 1998 (Act 36 of 1998) (NWA).* Specifically, Section 19 of this act stipulates that mineral rights holders are required to take all reasonable measures to prevent pollution. Other legislation which applies to the treatment of polluted water includes the *Environmental Conservations Act*, the *National Environmental Management Act* and the *Hazardous Substances Act*. Mining houses are faced with the need to monitor and manage their long-term water quality problems in innovative and sustainable ways. If mining houses do not comply with long-term water quality treatment standards, authorities will not issue the mines with closure certificates (Coetser, Molwantwa, Heath, & Pulles, 2004)

There are two main groups of mine water treatment, namely active and passive water treatment.

"Active water treatment is the improvement of water quality by methods which require ongoing inputs of artificial energy and/or (bio) chemical reagents"(Younger, Banwart, & Hedin, 2002)

"Passive water treatment is the deliberate improvement of water quality using only naturally available energy sources (for example gravity, microbial energy, photosynthesis) in systems which require only infrequent (albeit potentially regular) maintenance in order to operate effectively over the entire system design life) (Pulles, Coetser, Heath, & Muhlbauer, 2004)

Table 1 shows the key advantages and disadvantages between active and passive water treatment systems. Both systems have areas of strength and areas of weakness (Muller, 2013).

Table 1: Comparison between Active and Passive water treatment systems

Water Treatment		
Key aspect	**Active**	**Passive**
Feed water flow	Not limited	<1 ML/day
Typical water quality parameters	Can treat almost all water quality parameters	Sulfides and monovalent ions in current research cannot be treated
Final water quality	Potable water	Lower quality of water
Technology	Well established treatment technology	Gaps in research
Operational aspects	Requires 24 hour operations	Mainly self-sustaining system
Site requirements	Small footprint (needs security)	Large footprint and a sloped site is required
Costing	High CAPEX, OPEX, replacement and electrical costs	High CAPEX costs but little to no other costs
Waste generation	Large quantities of hazardous waste and brine	Some waste stays in the system

In the past decade, society has started to understand the severity of a potential water crisis. Many engineers and scientists have begun to research new ways of purifying contaminated water. Specifically, engineers have looked towards nature to see how the earth purifies water naturally. One way in which the earth purifies water is through naturally occurring wetlands (passive system). Naturally occurring wetlands are one of nature's particularly useful natural phenomena. Wetlands function both as *"nature's supermarkets,"* because of their wide-ranging biodiversity and *"nature's kidneys,"* because they function as a downstream catchment for water and waste (Mitsch & Gosselink, 2007). Wetlands occur naturally in almost all parts of the earth where fauna and flora live, as well as amongst standing water or saturated soils (Mitsch & Gosselink, 2007).

The word *"wetland"* only started to become popular jargon around the 20th century and one of the first publications containing the word was entitled *Wetlands of the United States (Shaw & Fredine, 1956)*. However, society knew about wetlands long before then; they simply called wetlands by different names such as "swamp", "marsh", "bog", "fen", "mire" and "moor". For a long period of time, society misunderstood wetlands and before the mid-1970s, wetlands

were being drained and destroyed to make way for agriculture, commercial and residential development. At that time, wetlands were perceived to be more of an obstacle than a resource. Fortunately, since the 1980s, more engineers and scientists have been conducting research on wetlands and slowly, society's knowledge and perceptions of wetlands are changing (Mitsch & Gosselink, 2007).

Due to wetlands' natural cleaning ability, coupled with the high costs of conventional water treatment, mining houses and researchers have found the logical step of using wetlands to treat polluted water. Engineers and scientists have started using manmade/ constructed wetlands to utilize wetlands' natural cleaning ability, at the source of the polluted water.
According to *National Water Act of 1998* (Act 36 of 1998) (NWA), it is now illegal to pollute natural wetlands.

The fundamental goal in utilizing manmade/ constructed wetlands is to try and replicate natural wetlands' processes as closely as possible. However, the challenges in trying to replicate natural wetlands are that natural wetlands are extremely diverse ecosystems (Mitsch & Gosselink, 2007). Much research still needs to be done in order to understand the many different components of natural wetlands and the interactions thereof, before manmade wetlands can perform to their full potential.

It is important to note that the concept of creating "green" ecosystems that have the potential to treat any mine water pollution is still some way away. The water currently being treated is usually so severely polluted that ecosystems are strained to their limits and underperform as a result. There are, however, several facets in the mining process that lend themselves to treatment by wetlands if the right sets of circumstances occur (Coetser et al., 2004).

Since mine water pollution or AMD is not easily treated with conventional wetlands or constructed wetlands, engineers and scientists have come up with a third solution; a hybrid systems solution (Ávila, Bayona, Martín, Salas, & García, 2015; Vymazal, 2014). Hybrid systems borrow treatment processes from both active water treatment and passive water treatment, utilising the most suitable and cost effective processes from each system (Ávila, Garfí, & García, 2013; Zheng, Wang, Xiong, Liu, & Zhao, 2014), as shown in Figure 6.

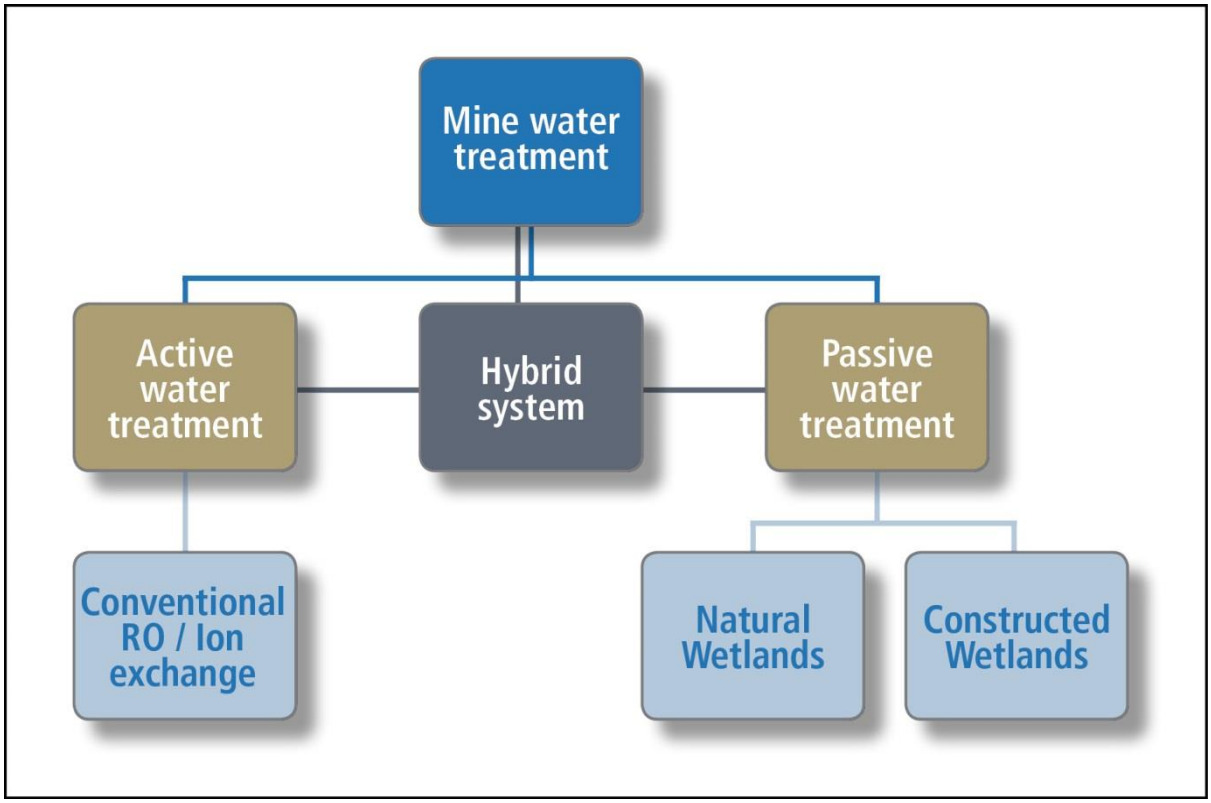

Figure 6: Mine water treatment hierarchy

Figure 7, (Muller, 2014) depicts a general decision tree used as an initial indication on the typical mine waste water and the various options which can be used to treat it. The decision tree depicts the usefulness of hybrid treatment technologies and its broad range of treatment options.

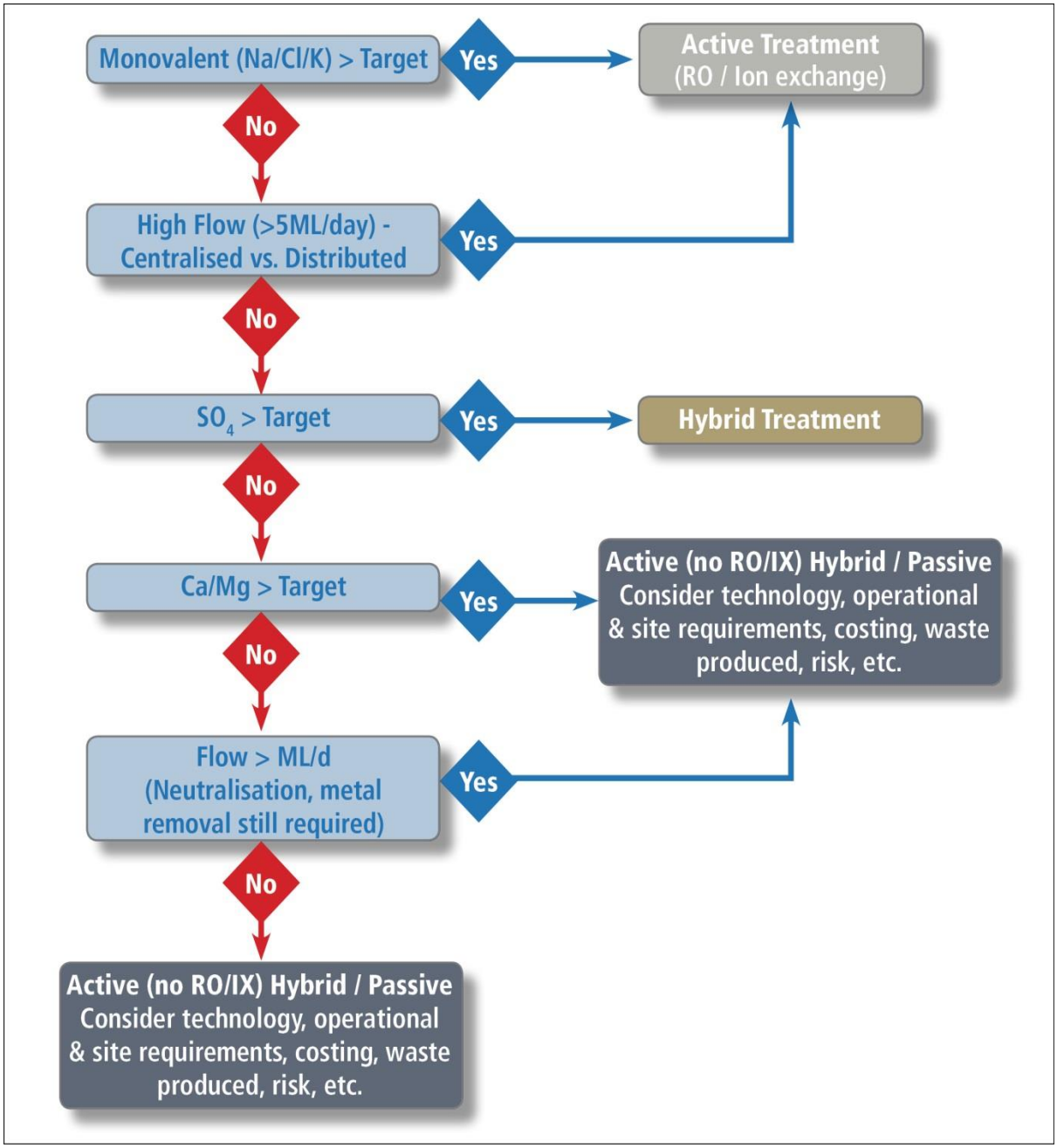

Figure 7: Water treatment decision tree (Muller, 2014)

Hybrid systems use a segmented approach to treating water by targeting a specific pollutant at a specific position in the treatment chain. Hybrid systems are tailor-made to treat a specific pollution cocktail (Coetser et al., 2004). A typical hybrid treatment chain can be seen in Figure 8.

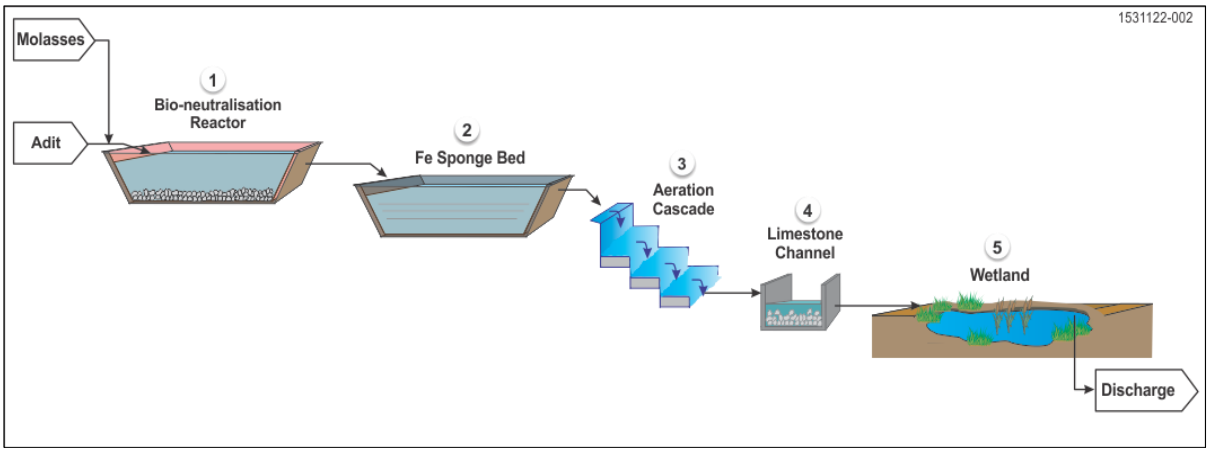

Figure 8: Typical hybrid treatment chain (Aspeling, 2015)

The main pollution problems existing in South Africa's Mpumalanga coal fields mine-polluted water include acidification, salinization and a large amount of metals (Coetser et al., 2004) and (Pinetown, Ward, & van der Westhuizen, 2007). The main issues needing to be addressed in a typical mine water mixture are:

- Neutralisation, sulfate reduction and metal precipitation;
- Sulfide removal;
- Removal of organic material, ammonia, phosphates and toxic metals;
- Manganese removal; and
- Final polishing (removal of all trace substances, precipitation of calcium and magnesium, and water softening, pH adjustment).

There are numerous different active and passive technologies to deal with the above pollutant mine water cocktail (Hengen, Squillace, O'Sullivan, & Stone, 2014). These technologies vary greatly in terms of factors such as cost, efficiency and size.

As part of this dissertation, the researcher investigated sulfate reduction, metal precipitation and pH neutralisation of typical Mpumalanga coal fields AMD (Acid Mine Drainage).

AMD (also known as Acid Rock Drainage or ARD), develops from mineral pyrite which is in contact with oxygenated water. A two stage oxidation process is undergone with the pyrite. Firstly, the reaction produces sulfuric acid and ferrous sulfate. Thereafter, it produces ferric hydroxide and more sulfuric acid (McCarthy, 2011). The general AMD chemical equation is shown:

(i) $$4F_eS_2(s) + 15O_2(g) + 14H_2O(l) \rightarrow 4F_e(OH)_3(s) + 8SO_4^{2-}(aq) + 16H^+(aq)$$

The aforementioned mineral deposits occur naturally within the ore body during the natural wreathing of these minerals. Acid is therefore produced at extremely slow rates. This acid is produced at such a slow rate that the natural neutralization process occurs. During the mining process, the rock has to be broken, thereby increasing the surface area and the rate of acidification (McCarthy, 2011).

In a hybrid system, the assumed leading technology in dealing with sulfate reduction, metal precipitation and pH neutralisation occurs in the *Degrading Packed Bed Bioreactor* (DPBR) (Pulles et al., 2004). The DPBR uses layers of organic substrate and SRB (Sulfate Reducing Bacteria) in anaerobic conditions to reduce sulfate, precipitate metals and neutralize the pH of the AMD.

The DPBR's different organic media layers, as well as the orientation of its layered packing are patented by Willium Pulles, patent number US 7306732 B2 (Pulles & Rose, 2002). The basic design of the DPBR was developed by Golder Associates.

DPBRs are usually rectangular and/ or square-shaped reactors which are constructed as part of the natural landscape. The DPBR can be constructed with two different materials; a concrete or HDPE (high density polyethylene) liner. Concrete has a higher capital cost than HDPE liner. However, HDPE liner needs to be constructed into a trapezoidal shape, thereby increasing the reactor's surface area and encouraging dead volume around the reactor's edges which leads to inefficiency and a reactor which is larger than design specifications. McCauley and colleagues concluded that hydraulics plays a key role in bioreactor performance. In their study, vertical-walled reactors outperformed the trapezoidal reactors with regard to contaminant removal (McCauley, O'Sullivan, Milke, Weber, & Trumm, 2009).

AMD is normally gravity fed into a series of manifold pipes, these manifold pipes can be seen in Figure 10 as a rendered image as well as Figure 11 and Figure 12 as actual constructed DPBR's. These spread the AMD evenly over the entire upper surface of the DPBR. A layer of rock is place around the manifold pipes to keep them in place. Underneath the manifold pipes

and stone layer is a geofabric protection layer. This prevents any fine material from the organic substrate migrating up into the manifold pipes and blocking them.

The treatment of AMD occurs in the organic substrate layer. The organic substrate material in the DPBR is therefore key to AMD treatment and various carbon sources are packed in layers underneath the geofabric protection layer. A second protection layer of geofabric is used underneath the organic substrate material for the same reason as the first layer: to prevent any fine material from the organic substrate material, migrating down into the drainage pipes and blocking them. Figure 9 depicts typical layer configuration of a DPBR.

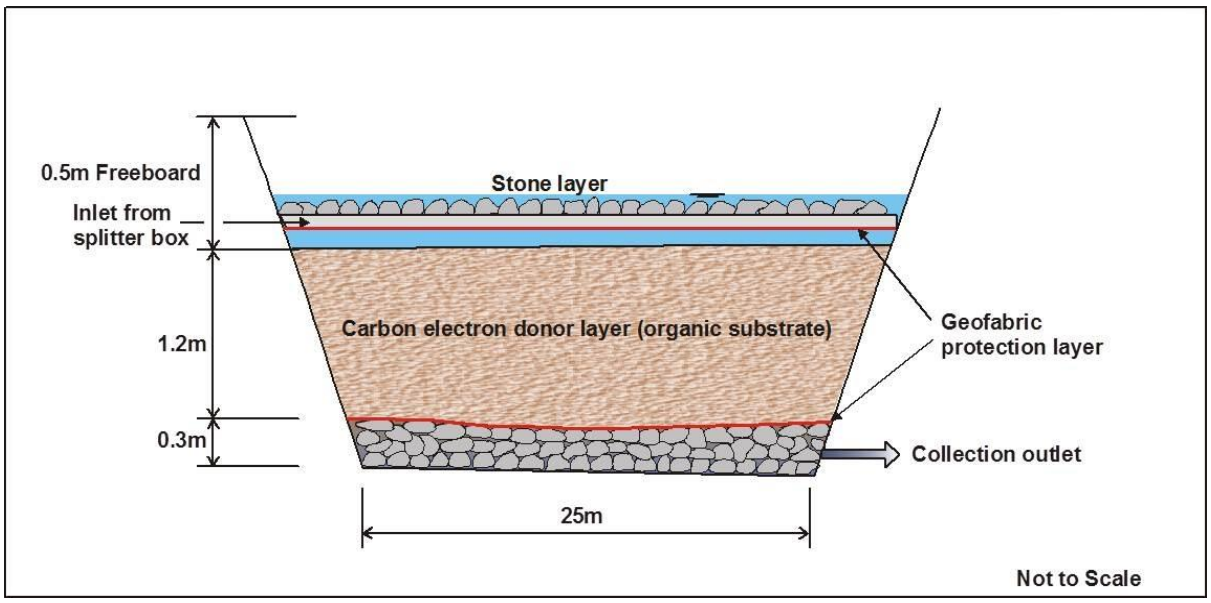

Figure 9: Typical depiction of different layers in DPBR

The DPBR needs to have anaerobic conditions at all times for the Sulfate Reducing Bacteria (SRB) to function. For this reason, a level control needs to be installed at the outlet of the DPBR to ensure fully flooded conditions at all times.

The DPBR relies on a number of layers of organic substances to donate electrons in anaerobic environments. Its process relies on three reactions. SRB use sulfate in the water system to feed on simple organic compounds which break down the sulfate into sulfide and alkalinity.
The first reaction, numbered (ii), shows the sulfate reduction equation, whereby the SRB reduce the sulfates in the reactor into sulfides and alkalinity.

(ii) $2CH_2O + SO_4{}^{2-} \leftrightarrow 2CHO_3{}^{-} + H_2S\ (g\ or\ aq)$

Sulfate reduction

The sulfides in the solution are present in the form of hydrogen sulfides. As seen in the second equation, numbered (iii), these hydrogen sulfides react with any heavy metal in the leachate solution, precipitating the metals there in (Coetser et al., 2004). Thereafter, the metal precipitate is in the form of metal sulfides. The "M" in the reaction stands for metal, which typically includes metals such as iron, lead or zinc.

(iii) $H_2S + M^{2+} \rightarrow MS\ (s) + 2H^{+}$

Metal precipitation

Equation (iv) shows the final step in the process, whereby the bicarbonate ions in the solution react with positively charged protons, forming carbon dioxide and water (Coetser et al., 2004). The carbon dioxide and water neutralize the acid in the solution, thereby increasing its pH.

(iv) $HCO_3^{-} + H^{+} \rightarrow CO_2(g) + H_2O$

Neutralization

Figure 10 is a rendered image of the designed DPBR. Figure 11 and Figure 12, depict a constructed images of a working DPBR. The images were taken in the northern KwaZulu-Natal as part of a Golder passive water treatment project.

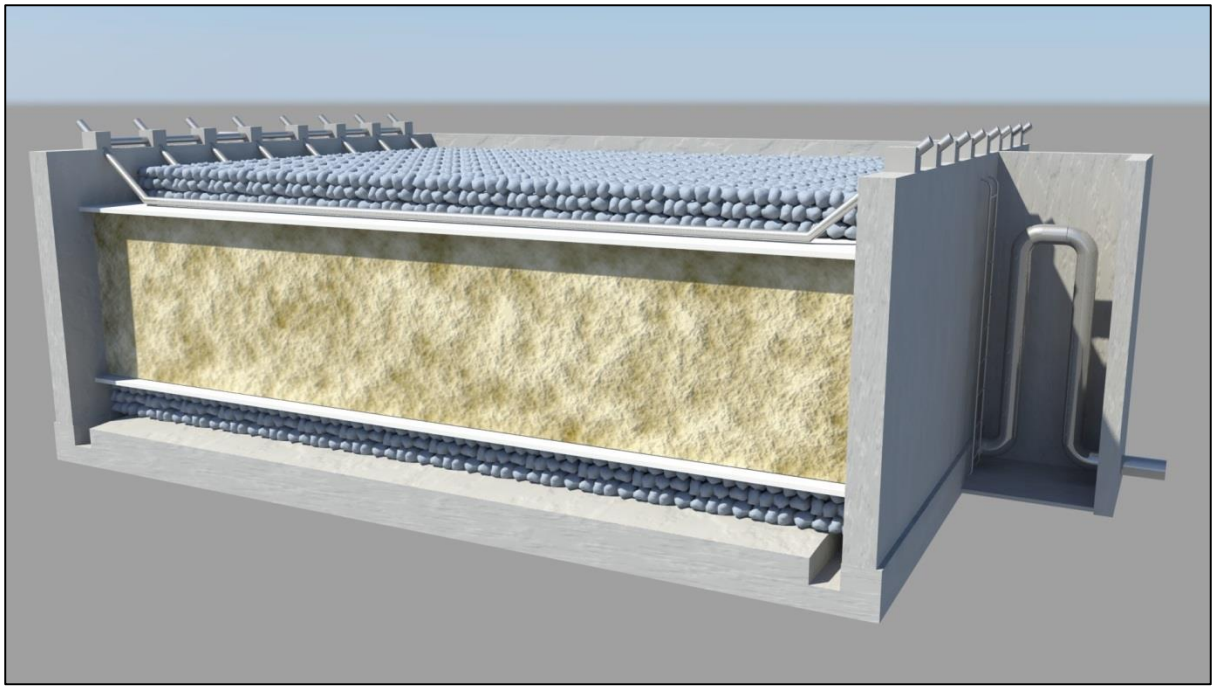

Figure 10: Rendered design image of DPBR

Figure 11: Constructed image of DPBR (Pulles & Meyer, 2012)

Figure 12: Constructed DPBR with inlet manifold pipes (Pulles & Meyer, 2012)

The DPBR utilizes waste products high in carbon to remove sulfates and metals from AMD and to increase pH levels. Typical waste products that are used include (but are not limited to) manure, straw, hay, compost, wood chips/shavings and sewage sludge. The true value of the DPBR lies in its utilization of waste material to treat waste water. Very little is known about the hydraulics of the organic substrate in the DPBR. As such, there are associated areas that require further research. However, if the DPBR operates within the appropriate design specifications, it can be used to remove sulfates, metals and increase the pH of the polluted mine effluent.

The DPBR is normally found in one of the first two phases in the hybrid water treatment chain. It is therefore of utmost importance that the reactor operates in accordance with the assumed hydraulic basis of design. If the DPBR had to fail, the equilibrium in the hybrid system would be disturbed and could lead to entire system failure. A number of failures could occur; four of such failures are described below:

- Manifold pipes clogging the system;
- Uneven distribution of AMD in the DPBR causing dead zones;

- Uneven layers in the packing of the organic substrate could cause short circuiting of the system; and
- A lack of AMD entering the DPBR could turn the anaerobic conditions into aerobic conditions, thereby killing the SRB and reducing the AMD treating ability of the DPBR. This would have an effect on any downstream biological reactors in the treatment chain.

The above failures and risks can and are for a large part designed out of the DPBR system. For example, the geofabric and stone layer ensure no clogging of the manifold pipes. One can ensure that the layers of organic substrate are evenly packed and a level cut off switch can be added to the outflow system, to ensure that the DPBR remains anaerobic at all times.

Clogging of the organic substrates is not as easily designed out of the system as the above examples. This is because clogging in organic substrates is not yet fully understood. One of the main causes of system failure in the DPBR is clogging. The term "clog" is defined as to "*Block or become blocked with an accumulation of thick, wet matter" ("Oxford Dictionaries," 2015).* Designers of DPBRs combat the clogging phenomenon by removing the organic substrate after a certain period of time and repacking the system with new organic substrate. Once the new organic substrate is packed, the SRB has to build up to effective treating capacity once again. Although repacking the organic substrate is viable option, a few related questions emerge: How often does one repack the reactor? Does one repack the DPBR before or after the carbon in the organic substrate has been depleted? How permeable is the organic substrate at the point at which the organic substrate is depleted? These questions show that the clogging of organic substrates needs to be more fully understood.

Clogging lessens the amount of AMD that comes into contact with SRB in the DPBR, thereby reducing the efficiency of the bioreactor. In severe cases, clogging can prevent all AMD from moving through the bioreactor, rendering the process obsolete and an environmental hazard. In this dissertation, the researcher asked the following question: How does the permeability of the bioreactor (DPBR) drop over time due to clogging within the reactor? Answering this question could assist in producing a set of guidelines for future design and maintenance of the DPBR with certain permeable carbon sources.

2. BACKGROUND INFORMATION

The mining sector is in need for passive water treatment technology, that has low maintenance and operating costs, yet has efficient water treatment ability (Coetser et al., 2004).

Hybrid water treatment systems could make a significant contribution to low cost water treatment in South Africa. However, such systems have high initial capital expenditure (CAPEX) costs to set up the treatment chain, as numerous steps are needed to treat mine effluent. Nevertheless, hybrid water treatment systems do save money on long-term operation and maintenance costs (Johnson & Hallberg, 2002).

In order for hybrid systems to become a widely used and trusted water treatment technology, the knowledge gaps within the system need to be addressed in research. Hybrid systems also need to be tested in pilot- and full-scale experiments. There are numerous areas within the hybrid treatment system with very little or no information about them. These areas form part of the system purely because of past experience. These areas need to be studied and optimized.

One fairly unknown area in hybrid treatment technology is the DPBR. The DPBR's main action is to convert sulfates into sulfides and alkalinity. It does this by allowing polluted water to trickle through layers of different organic matter. The organic matter donates electrons to the sulfate-reducing bacteria, thus reducing sulfates into sulfides. Although the chemical process is well understood, the hydraulics of such a system remains unclear.

Polluted water is fed through a trickle system, onto the organic matter. The polluted water needs to remain in and amongst the organic matter long enough for the reaction to take place, yet not too long to render the technology ineffective. This is called the hydraulic retention time.

The hydraulic retention time of the DPBR will be an important attribute to understand. Neculita et al, 2008 explain that for a passive system to operate efficiently under long term operation, the correct choice of hydraulic retention time needs to consider the desired discharge limits for acidity and metals. These limits need to weigh up against the problem of water movement though the reactor due to deterioration of organic material reducing the hydraulic conductivity. To optimize the time taken in the DPBR, the organic materials' hydraulic properties need to be

investigated. The AMD needs to stay in the bioreactor for the ideal residence time (Neculita, Zagury, & Bussière, 2008).

Hydraulic retention time is also known as the hydraulic residence time and is depicted with the symbol "τ". Ideal residence time is measured by taking the volume (V) and dividing it by the volumetric flow rate (Q) (Sheridan, 2012).

$$\text{(v)} \qquad \tau = \frac{V}{Q}$$

Ideal resistance time

$\tau = Ideal\ residence\ time$

$V = Reactor\ volume$

$Q = Volumetric\ flow\ rate$

The ideal residence time is used as a calculating parameter for two ideal reactor models, namely the ideal plug-flow reactor and the ideal continuously stirred reactor (CSTR). Plug flow reactor assumes no lateral mixing or diffusing of the liquid in the flow direction, whereas the continuously stirred reactor assumes that the liquid is perfectly mixed (Sheridan, 2012).

$$\text{(vi)} \qquad C_{out} = C_{in} \times e^{-k\tau}$$

Plug flow reactor

$$\text{(vii)} \qquad C_{out} = \frac{C_{in}}{(1+k.\tau)}$$

Continuously stirred reactor

$C_{out} = Exit\ concentration$

$C_{in} = Inlet\ concentration$

$k = Rate\ constant$

Ideal plug-flow reactors and continuously stirred reactors explained above rarely occur in practice due to things like short circuiting, dead zones and dispersion of the liquid.

Short-circuiting occurs when void spaces link together to form larger void spaces (Villholth & Jensen, 1998). Larger void spaces allow effluent to pass through the bioreactor at a higher rate, thereby bypassing favorable reactions with the organic matter. Figure 13 below shows the process of short-circuiting (indicated in grey), whereby the tracer passes through the bioreactor at a quicker rate than is expected of an ideal reactor (indicated in blue).

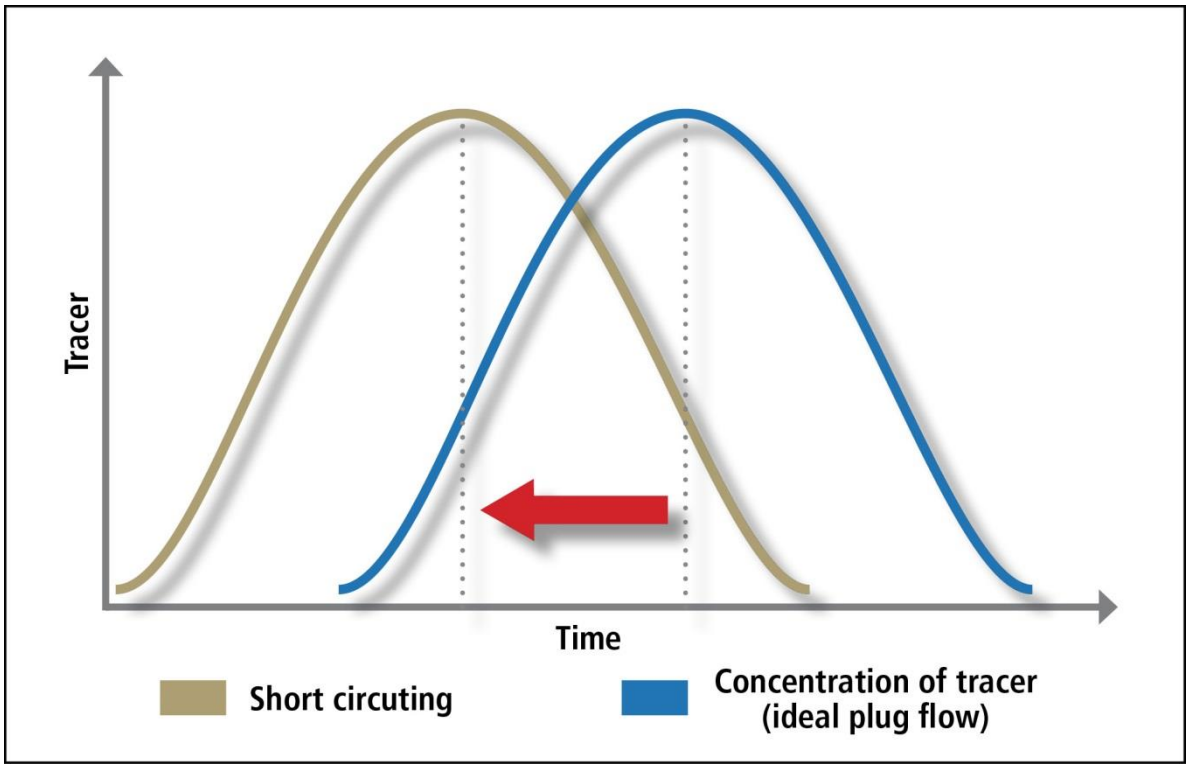

Figure 13: Graph depicting short circuiting (Lightbody, Nepf, & Bays, 2009)

Dead volumes, also known as stagnant volumes, are areas or regions within the reactor which have little to no effluent movement (low flow areas). These areas reduce the designed volume of the bioreactor (Fogler, 2005) as cited by (Sheridan, 2012).

In practice, dispersion of the liquid within the bioreactor also causes reactors to deviate from an ideal plug flow. There are commonly two types of dispersion within a bioreactor, axial and radial dispersion. Axial dispersion negatively affects the absorption properties of the bioreactor (Albright, 2009). Conversely radial dispersion increase the absorption properties of a bioreactor (Albright, 2009). The difference between axial and radial dispersion is the direction in which they work. Axial dispersion works in the same direction as the fluid flow and widens (dilutes) the typical tracer graph (Albright, 2009). Radial dispersion narrows this graph allowing it to act more like an ideal plug flow reactor (Albright, 2009).

Four main physical properties that would influence the hydraulic traits of organic matter would be particle size, particle size sorting, porosity (Cameron & Schipper, 2012) and distribution of feed inlet and outlet locations (Sheridan, 2012).

The particle size of the packing material plays an integral role in the hydraulic traits of the bioreactor. Zhang et al, 2013 looked at the effects of particle packing sizes of organic material and bacteria attachment rates. The quicker the bacteria attached to the organic material, the faster the bacterial colony grew. This resulted in the formation of biofilm, which clogged up the pore space between the organic materials, reducing the bioreactor's permeability. It was found that the larger the packing radius, the longer it took for the bacteria to attach to the organic material (Zhang, Chen, Liao, & Zhu, 2013). Organic material almost never has a uniform particle size. There is normally a distribution of various particle sizes within the same material- particle size distribution therefore comes into play.

Particle size distribution, according to (Brix, Arias, & del Bubba, 2001), is an important property to consider when constructing a subsurface flow constructed wetland. To minimize the risk of clogging, (Brix et al., 2001) proposed that the effective grain size d_{10} should be in the range of 0.3 to 3 mm and the d_{60} should be 0.5 and 8 mm. The terms d_{10} and d_{60} refer to the diameter at which 10% and 60% of the sample's mass is comprised of particles with a diameter less than the proposed grain sizes during a standard sieve analysis. The authors also suggested checking the uniformity coefficient of the particles by dividing the d_{60} value by the d_{10}:

$$\frac{d_{60}}{d_{10}} \quad \text{(viii)}$$

The uniformity coefficient should be less than 4 to ensure the correct hydraulic conductivity for the removal of phosphorous in subsurface flow wetlands.

Different particle shapes and gradings have a profound influence on flow through packed bed reactors [(Scheidegger, 1974) and (Tukac & Hanika, 1992) as cited by (Nemec & Levec, 2005)]. Nemec and Levec (2005) looked at flow through packed bed reactors, specifically observing particle size and shape along with different particles' packings and how they would affect the hydraulic capabilities of trickle bed bioreactors (Nemec & Levec, 2005). Their work showed that the porosity of the material can be simulated to within 10%, using Ergun's

mathematical equation. It is, however, quite a simplistic formula that only applies to a narrow range of porosities and flow rates. Another gap in the knowledge is that Ergun's equation is formulated for basic shape types (spheres, cylinders, rings, trilobes and quadralobes) which rarely occur in organic materials. There is little to no literature on hydraulics in terms of randomly shaped organic matter (Nemec & Levec, 2005). Ergun's equation can be seen as equation (x) below:

$$\text{(ix)} \qquad \frac{\Delta p}{L} = \frac{150\mu(1-\epsilon)^2\mu_O}{\epsilon^3 dp^2} + \frac{1.75(1-\epsilon)\rho\mu_O^2}{\epsilon^3 d_p}$$

$\Delta p = the\ pressure\ drop\ (N/m^2\ or\ Pa)$
$L = the\ height\ of\ the\ bed\ (m)$
$\mu = the\ fluid\ viscosity\ (kg/s.m)$
$\epsilon = the\ void\ space\ of\ the\ bed\ (dimensionless)$
$\mu_O = the\ fluid\ superficial\ velocity\ (m/s)$
$d_p = the\ partical\ diameter\ (m)$
$\rho = the\ density\ of\ the\ fluid\ (kg/m^3)$

Other important hydraulic traits of the organic material and the bioreactor include the inlet and outlet configurations (Sheridan, 2012). The influence of inlet and outlet configurations, flow rate and filter size were tested by (Wang et al., 2014) with the use of Sodium Chloride (NaC*l*) and dye tracer testing. (Wang et al., 2014) did numerous tests with the inlet being either at the bottom, middle or top of the constructed horizontal subsurface flow wetland. The outlet configuration was also tested at the bottom, middle or top positions within the constructed wetland. (Wang et al., 2014) concluded that for a homogeneous substrate, the inflow rate and the inlet/ outlet configurations are the key factors determining the hydraulic efficacy. For the constructed horizontal flow wetland, slower inflow rate with the inlet configuration at the middle and the outlet at the top were determined to have the best hydraulic efficacy.

It has been found that certain configurations of particles influence permeability through certain layers [(Scheidegger, 1974) and (Tukac & Hanika, 1992) as cited by (Nemec & Levec, 2005)]. Porosity is a well-researched physical property and forms part of everyday terminology. Porosity is a key physical property in determining the hydraulic properties in DPBRs. In

organic material, just as in geology, there are two kinds of porosity primary and secondary porosity (Hiscock, 2005).

Primary porosity represents the open pores in-between particles, during original packing of the particles (Hiscock, 2005).

Three large horizontal subsurface flow constructed wetlands where tested for primary porosity in Dakahliya, Egypt. Authors (Zidan, El-Gamal, Rashed, & El-Hady Eid, 2015) showed that there is noteworthy reduction in porosity of the horizontal subsurface flow system within the first 90 days of wetland operation. This was mainly due to clogging of the primary porosity due to sedimentation, degrading of fine particles, suspended solids from plant roots and biofilm growth (Zidan et al., 2015). It was noted that at 180 days, the porosity reduction stabilized and the pore size remained fairly stable. The water treating potential only increased once biofilm started developing around the media and plant roots (Zidan et al., 2015).

Secondary porosity develops as fractures in material, once the material has been deposited (Hiscock, 2005). Secondary porosity can lead to short-circuiting of the system (Villholth & Jensen, 1998).

Another key term in understanding porosity is effective porosity (ϕ). Effective porosity is the number of pore spaces allowing water to move freely through a layer (Gibb, Barcelona, Ritchey, & LeFaivre, 1984). Over time in the DPBR, biofilm growth as well as metal precipitation starts reducing the effective porosity of the bioreactor.

$$\text{(x)} \qquad \emptyset = \frac{V_p}{V_b}$$

$\emptyset = effective\ porosity\ (dimensionless)$

$V_p = total\ volume\ of\ interconnected\ voids\ (cm^3)$

$V_b = bulk\ volume\ (cm^3)$

Although there are numerous publications on the topic of porosity and various mathematical models trying to predict porosity of materials with different results, there is very little information on porosities of organic materials. The limited research that has been done on porosities and permeabilites of organic materials looks at flow and transport parameters in a

woodchip based bioreactor (Chun, Cooke, J.W, & Kang, 2009). This research mainly focuses on a single uniformly graded organic material.

In literature, there have been studies on different organic materials and their effectiveness in removing nitrates or sulfates (Blowes, Robertson, Ptacek, & Merkley, 1994), (Greenan, Moorman, Kaspar, Parkin, & Jaynes, 2006) and (Wildman, 2002) as cited in (Chun et al., 2009). Nevertheless, very little is known about the general permeability and porosity values of organic materials such as:

- Manure;
- Hay/ straw;
- Vegetable food processing waste (compost);
- Wood shavings;
- Chicken litter; and
- A composite sample of equal layers of all of the above carbon sources. (Pulles & Rose, 2002)

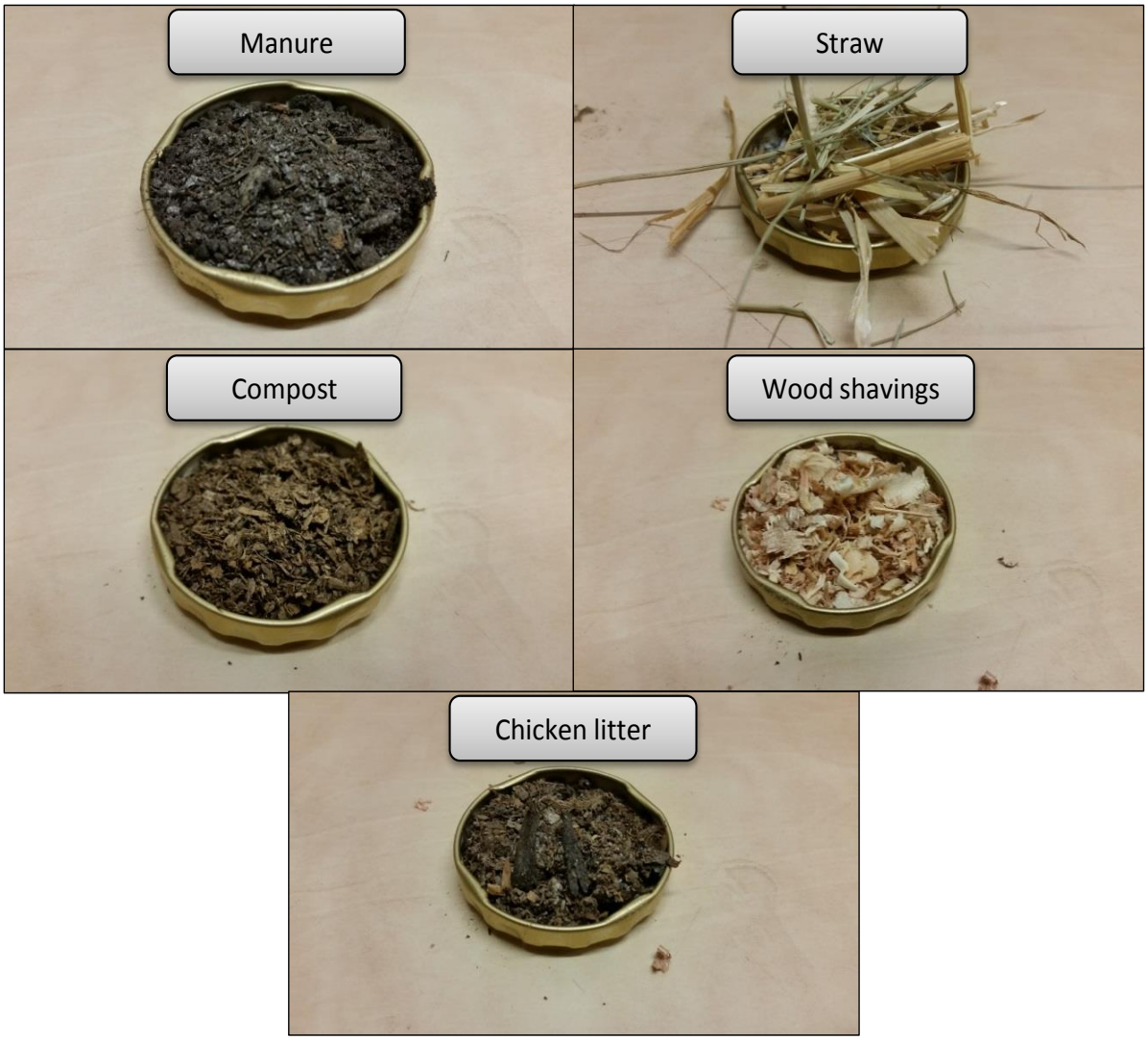

Figure 14: Carbon sources

The aforementioned Figure 14 organic materials make up a typical packing for the DPBR. The DPBR has numerous layers of these materials, placed on top of one another. In practice, the availability of the carbon sources, as well as their economic value and their distance to the DPBR are all weighed up and experimented, before the use of a specific carbon source is selected. (Gusek, 2008) explains that in order to increase the possibility of success within hybrid treatment chains, experimentation is extremely important. Furthermore, Gusek 2008 recommends a staged approach when designing such systems. The various stages are:

- Laboratory testing;
- Bench scale testing;
- Pilot scale testing; and finally
- Full scale implementation.

In this research, the basic permeabilities and porosities of the aforementioned organic materials will be investigated, as well as a combination of all the layers put together. This is envisaged to contribute to a better understanding of the flow of water through a multilayered organic bioreactor.

Once engineers and scientists have a better understanding of the porosities and permeabilities of the multiple layers in the DPBR, this could form the guidelines for the design of a reactor. It is important to understand the flow rate through the bioreactor; otherwise the whole downstream chain of the DPBR could underperform or in the worst case scenario, even be rendered obsolete.

It would be inaccurate to design a DPBR for the initial case of water flow through the multiple layers of organic materials because the multiple layers are of varying size, shape, packing and porosity. One of the worst parameters that influence the flow of water through constructed wetlands, is clogging (Yu, Wu, & Xu, 2006) as cited in (Guiping, Zhang, Chen, & Chen, 2013). In recent years the investigation into clogging has become slightly more prevalent in journal articles (Knowles, Griffin, & Davies, 2010). These articles look at methods to investigate clogging.

Guiping and colleagues (2013) and (Zhao, Zhu, & Tong, 2009) describe clogging as an extremely intricate process which is not well understood. It is clear that the clogging phenomenon contains large gaps of knowledge for future research. Clogging can occur by two broad methods: clogging by mechanical means and biological clogging. Through clogging by mechanical means, physical particles in the treatment water get lodged between the organic materials, reducing the organic materials' effective porosity. This process is also known as plugging (Iliuta & Larachi, 2005).

(Pozo-Morales, Franco, Garvi, & Lebrato, 2014) found that the entrance of a horizontal subsurface flow wetland has the highest potential for clogging, followed by the outlet of the system. The DPBR is vulnerable to clogging of the upper layer of the organic material; this would render the rest of the organic material redundant.

The key factor in designing for limited clogging within the DPBR is time. The designer needs to know at what point in time the DPBR becomes ineffective, in order to decipher at what stage the DPBR's organic materials would need to be removed and repacked (Langergraber, 2005) as cited by (Wichern, Lindenblatt, Lubken, & Horn, 2008). A large part of the treatment process is done by using active biofilm (Langergraber, 2005) as cited by (Wichern et al., 2008). The same biofilm that is being used to treat water is simultaneously clogging up the reactor. This key trade-off between active biofilm and clogging has also been elaborated upon by (Gibert et al., 2013). The question of when to repack the DPBR is important, as a balance between flow through the reactor and treatment potential needs to be found. Therefore, in this research, a key trade off study between clogging of the bioreactor and depletion of a carbon source was undertaken. This trade off study was conducted to determine which process over time would dictate when the bioreactor needs to be repacked.

Biofilms accrue naturally in most ecosystems where micro-organisms are found on solid surfaces. In unfavorable systems, biofilms tend to comprise of a single layer of attached cells but in favorable, high nutrient systems such as some constructed horizontal flow wetland environments, biofilms tend to be more extensive (Van Loosdrecht & Heijnen, 1993). Biofilms generally attaches to solid surfaces due to the plug flow characteristics (high dilution rate) of natural systems; to survive, organisms have to attach themselves to solid surfaces (Van Loosdrecht & Heijnen, 1993).

According to (Velten et al., 2011), the key parameters influencing biofilm growth rates are temperature, hydraulic conditions and the way in which the reactor is backwashed. The DPBR is not backwashed and the organic material is left in the reactor until most of the carbon has been utilized or until the reactor is clogged. Backwashing is not utilized in the DPBR, because it is designed as a passive system which works under gravity. If the DPBR is clogged, it could potentially cause spillage, which would be an environmental risk to the mining house.

To design a hybrid passive water treatment chain, each link in the water treatment process must be fully understood. The DPBR has three clear knowledge gaps. The first gap that needs to be understood includes the permeabilities and porosities of combined organic layers. The second gap that needs to be understood is the relationship between permeability and retention time of the composite organic layers (Chun et al., 2009). Finally the third gap that needs to be

understood is when the DPBR has to be repacked. This would be done by determining how long it takes for the carbon sources to clog the reactor and whether this occurs before or after the carbon in the bioreactor has been depleted. In this study, the permeabilities and porosities of the composite organic layers were determined, an indication on when the DPBR should be repacked was understood, in order to compile basic design guidelines which will guide future designs of the DPBR. These objectives are explicitly described in the next chapter.

3. RESEARCH OBJECTIVES

In order to connect the study's research question effectively with the data that is collected, it was essential to keep in mind the aims of the study (Leedy & Ormrod, 2014).

3.1 Main Aim

The main aim of this study was to determine how the permeability of the bioreactor drops over time due to clogging.

3.2 Sub-Aims

To achieve the main aim of the research project, a series of sub-aims were developed:

- To determine the operating range (the range in which the DPBR allows water to pass through the bioreactor at a sufficient rate as well as remove sulfates, precipitate iron and increases the pH to design levels), in order to classify the DPBR as working efficiently;
- To establish how long it takes before the bioreactor is classified as clogged; and
- To establish how often the packing material in the DPBR will have to be replaced through looking at whether the carbon source gets depleted before or after the bioreactor is clogged.

4. MATERIALS AND METHODS

4.1 Scope of the study

The equipment for the true experimental procedure was set up so as to control most of the variables in the experiment (Blumberg, Cooper, & Schindler, 2005). A small scale DPBR was simulated in the following way: A water reservoir (25*L* drum) containing the leachate (synthetic AMD) was linked to two identical peristaltic pumps with suitable piping. The pump was set to feed a constant flow rate into the six bioreactors from the same source water drum. The pump's exit lines were connected to the tops of the six bioreactors. AMD was pumped into all six reactors at a constant flow rate. The AMD would move through the organic media to the bottom of the bioreactor. The treated water would then be expelled through the bottom of the reactor. This is shown in Figure 18 and Figure 19 in Section 4.7.

4.1.1 Parameters in the scope of study

In the study, the permeability, as well as the total porosity of individual and composite organic layers of manure, straw, vegetable food processing waste (compost), wood shavings and chicken litter were determined over a period of 3 months. In this experimental procedure, certain variables were manipulated in order to see their effect on the experiment.

The key parameters included in the study were:

- Permeability;
- Porosity;
- Flow rates;
- Concentration of iron and sulfides;
- pH;
- Clogging;
- Effective void volume; and
- Time.

4.1.2 Parameters outside the scope of study

Even though they play an integral part to DPBRs, the following parameters fell outside the scope of this study:

- Temperature (although daily temperatures readings were taken);
- Atmospheric pressure;

- Wall effects;
- Bio-film growth patterns;
- Sulfate-reducing bacteria;
- Mass balance; and
- Climate effects.

4.2 Variables

"*In practice the term, 'variable' is used as a synonym for the construct or property being studied*" (Blumberg et al., 2005).

In this study, the dependent and independent variables investigated were quantitative. The dependent variables in the experiment were permeability, porosity, concentration and flow rate. The independent variable in the experiment was time.

The inflow rate was kept constant by connecting the bioreactors to low flow peristaltic pumps. These pumps supplied AMD at a smooth, continuous flow throughout the experiment's design life. The concentration of certain constituents within the AMD was measured at the exit of the bioreactor.

4.3 Experimental structure and procedure

The experimental structure followed in this dissertation started with three pre-experiments followed by the main experiments. Each pre-experiment had clear research questions which, in answering, helped the researcher gain understanding and background to the main experiment. The flow of the experimental structure and procedure is shown in Figure 15.

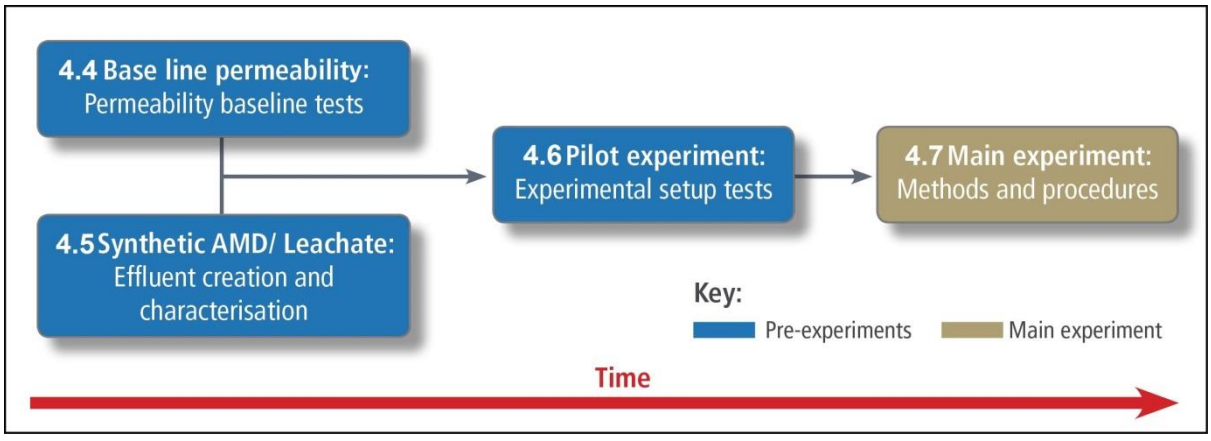

Figure 15: Experimental and dissertation structure

The pre-experiments are described in detail in the following sections:

4.4 Baseline permeability;

4.5 Synthetic AMD/ Leachate; and

4.6 Pilot experiment.

The first pre-experiment was to determine the different carbon sources' baseline permeabilities. This was done so that the main experiment could work with a firm baseline of permeability data. The next pre-experimental procedure was to create synthetic AMD of similar quality to that of typical AMD found in the Mpumalanga coal fields. The final pre-experiment was the pilot experiment. The pilot experiment included the use of a single bioreactor which simulated the experimental procedure of the main experiment.

Various learnings and results from the pre-experiments were obtained and are discussed in Section 5 of this dissertation. These learnings and results were used to set up the main experimental procedure.

4.4 Baseline permeability

The permeability of the individual layers of carbon material within the DPBR was determined using the American Society for Testing and Materials' (ASTM D2434) C*onstant Head Permeability Test* as well as the (ASTM 5084-3) *Falling Head Permeability Test*. Samples of the various carbon sources used [manure, straw, vegetable food processing waste (compost), wood shavings and chicken litter] were taken to a South African National Accredited System (SANAS) laboratory, Soillab (PTY) Ltd. The permeabilities acquired from the tests conducted by the laboratory formed the remolded base permeability figures for each of the carbon sources. Both the falling head permeability and the effective porosity tests were done using water at room temperature.

4.4.1 Baseline permeability questions

The baseline permeability tests were conducted in order to answer the following questions before moving onto the main experiment:

- What are the remolded steady state permeability values for the various carbon sources?
- What is the permeability of all the layers as a whole (composite value)?
- What is the effective porosity of the various carbon sources?

- Does the main experiment fall within the correct permeability range as compared to the SANAS laboratory? and
- How is the hydraulic efficiency affected by different layers of carbon sources with different permeabilities?

4.4.2 Baseline permeability data collection and recording

The baseline permeabilities were conducted by Soillab (PTY) Ltd. The ASTM permeability tests were developed to determine the permeabilities of undisturbed samples of soil. Since the various samples of carbon sources used in the experiments were not undisturbed samples, the carbon sources had to be remodeled to a specific density. The samples were then moved into the falling head apparatus to determine their permeabilities. The permeabilities were measured by timing the length of time it took for water to run through the samples. This was repeated to get representative permeabilities.

4.5 Synthetic AMD/ leachate

Synthetic AMD/ leachate was used to feed through the bioreactors in the pilot study and main experiment. The synthetic AMD was based upon samples of actual AMD taken from the eMalahleni region, in the Mpumalanga coal fields. These samples were analyzed and their chemical compositions were found to be:

- 3100 *mg/l* ***sulfate***;
- 208 *mg/l* ***iron***; and
- ***pH*** of 2.6

In order to replicate the AMD for the pilot and main experiments, the following chemicals were used:

- Sulfuric acid (H_2SO_4) 99% pure;
- Ferrous sulfate heptahydrate ($FeSO_4$); and
- Bicarbonate of soda ($NaHCO_3$).

A 25*L* drum was used as the parent container to house the synthetic AMD. Ferrous sulfate heptahydrate and sulfuric acid were added to the parent drum in predetermined quantities, based on the sample of actual AMD. Thereafter, bicarbonate of soda was added to the synthetic AMD to bring the pH up to 2.6, in line with the actual AMD. Throughout this process, the pH was tested with the Hanna pH and EC probe HI 9511-5.

To ensure the correct readings, the Hanna Instruments (HI 9511-5, Italy) probe was calibrated with *Hanna Instruments calibration solutions* (Figure 16).

Figure 16: Hanna calibration solution and instrument

As a secondary measure to ensure the accuracy of the synthetic AMD content, it was tested with (Macherey-Nagel, Germany) litmus paper (Figure 17). The parent drum was tested once a week during a testing period to ensure that the pH of the mixture did not deviate from the targeted pH of 2.6.

Figure 17: Macherey-Nagel, Germany litmus paper

4.6 Pilot experiment

The purpose of the pilot study was to identify and correct flaws in the experimental setup. It also ensured that the data collected in the main study would be of sufficient quality to answer the research question and assisted in determining validity of the experimental procedure (Leedy & Ormrod, 2014).

The pilot experiment consisted of the following experimental setup: A single sample of manure (0.0012 m3) was placed into the (0.002 m3) bioreactor. The bioreactor was then filled with synthetic AMD, to the level of the design start water level mark. The amount of synthetic AMD needed to saturate the sample was recorded to determine its effective porosity. The initial start time, date and manometer readings were recorded. The peristaltic pump was set to pump synthetic AMD at a rate of 0.31ml/min (Constant head permeability test).

The pilot experiment was designed to work as a constant head permeability test. The constant head formula is as follows:

$$k = \frac{q\,l}{A\,\Delta h} \quad \text{(xi)}$$

$k = permeability\ (m/min)$

$q = flow\ rate\ (l/min)$

$l = length\ of\ the\ sample\ (m)$

$A = cross\ sectional\ area\ (m^2)$

$\Delta h = constant\ head\ causing\ flow\ (m)$

The pilot experiment ran over a period of 35 days.

4.6.1 Pilot experimental questions

The pilot study was conducted in order to clarify the following aspects, before moving onto the main experiment:

- Typical time over which the experiment would need to be conducted;
- Experimental setup issues;
- Adverse events;
- Data collection procedures; and
- Feasibility of the experiments.

4.6.2 Pilot study data collection and recording

Over the one month period, temperature, manometer readings and the amount of general standing water above design water level readings were taken daily at 07:00am and/or 04:00pm.

4.7 Main experiment: Materials and apparatus

In the manufacture of the simulated DPBR, a variety of materials and apparatus were utilized. 2L measuring cylinders were utilized to act as the bioreactors' outer casing. Measuring cylinders were utilized because they are impermeable, acid resistant, robust and relatively inexpensive. The measuring cylinders could be purchased from most laboratory distributers. Two Watson Marlow 120DM3 three channel laboratory peristaltic pumps were used to feed the AMD into the bioreactors. The tubing used to transport the AMD from the parent drum to the bioreactors was PVC tubing. Special, Marprene tubing was used in the peristaltic pumps as normal PVC hardens over time due to continual deformation in the peristaltic pump. A schematic of the experimental layout can be seen in Figure 18 and a 3D image of the experimental setup is shown in Figure 19. A photo of the actual experimental setup is shown in Figure 20.

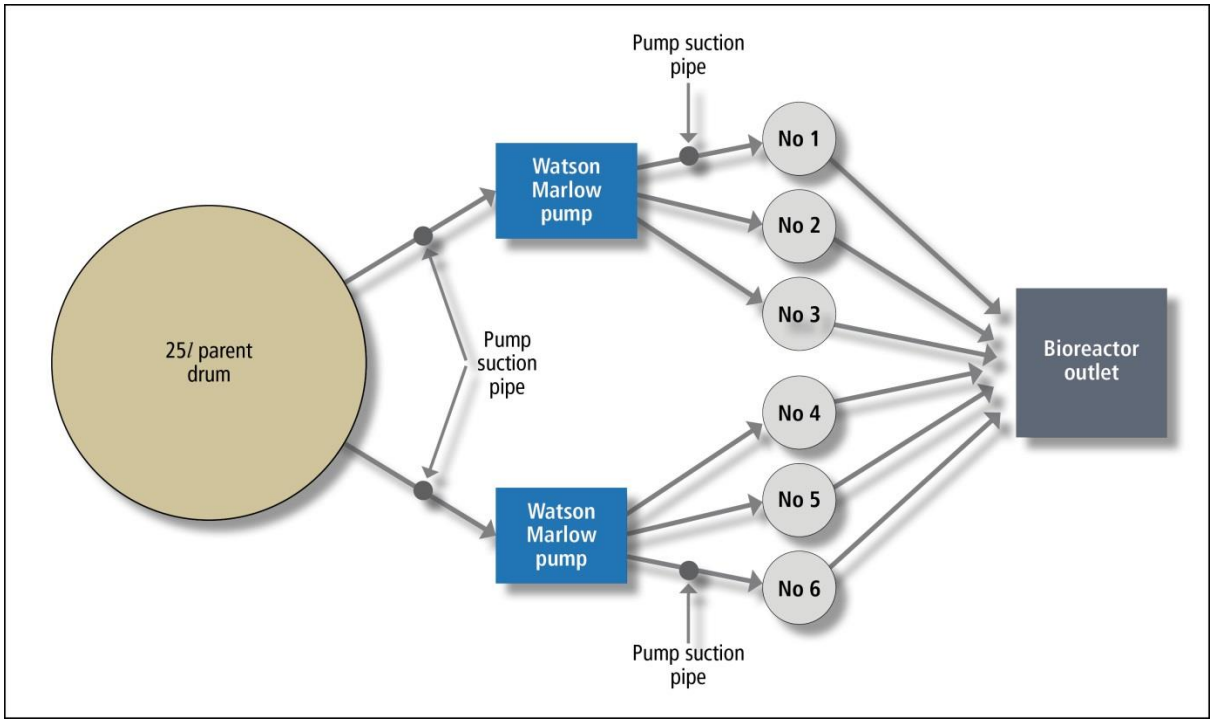

Figure 18: Experimental Setup

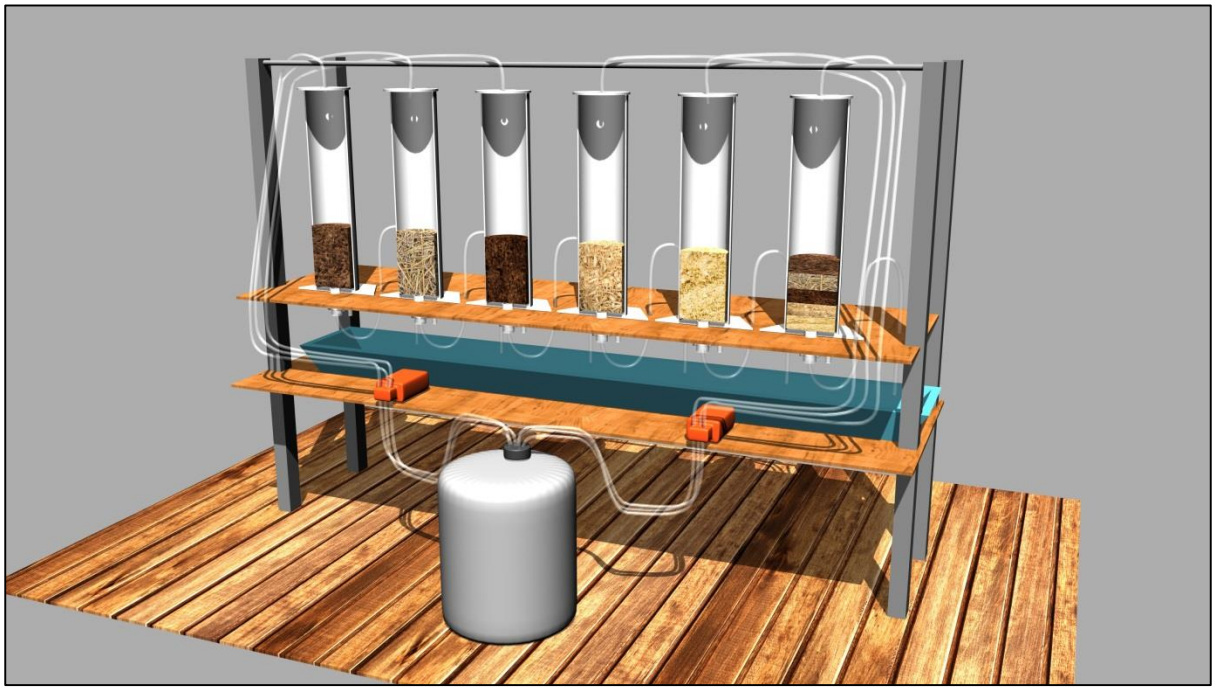

Figure 19: 3D image of the experimental setup

4.7.1 Materials

The materials that were used in the construction of the main experiment are as follows:

- Synthetic AMD/leachate (Ferrous sulfate heptahydrate, sulfuric acid and bicarbonate of soda);
- Manure, straw, vegetable food processing waste (compost), wood shavings and chicken litter (Pulles & Rose, 2002);
- PVC and Marprene tubing; and
- Experimental framework to house the six bioreactors.

The experimental setup along will the different carbon sources and materials used can be seen in Figure 20.

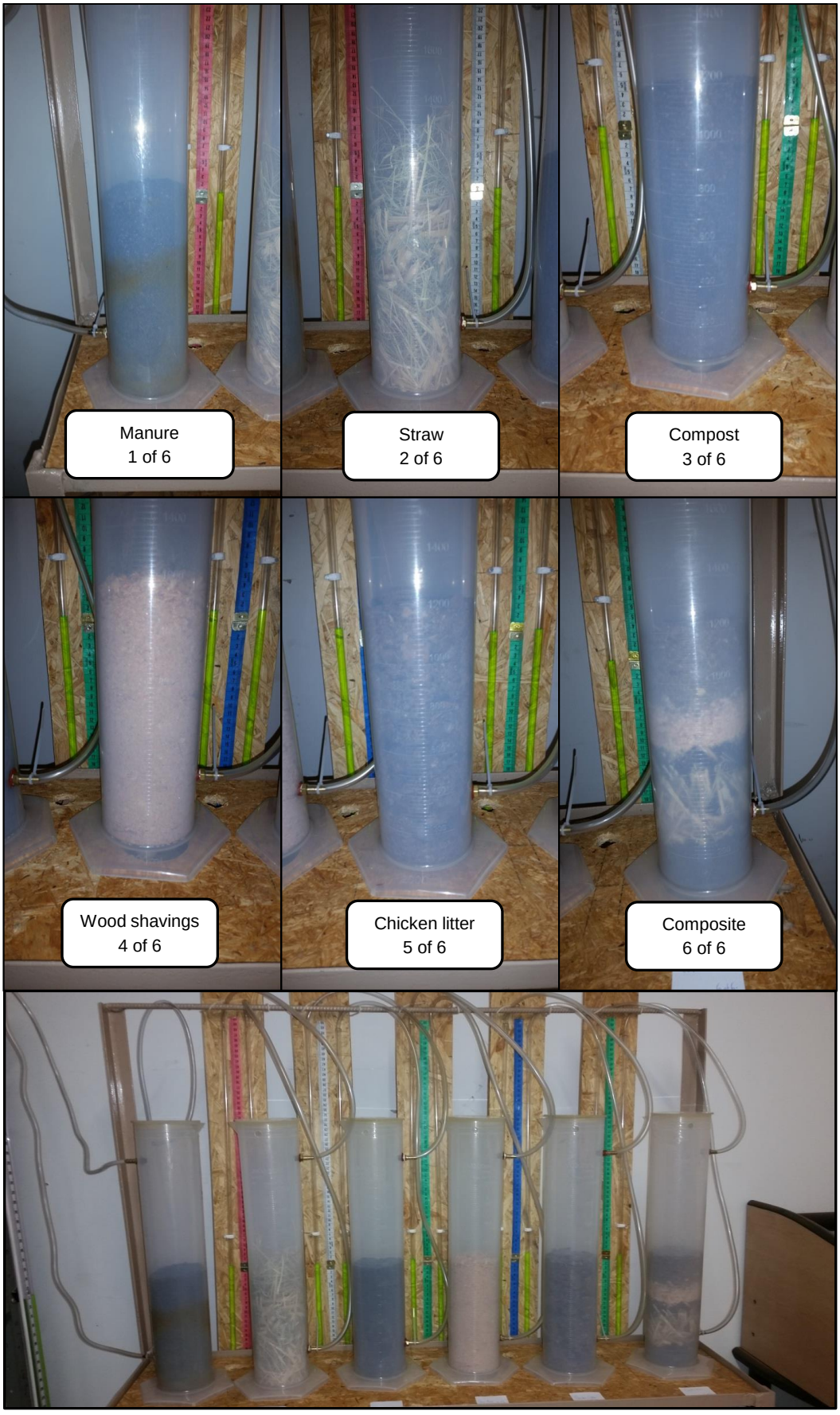

Figure 20: Experimental setup and the various carbon source bioreactors

4.7.2 Apparatus

The following apparatus was used in the construction of the main experiment:

- Watson Marlow 120DM3 three channel laboratory peristaltic pump;
- Dwyer u-tube manometer 1223-M1000-W;
- Measuring jug;
- 2*L* measuring cylinder;
- 25*L* parent drum;
- Experimental stand with wooden base;
- Macherey litmus paper;
- Hanna HI 9511-5 pH and conductivity meter (probe); and
- Stopwatch.

4.7.3 Main experimental procedure

Once all of the learnings from the pilot experiment were incorporated into the main experiment, a start date for the main experiment was established and noted. For the main experiment, five bioreactors with their own carbon source [manure, straw, vegetable food processing waste (compost), wood shavings and chicken litter] were filled to 0.0012 m^3 of each bioreactor. The sixth bioreactor was filled with alternating layers of the first five carbon sources. The bioreactors were then filled with the synthetic AMD until the design start water level marked 1200ml.

A 25L parent drum was filled with synthetic AMD/leachate, which was made according to the AMD samples from Mpumalanga coal fields, as described in (Section 4.5 Synthetic AMD/ leachate)

Initially, the synthetic AMD was fed through into the six bioreactors to a level of approximately 1600*ml* and the stopwatches were started. When the water level reached the sample level of 1200*ml*, the stopwatches were stopped and the time recorded (*Falling head permeability test*).

$$\text{(xii)} \quad k = \frac{al}{At} \times ln\frac{h_0}{h_1}$$

$k = permeability\ (m/min)$

$a = internal\ cross\ sectional\ area\ standpipe\ (m^2)$

$l = length\ of\ the\ sample\ (m)$

$A = cross\ sectional\ area\ (m^2)$

$t = time\ it\ takes\ for\ water\ level\ to\ drop\ from\ h_0\ to\ h_1\ (min)$

$h_o = starting\ height\ of\ water\ above\ sample\ (m)$

$h_1 = final\ height\ of\ water\ above\ sample\ (m)$

This process was repeated daily for 3 months or until the reactor was fully clogged.

On a daily basis, the following data were captured:

- Daily temperature readings; and
- The time it took for the AMD to drop from 1600*ml* to 1200*ml* through the sample.

On a weekly basis, the following data were captured:

- A sample of the exit leachate was taken from all six bioreactors on the Wednesday mornings during every week of the experiment; the samples can be seen in Figure 21. The constituents which were tested for included soluble iron, sulfate and pH. Once the samples were taken and marked, they were put in a cooler box with ice packs and transported to the SANAS accredited GARL (Golder Associates Research Laboratory) for testing.

Figure 21: Exit samples

At the start and at the end of the experiment the effective porosity of each carbon source was determined before the main experiment was started and once the main experiment was concluded. This was done to determine the effective porosity drop over the experimental

lifespan. The effective porosity was determined by using the effective porosity equation, as shown in equation (x) above.

At the beginning of each experiment, the total volume of water up to the 1200ml mark was recorded as the bulk volume. Thereafter, the carbon sources were placed in the bioreactors up to the same 1200*ml* mark. Synthetic AMD was then poured from a 1500*ml* beaker into the bioreactor up to the 1200*ml* mark. The total interconnected voids were deduced from the amount of AMD which fit into the bioreactor with the organic matter, to the marker point of 1200*ml.*

The data recording procedure was followed on a daily basis until the bioreactor clogged completely (no further AMD moved through the sample).

4.7.4 Reliability of experimental procedure

In order to increase the reliability and repeatability of the experimental procedure, the pumps were calibrated before any testing commenced. Calibration was done according to the instrument's user manual, prescribed by the manufacturer. Samples of every parent batch of synthetic AMD were analyzed and tested. Spot pH tests were done on the parent AMD on a weekly basis, with a probe and litmus paper. Pre-experiments were carried out in order to check if all of the measuring equipment was functioning acceptably. The highly accurate, low flow peristaltic pumps allowed the same volume and chemical make-up of the parent AMD to be injected into each bioreactor.

5. RESULTS AND DISCUSSIONS

5.1 Results and discussion structure

The results and discussion structure follows the headings in Section 4. A depiction of the results and discussion structure which follow from Section 4 can be seen in Figure 22.

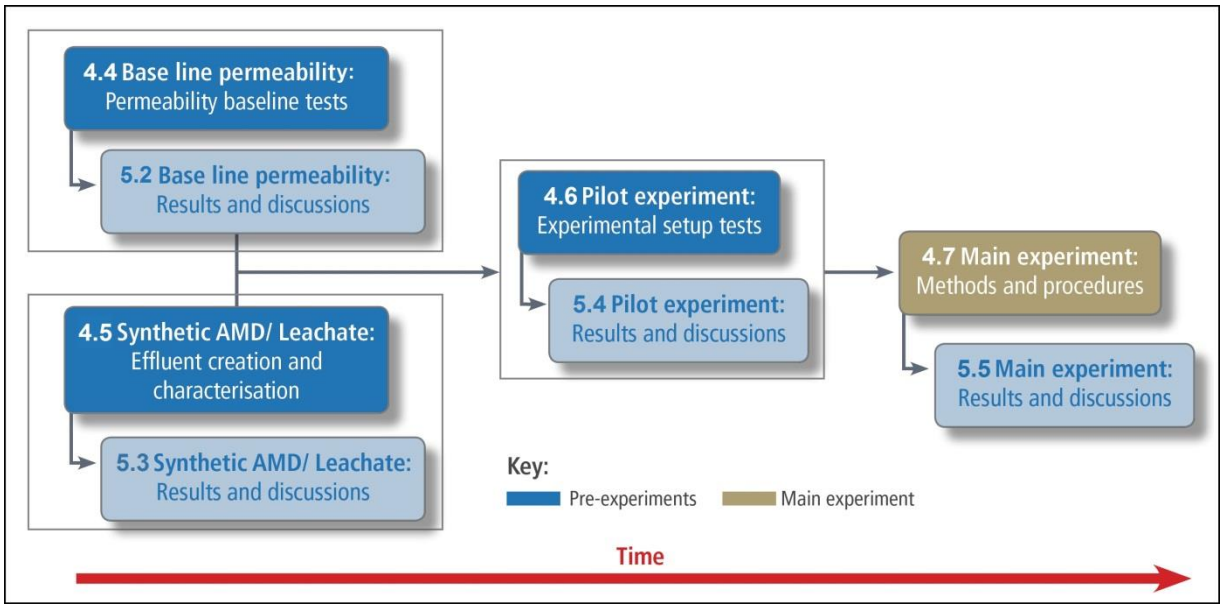

Figure 22: Results and discussion structure

5.2 Baseline permeability

5.2.1 Baseline permeability results

Due to the large porous spaces between the carbon sources (high permeabilities); the pressure controllers for the (ASTM D2434) C*onstant Head Permeability Test* could not maintain a minimum constant pressure of 10kPa. Therefore, the results received from this test reported the maximum flow rate of the pressure controllers and not the true permeability of the carbon sources. However, the (ASTM 5084-3) *Falling Head Permeability Test* did render permeability results.

The densities of the remolded carbon sources were:

- Manure 804 kg/m^3;
- Straw/Hay 53 kg/m^3;
- Compost 543 kg/m^3;
- Wood shavings 170 kg/m^3;

- Chicken litter 536 kg/m^3; and
- Composite sample 376 kg/m^3.

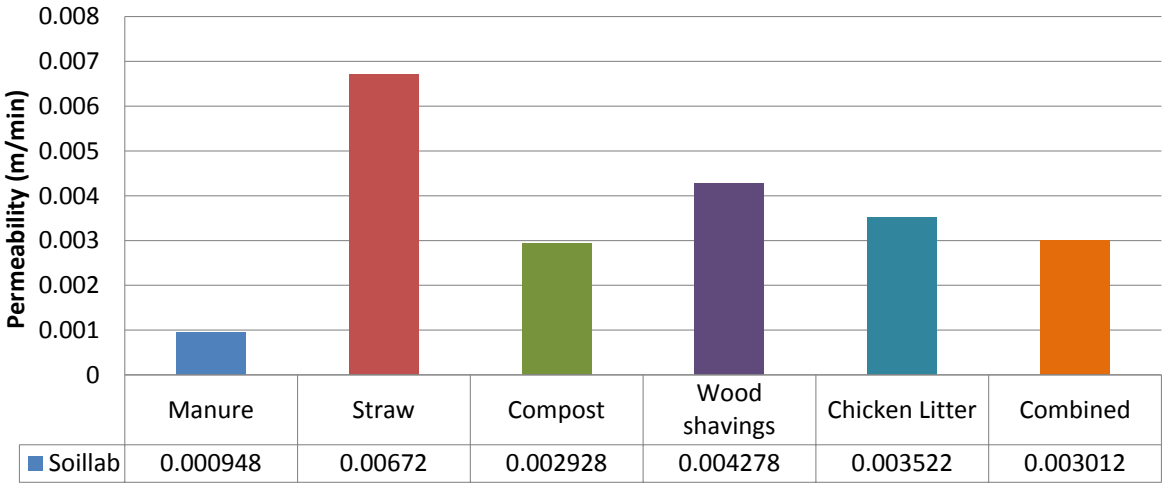

Figure 23: Falling head permeability results

Soillab represents the laboratory that was used to test the permeability of the different carbon sources. Figure 23 depicts the steady state permeabilities for the various carbon sources, with straw being the most permeable and manure being the least. The combined samples' permeability and density deviated below the mean by 18 and 11%, respectively. By layering the five different carbon sources in precisely uniform layers, the combined sample averaged out the permeability and density of the extreme values (straw and manure).

The effective porosities of the carbon samples followed the trend of the permeability graph, with straw having the highest effective porosity and manure the least. The correlation between permeability and effective porosity were plotted and is shown in Figure 24. The correlation coefficient was 0.8, indicating a strong positive linear relationship for the specific carbon sources.

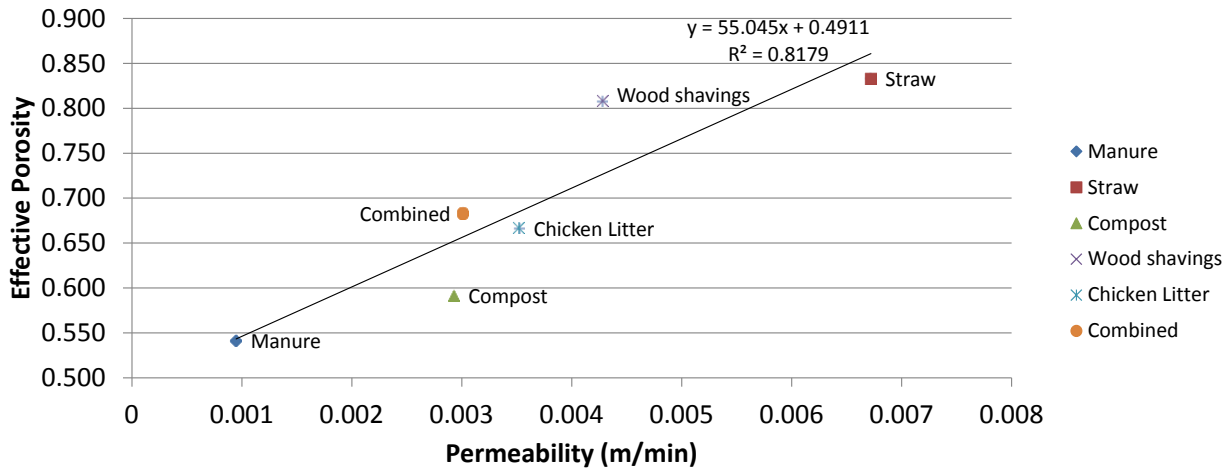

Figure 24: Permeability and effective porosity

As seen in Figure 24, an increase in effective porosity resulted in an increase in permeability. The carbon samples with the larger, more irregularly shaped particle sizes were plotted on the upper end of the graph, with the smaller and more uniform particle sizes at the bottom of the graph.

5.2.2 Baseline permeability discussion

The following learnings developed from the baseline permeabilities:

- *The steady state permeability values for the various carbon sources:* The carbon sources had to be remolded to a predetermined density before they could be inserted into the falling head permeability apparatus. These permeability results would be slightly different to the actual packing of a DPBR because of the manner in which the DPBR is packed. The main experiment should be packed and not remolded;
- *The permeability of all the layers as a whole (combined):* By layering the five different carbon sources in precisely uniform layers, the combined sample, averaged out the permeability, effective porosity and density of the extremes values; and
- *How the hydraulic efficiency is affected by different layers with different permeabilities:* The carbon samples with the larger, more irregularly shaped particle sizes had larger permeabilities and porosities. The smaller and more uniform particle sized carbon sources had lower permeabilities and porosities.

5.3 Synthetic AMD/ leachate results

Throughout the experiment, four "parent tanks" of AMD were made. Each tank was tested at a SANAS laboratory for sulfate, iron and pH as discussed in the methods.

These samples were analyzed and their chemical compositions were found to be:

- 3100 *mg/l* ***sulfate***;
- 208 *mg/l* ***iron***; and
- ***pH*** of 2.6

5.4 Pilot experiment

5.4.1 Pilot experimental results

The pilot experiment was initiated to determine the time over which the main experiment would have to be conducted. During the pilot experiment, further aspects emerged:

- Experimental setup issues;
- Adverse events;
- Data collection procedures; and
- Feasibility of the experiments.

In the pilot experiment, manure was used as the test substrate. Manure was used as it had the lowest permeability out of all the different carbon sources, giving an accurate time period over which to run the main experiment.

The pilot experiment was designed to work as a constant head permeability test. The results of the constant head permeability test are shown in Figure 25.

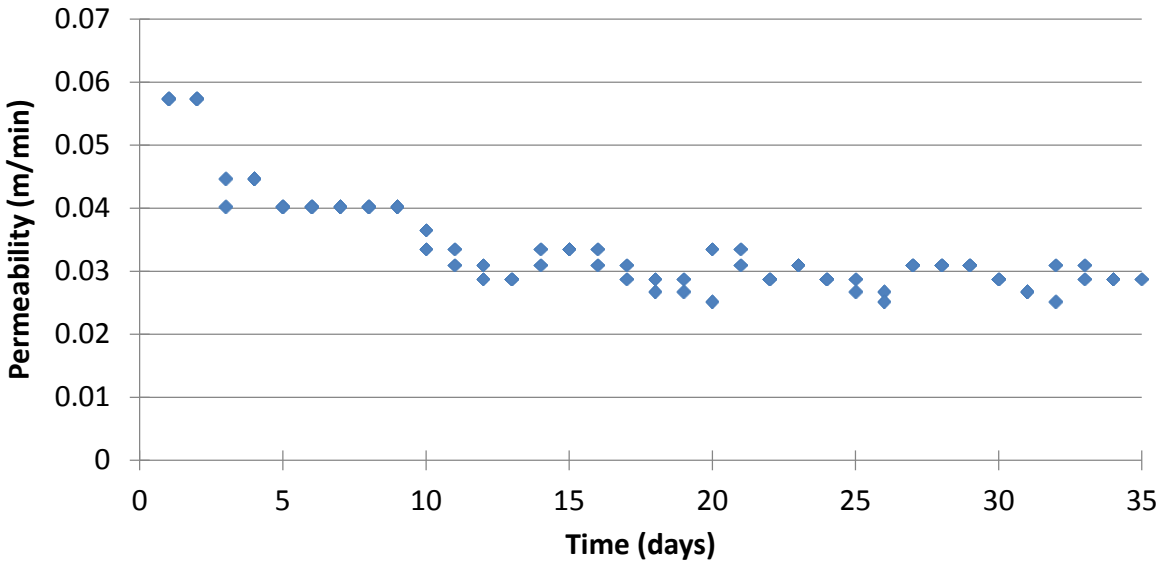

Figure 25: Constant head permeability results

The permeability values differed from the SANAS accredited laboratory by an order of magnitude. This difference can be attributed to the incorrect laboratory method that was used during data collection. Since the researcher wanted to determine the clogging effect of the carbon source in the bioreactor over time, the falling head permeability test should have been used. However, the results from the pilot experiment did allow the researcher to uncover an oscillating effect in the permeability readings, as seen in Figure 25 and Figure 26.

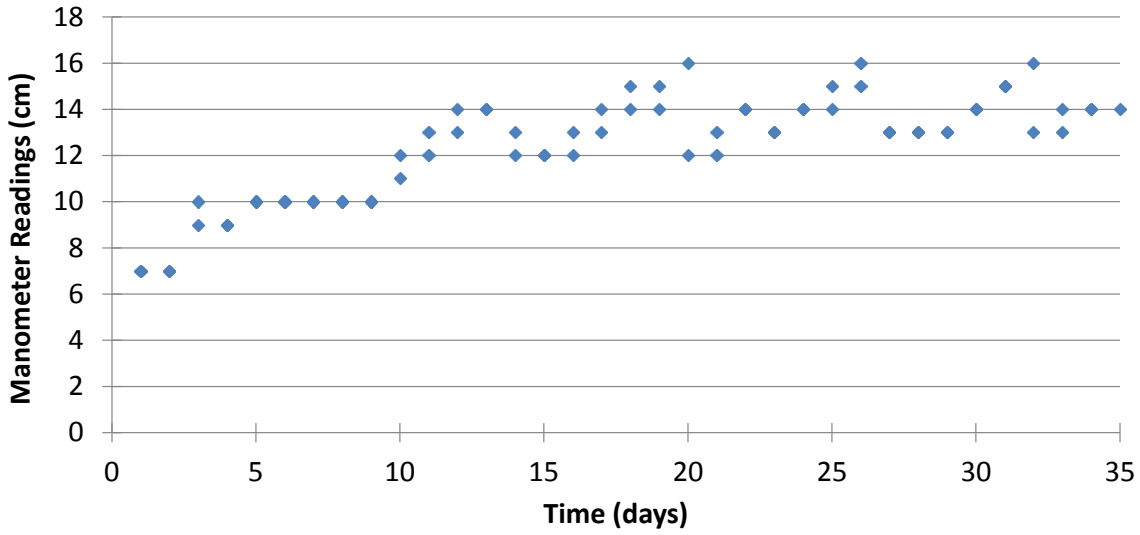

Figure 26: Manometer reading over time

The oscillating readings from the manometers were obtained at regular intervals. Through further investigation, it was found that as the AMD in the bioreactor built up to a certain static head, a small vacuum was caused in the exit tubing of the bioreactor. This pushed small air bubbles out of the exit tubing, causing a negative pressure and thereby "sucking" the synthetic AMD through the bioreactor, decreasing the manometer reading and causing rhythmical jumps in the data (seen in Figure 25 and Figure 26).

5.4.2 Pilot experimental discussion

The following learnings developed from the pilot experiment:

- *Typical time over which the experiments need to be conducted:* It was found that the pilot experiment took approximately one month to clog. The main experiment would be conducted over a period three times as long, taking into consideration the fact that other carbon sources could have larger lag times for the SRB to build up. Other carbon sources did not break down as quickly as manure, therefore taking longer to clog the bioreactor;
- *Experimental setup issues:* To ensure that the bioreactor remained anaerobic and that the top water level remained constant at the height of the sample, the exit tubing was raised to the same level as the intended water level, as seen in Figure 27. This ensured that the sample remained saturated at the designed level. This is vital as SRB needs anaerobic conditions to function;

Figure 27: Bioreactor with level control

- *Adverse events:* It was found that the bioreactor clogged up to a point and then the AMD subsequently pushed through the bioreactor. The cause of this phenomenon was observed to be a vacuum in the "level regulator" exit tubing. When the bioreactor clogged and pushed back on the system, the static head built up to a point and then pushed the air bubble out of the system, causing a slight vacuum (the exit tubing was under full flowing conditions). This problem was overcome by adding a siphon break on the exit tubing. The way in which the data was collected was also reconfigured to ensure that the static head would not build up to the point at which it would have this effect on the sample in the experiment;
- *Data collection:* The data collection and empirical formula used to determine the permeability were altered so that the experiment could be started again every morning.

This ensured that the static head would not build to the point at which it would have an effect on the sample in the experiment. The falling head permeability method was subsequently used to determine the permeabilities in the main experiment; and

- *Feasibility of experiment:* The data from the pilot experiment was analysed to determine if the experimental setup was correct. Numerous items within the setup were changed and tested until they were functioning correctly. The permeability values from the reconfigured experimental setup and methodology largely matched the permeability derived from SANAS laboratory Soillab. Feasibility was thus established for the main experiment.

5.5 Main experiment

5.5.1 Permeability of bioreactors over time results

During the experimental life span, six different experiments were conducted on the different carbon sources. The results are shown in Figure 28 and 29, the graphs are labeled as follows:

A) Manure;
B) Straw;
C) Compost;
D) Wood shavings;
E) Chicken litter; and
F) Combined Combination of the other carbon sources.

Manure and chicken litter were noted to clog most rapidly, as seen in graphs A and E respectively. None of the other experiments clogged fully over the experimental lifespan.

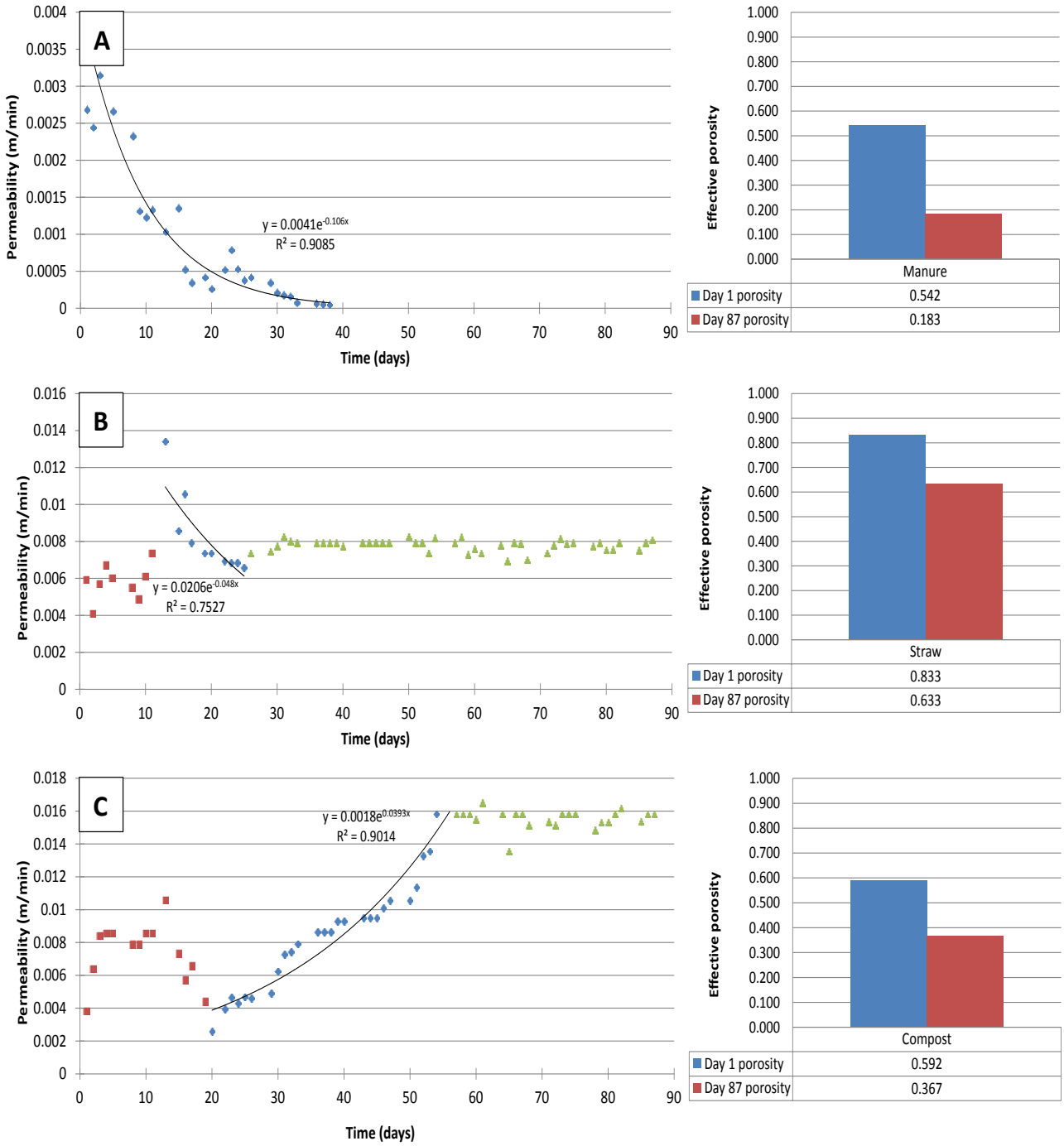

Figure 28: Permeability of the six different bioreactors over the three month period as well as the decrease in effective porosity from the start of the experiment to the end. A-Manure; B-Straw and C-Compost

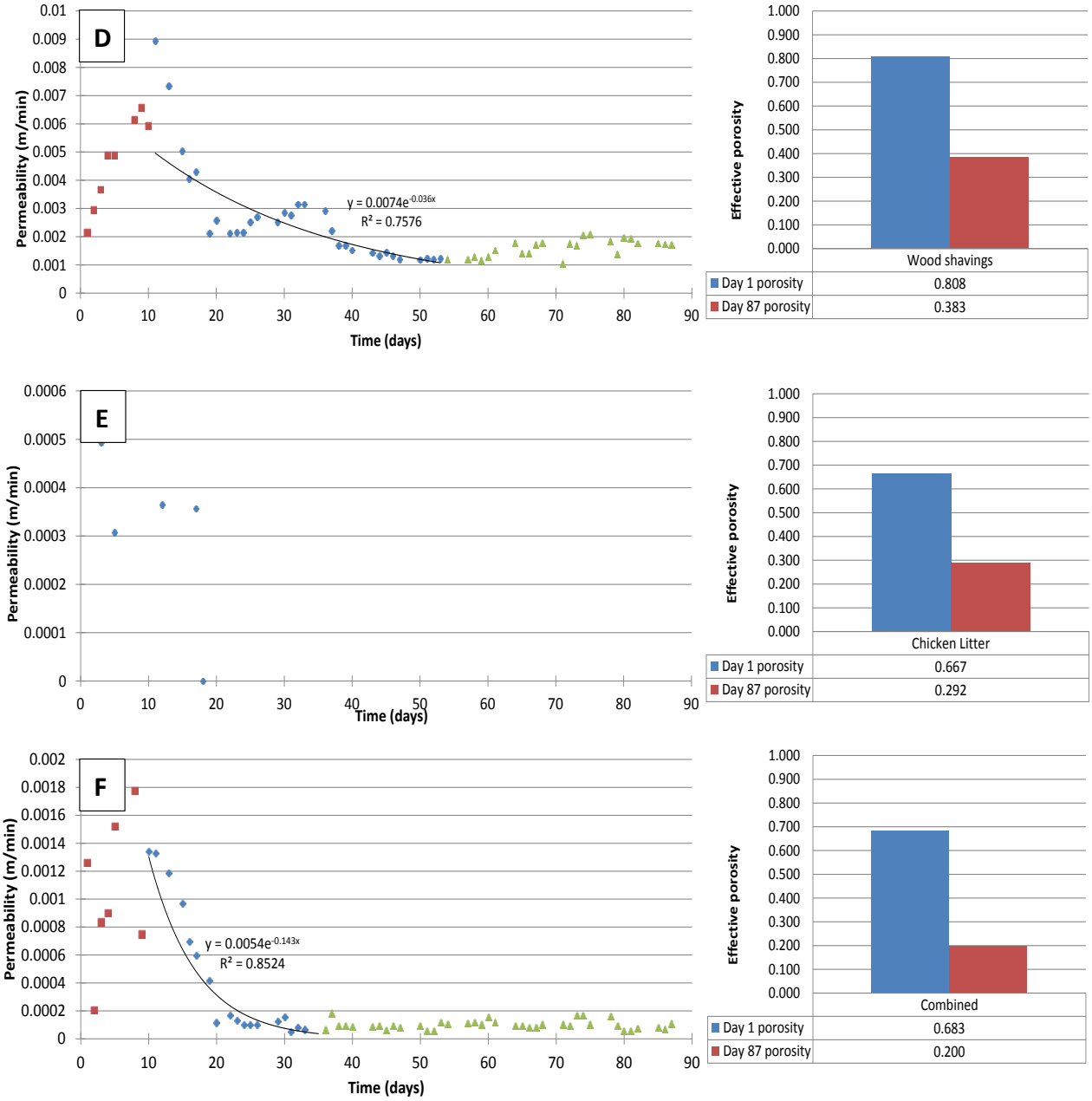

Figure 29: Permeability of the six different bioreactors over the three month period as well as the decrease in effective porosity from the start of the experiment to the end. D-Wood shavings; E-Chicken litter and F-Combined sample

Three phases could be seen on the permeability graphs shown in Figure 28 and 29, namely:

- Establishment phase: Depicted by the red data points;
- Exponential phase: Depicted by the blue data points; and
- Stabilisation phase: Depicted by the green data points.

As seen in Figure 28 and 29, all of the carbon sources, with the exception of the manure and chicken litter, had an establishment phase (shown by the red data points), where the initial

reading of permeability varied with no obvious trend or pattern in the data. After the establishment phase, exponential trends started developing (shown by the blue data points) these trends started to develop as the bioreactor started to clog. These exponential trends were mainly in the negative direction (clogging of the bioreactor), with the exception of the compost bioreactor. The final phase identified was the stabilisation phase (shown by the green data points). Four of the carbon sources (straw, compost, wood shavings and combination bioreactor) showed a clear stabilisation phase, whereby the permeability values continued to decrease but at a vastly decreased rate for the remainder of the experimental lifespan. This is key as a relatively constant permeability is reached in the bioreactor. This stabilisation value would be the true permeability design value for the specific carbon source.

Table 2 shows the summarized phase lengths of the different carbon sources. The table indicates the start and end days for each phase, from the initiation of the experiment.

Table 2: Different phases of the carbon sources

Carbon Source	Startup phase	Exponential phase	Stabilization phase
Manure-A	1-2 days	3-38 days	Clogged
Straw-B	1-11 days	12-25 days	26 > days
Compost-C	1-19 days	20-62 days	62 > days
Wood shavings-D	1-10 days	11-59 days	59 > days
Chicken litter-E	Clogged within 18 days		
Combination-F	1-9 days	10-35 days	35 > days

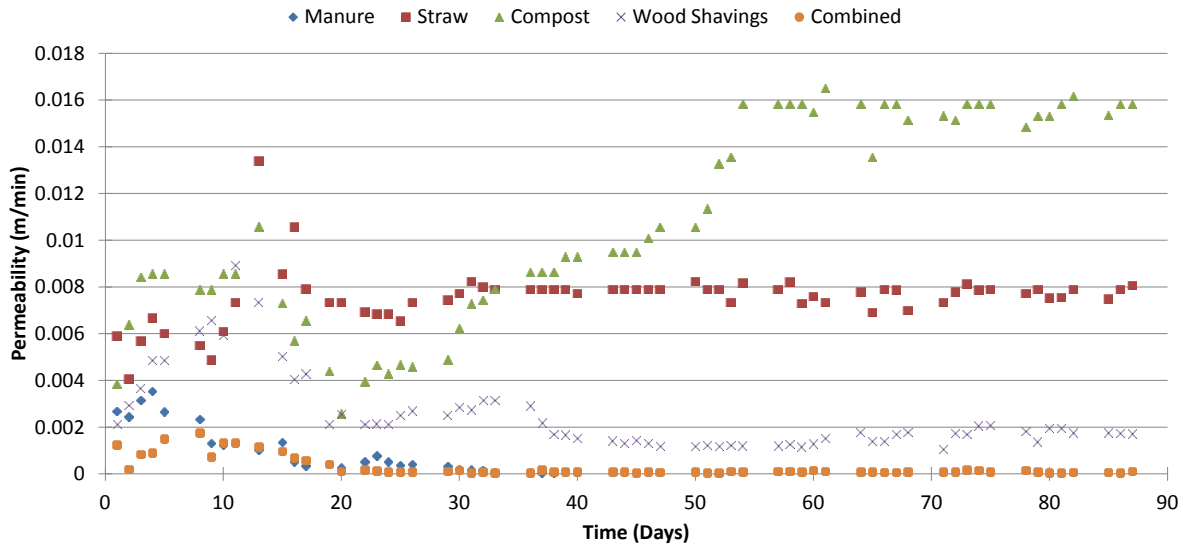

Figure 30: Permeability of different carbon sources

As seen in Figure 30, compost and straw had the overall highest permeabilities. Manure and the combined sample had the lowest permeabilities. Although the combination bioreactor never fully clogged, it was only as permeable as its least permeable layer, manure.

With the help of the SRB, the carbon source precipitated the metals within the AMD in the bioreactors, thereby reducing the effective porosities of the bioreactors. This can be seen in Table 3. The iron in the AMD precipitates in the carbon sources thereby reducing the amount of voids and reducing the effective porosity of the carbon source.

Table 3: Effective porosities of carbon sources

	Manure	Straw	Compost	Wood shavings	Chicken litter	Combined sample
Day 1 effective porosity	0.542	0.833	0.592	0.808	0.667	0.683
Day 87 effective porosity	0.183	0.633	0.367	0.383	0.292	0.2
% decrease in effective porosity	66.24	24.01	38.01	52.60	56.22	70.72

Also seen in Table 3, the manure and the combined sample had the largest reduction in effective porosity, with straw and compost having the least. The effective porosities obtained followed the carbon sources' permeabilities, as manure and the combined samples had the lowest permeabilities while straw and compost had the highest permeabilities.

The average permeabilities of the stabilisation phase for the bioreactor, which did not clog, was determined and can be seen in Figure 31.

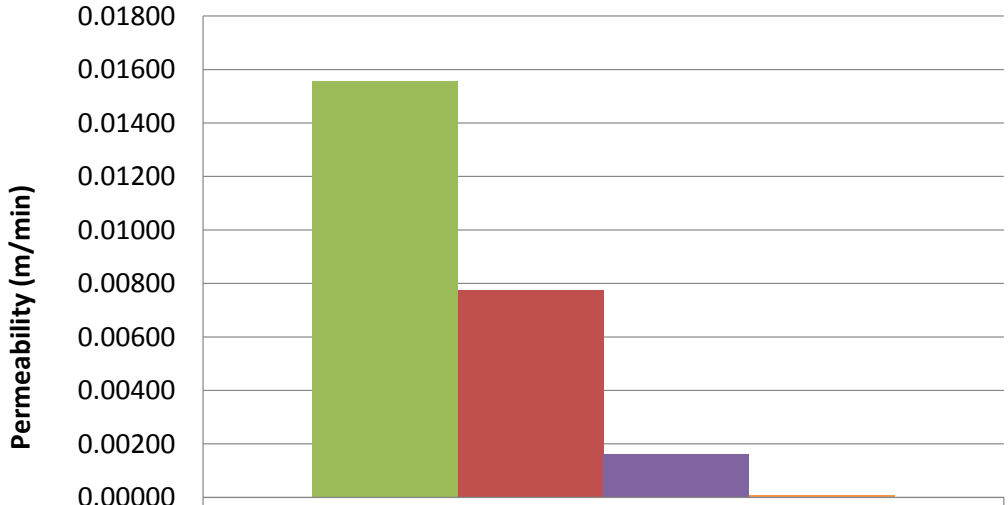

	Carbon sources
Compost	0.01557
Straw	0.00776
Wood Shavings	0.00161
Combined	0.000099

Figure 31: Average permeabilities of the stabilisation phase

The compost bioreactor had the highest stabilisation permeability and the combination bioreactor had the lowest. Although it was not proven, it is assumed that compost had an increasing permeability following the initial establishment phase, due to short circuiting through the bioreactor. The stabilisation phase is of significance because it impacts the steady flow of AMD passing through the bioreactors. The polluted water needs to remain in and amongst the organic matter long enough for this reaction to take place, yet not so long that it increases operating costs; as a result a larger bioreactor will be needed to treat larger volumes of AMD. This stabilisation permeability can be used as the hydraulic design permeability of the bioreactor.

5.5.2 Permeability of bioreactors over time discussion

The chicken litter carbon source had the lowest permeability from the start of the experiment. The chicken litter held large air bubbles between the larger clumps of litter. The air bubbles blocked the bioreactor, not allowing any flow of AMD through the bioreactor. The chicken litter completely clogged within 18 days after the initiation of the experiment. It is therefore recommended not to be used as a carbon source in the DPBR.

Manure showed the quickest establishment and started clogging from day 2 of the experiment. This could be seen as both an advantage and disadvantage. The advantage lies in the fact that the bioreactor does not waste time in precipitating metals. The disadvantage is the fact that the fast precipitation of metals clogs up the pores in the bioreactor, as can be seen by a 66% decrease in effective porosity. The manure was also one of two carbon sources which fully clogged on day 38 of the experiment.

The straw, compost, wood shavings and combination bioreactors all stabilised at a certain point in time and further reduction in permeability occurred at a slow rate thereafter. All four stabilisation points occurred at different times during the experiment, with the straw bioreactor stabilising the quickest and the wood shavings and compost bioreactors taking the longest. This stabilisation permeability can be used as the hydraulic design permeability of the bioreactor.

The combination bioreactor had a dilution effect. All five of the different constituent carbon sources found in equal layers within the bioreactor helped average out the different phases of the bioreactors. The overall permeability of the combination bioreactor was only as permeable as its lowest permeable layer, manure. The combination bioreactor's permeability closely followed the manure's permeability graph, with a decrease in effective porosity of 70%. However, the combination bioreactor did not clog over the experimental lifespan. Hydraulically, the combination bioreactor was the best performing reactor; it never fully clogged and the AMD moved through the bioreactor at a constant rate.

The main function of the DPBR is to treat sulfates and precipitate metals in AMD. Therefore, the operating range of the DPBR, which takes into consideration the permeabilities as well as the chemical treatment potential of the bioreactor, is extremely important. Therefore the chemical parameters are discussed against the permeability in the subsequent sections.

5.5.3 Permeability versus sulfate removal of bioreactors results

A typical Highveld AMD is high in sulfates. The DPBR aims to convert sulfates into sulfides with the help of SRB. No samples were taken for the chicken litter bioreactor as this bioreactor clogged before the first sample stage. The results for sulfate removal against the permeability of the bioreactors for each individual carbon source can be seen in Figure 32 and 33, the graphs are labeled as follows:

A) Manure;
B) Straw;
C) Compost;
D) Wood shavings; and
E) Combination of the other carbon sources

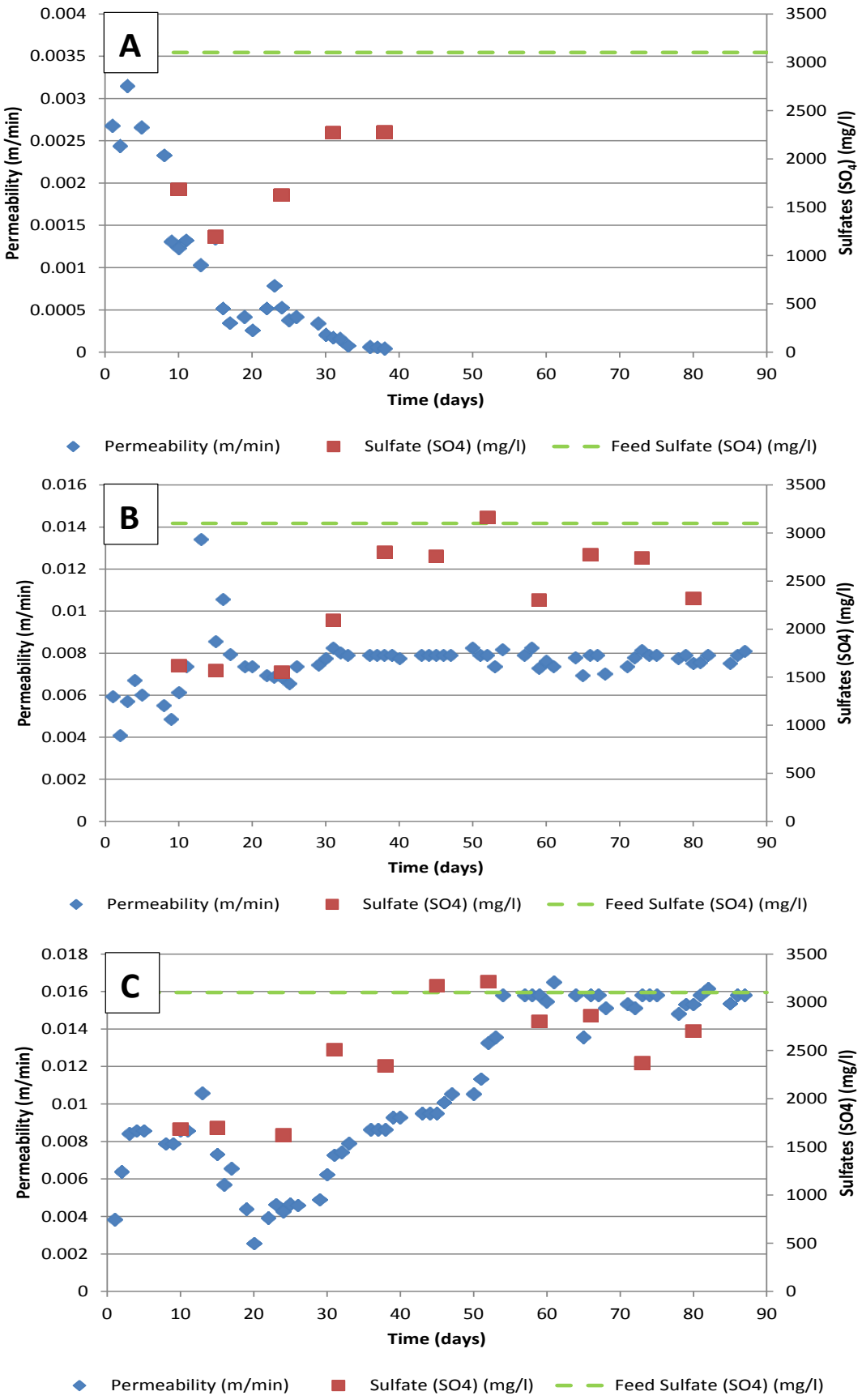

Figure 32: Permeability versus sulfate removal, for A-Manure, B-Straw and C-Compost

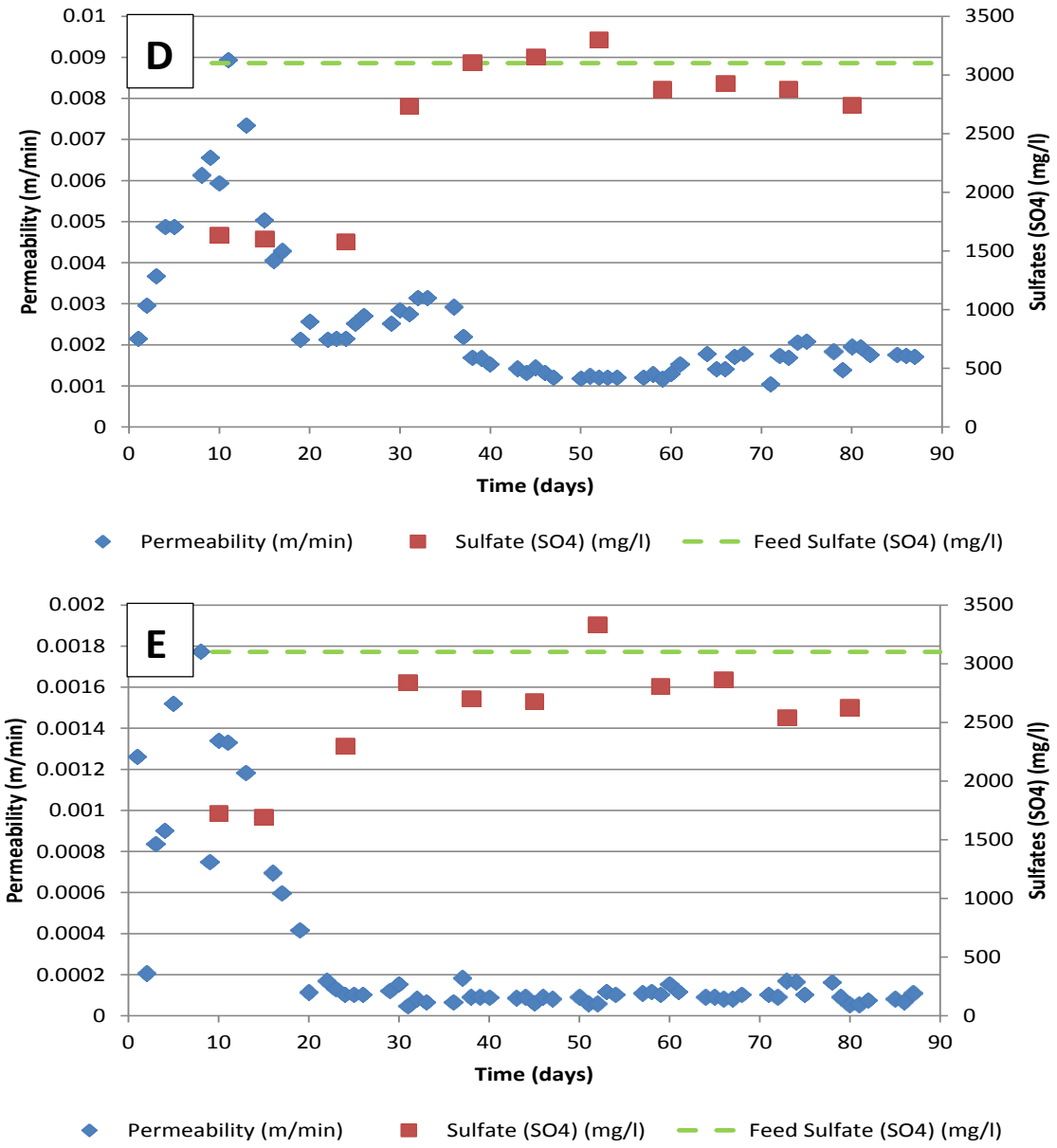

Figure 33: Permeability versus sulfate removal, for D-Wood shavings and E-Combined sample

The green dotted lines in graphs A though E in Figure 32 and 33 indicates the initial level of sulfate in the feed synthetic AMD (3100 *mg/l*). The blue points in graphs A though E indicates the permeabilities in (*m/min*) and the red points are the weekly sulfate samples in (*mg/l*) for each carbon sources.

Two distinct points are highlighted in graphs A through E, namely:

- Optimal sulfate removal point: This point indicates the time taken before the largest amount of sulfate is removed from the feed AMD;

- Point at which sulfate is no longer removed: This is the point in time when the leachate exiting the bioreactor matches the AMD entering the bioreactor, thereby indicating no further sulfate removal.

Table 4: Optimal sulfate removal point and final sulfate removal point

Carbon Source	Optimal sulfate removal point	Point at which sulfate is no longer removed
Manure-A	Day 15	Clogged before reaching 3100*mg/l*
Straw-B	Day 24	Day 52
Compost-C	Day 24	Day 45
Wood shavings-D	Day 24	Day 38
Combination-E	Day 15	Day 50

The manure (graph A) only has data up to day 38 because at this point, the bioreactor was completely clogged. The manure bioreactor at day 10 had lowered the sulfates by 45%. Day 15 was the manure's optimal sulfate removal point, as 61 % of the sulfate in the fed AMD was removed. Thereafter, the sulfates load started to trend towards the initial feed of 3100 *mg/l*, however the bioreactor clogged before further samples were taken. At the optimal sulfate removal point on day 15, the permeability of the bioreactor was 0.0013 *m/min*. After this optimal point, the bioreactor clogged further and the sulfate removal rate continued to decrease. Permeabilities higher than the optimal point also removed sulfates but at a lower quantity than that which occurred at the optimal point.

The straw (graph B) did not fully clog over the life span of the experiment. The straw bioreactor at day 10 had lowered the sulfates by 47.6%. Day 24 was the straw's optimal sulfate removal point as 50% of the sulfate in the fed AMD was removed. Thereafter, the sulfates load starts to trend towards the initial feed of 3100 *mg/l*. At day 52, the straw sample exiting the bioreactor was the same as the AMD entering the bioreactor. No further sulfates were removed after this point. At the optimal sulfate removal point on day 24, the permeability of the bioreactor was very close to the stabilised permeability of 0.0076 *m/min*. The straw bioreactor never clogged over the experimental lifespan but rather reached a stabilised permeability. The sulfate removal however, started to decrease from this optimal point and hovered around a general range from 2300 to 3100 *mg/l.*

The compost (graph C) also did not fully clog over the life span of the experiment, but rather increased in permeability until its stabilisation point. The compost bioreactor at day 10 had lowered the sulfates by 45.5%. Day 24 was the compost's optimal sulfate removal point as 47.7 % of the sulfate in the fed AMD was removed. Thereafter, the outlet concentration of sulfate started to trend towards the initial feed of 3100 *mg/l*. At day 45, the compost sample exiting the bioreactor was the same as the AMD entering the bioreactor. No further sulfates where removed after this point. At the optimal sulfate removal point on day 24, the permeability of the bioreactor increased towards it stabilisation point. The compost bioreactor never clogged over the experimental lifespan but reached a stabilised permeability. The sulfate removal and the permeability of the compost followed similar trends, with the sulfate removal curve preceding the permeability curve.

The wood shavings (graph D) did not fully clog over the life span of the experiment. The wood shavings bioreactor, at day 10, had lowered the sulfates by 47.2%. Day 24 was the wood shavings' optimal sulfate removal point, as 49 % of the sulfates in the fed AMD were removed. Thereafter, the outlet concentration of sulfate started to trend towards the initial feed of 3100 *mg/l*. At day 38, the wood shaving sample exiting the bioreactor was the same as the AMD entering the bioreactor. The sulfate removal levelled out after day 38 to a range just below the feed 3100 *mg/l*. At the optimal sulfate removal point on day 24, the permeability of the bioreactor was 0.0025 *m/min* and thereafter decreased toward its stabilisation permeability. The wood shavings bioreactor never clogged over the experimental lifespan but reached a stabilised permeability. The sulfate removal rate, however, started to decrease from this optimal point.

The final combination bioreactor (graph E) did not fully clog over the life span of the experiment. The combination bioreactor, at day 10, had lowered the sulfates by 44.4%. Day 15 was the combination bioreactors optimal sulfate removal point as 45.3 % of the sulfates in the feed AMD were removed. Thereafter, the outlet concentration of sulfate started to trend towards the initial feed of 3100 *mg/l*. At day 50, the combination reactor's sample exiting the bioreactor was the same as the AMD entering the bioreactor. Subsequent samples were all around the 3100 *mg/l* feed mark. At the optimal sulfate removal point on day 15, the permeability of the bioreactor was 0.0009 *m/min* and decreased sharply toward its stabilisation permeability. The combination bioreactor never clogged over the experimental lifespan but reached a stabilised permeability. The overall stabilisation permeability for the combination bioreactor was quite low.

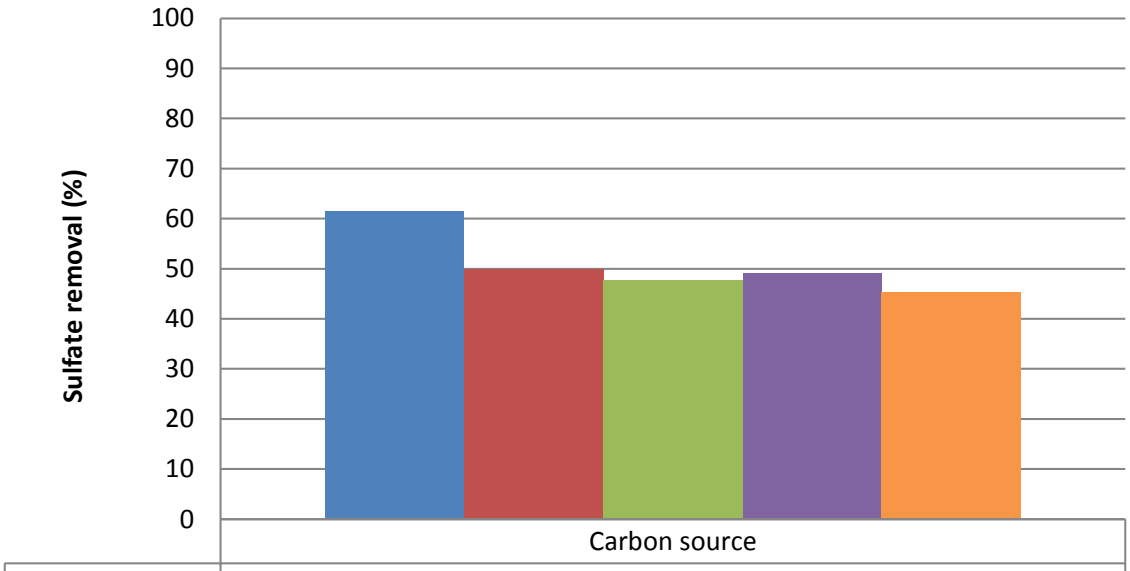

	Carbon source
Manure	61.5
Straw	50.0
Compost	47.7
Wood shavings	49.0
Combined	45.3

Figure 34: The percentage of sulfate removed at the optimal sulfate removal points for all the carbon sources

As seen in Figure 34, all of the carbon sources removed between 45 and 62 % of the sulfates from the fed AMD. Manure removed the highest percentage of sulfates with 61.5% and the combined bioreactor removed the least sulfates, with 45.3% sulfate removal. The point in time at which these optimal sulfate removal points accrued varied between the carbon sources, with manure and the combined bioreactor being approximately 15 days from the start of the experiment and the rest of the bioreactors at 24 days after the initiation of the experiment.

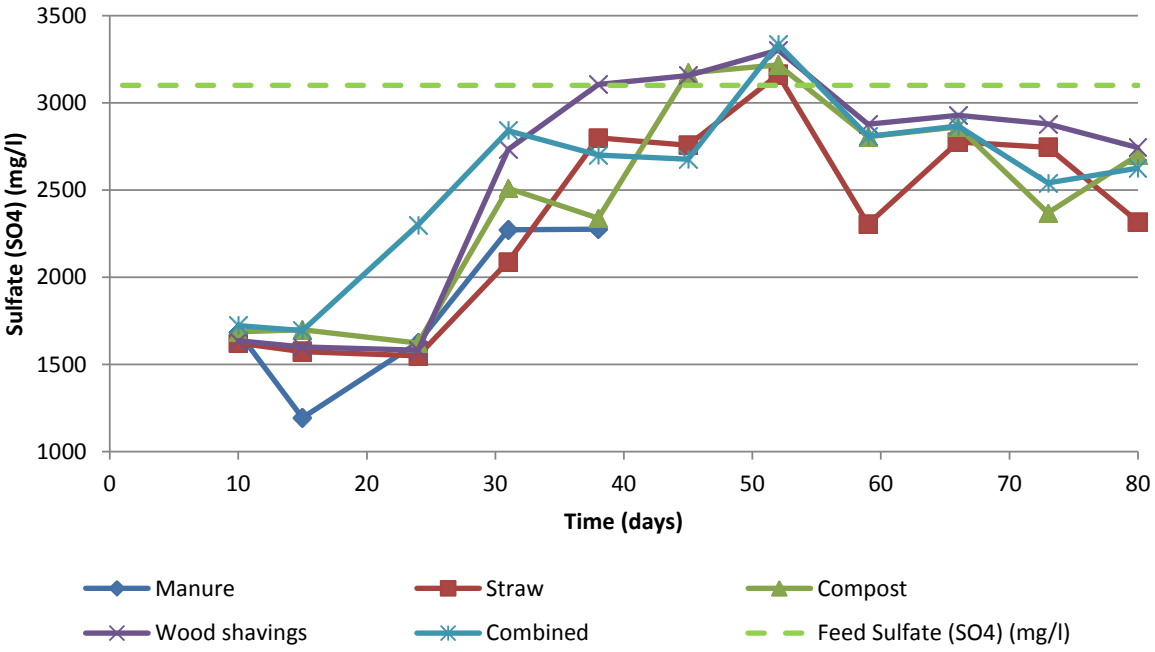

Figure 35: Sulfate break through curves for all carbon sources

As seen in Figure 35, all of the carbon sources optimally removed sulfates up to day 25 after the initiation of the experiment. Thereafter, the carbon sources lessened in the amount of sulfates being removed from the AMD, up to the point where the break through curve reached the feed sulfate load of 3100 *mg/l*. Wood shavings reached the fed sulfate load the quickest (this occurred at day 38) and straw took the longest time to reach the break through stage (this occurred at day 52). Once all of the carbon sources reached the breakthrough mark of 3100*mg/l*, the removal rate starts to taper off slightly and hover just under the 3100*mg/l* mark. The carbons sources at day 52 had sulfate loads higher than the initial fed load of 3100 *mg/l*, the carbon sources themselves could be adding small amount of sulfates to the exiting AMD.

5.5.4 Permeability versus sulfate removal of bioreactors discussion

At the optimal sulfate removal point, manure removed the highest amount of sulfates, with 61.5% of the sulfate being removed from the fed AMD. The combined bioreactor removed the lowest amount of sulfates, with 45.3% sulfate removal. The other bioreactors also fell within this range. Therefore, the overall average sulfate removal for the carbon sources in the bioreactors was about 50%. The sulfate was converted by the SRB to sulfides (hydrogen sulfide) and was removed from the system in a gas form (an egg like odor was noted as coming from the bioreactors).

Since all of the carbon sources' sulfate removal rates are within 17% of each other, the permeability variable plays a larger role in the decision on which carbon source should be used within the DPBR.

Out of all the carbon sources, manure showed the highest amount of sulfate removal from the fed AMD. In terms of permeability on the other hand, manure clogged the quickest of all the materials. For the DPBR to work efficiently, the amount of water moving through the DPBR as well as the amount of sulfates being removed need to be weighed up against each other to determine the optimal carbon source to be used. The combined bioreactor (which removed the lowest amount of sulfate) and the straw bioreactor allowed for a longer period of sulfate removal as they only reached the point at which no further sulfate was removed on days 50 and 52 respectively.

Wood shavings would be recommended for use within the DPBR for its high permeability and close to 50% sulfate removal. However, wood shavings' break through curve was the quickest at 38 days, rendering the high permeabilities worthless as no sulfate was removed after day 38.

Straw and compost would be recommended for use within the DPBR based upon their high stabilisation permeabilities, as well as having a sulfate removal rate close to 50%. Both their breakthrough points were more than 45 days. Therefore, straw and compost allowed a high, constant amount of AMD to flow through the carbon sources, without the carbon source completely clogging over the experimental lifespan.

5.5.5 Permeability versus iron removal of bioreactors results

Just as permeability was plotted against sulfate reduction in Section 6.5.3, the permeability of each bioreactor was plotted against the iron exiting each bioreactor. Samples of AMD exiting the five bioreactors were taken on a weekly basis. No samples were taken for the chicken litter bioreactor as this bioreactor clogged before the first sample stage.

The results for the remaining carbon sources can be seen in (Figure 36 and 37) and are labeled as follows:

A) Manure;
B) Straw;
C) Compost;
D) Wood shavings; and
E) Combination of the other carbon sources.

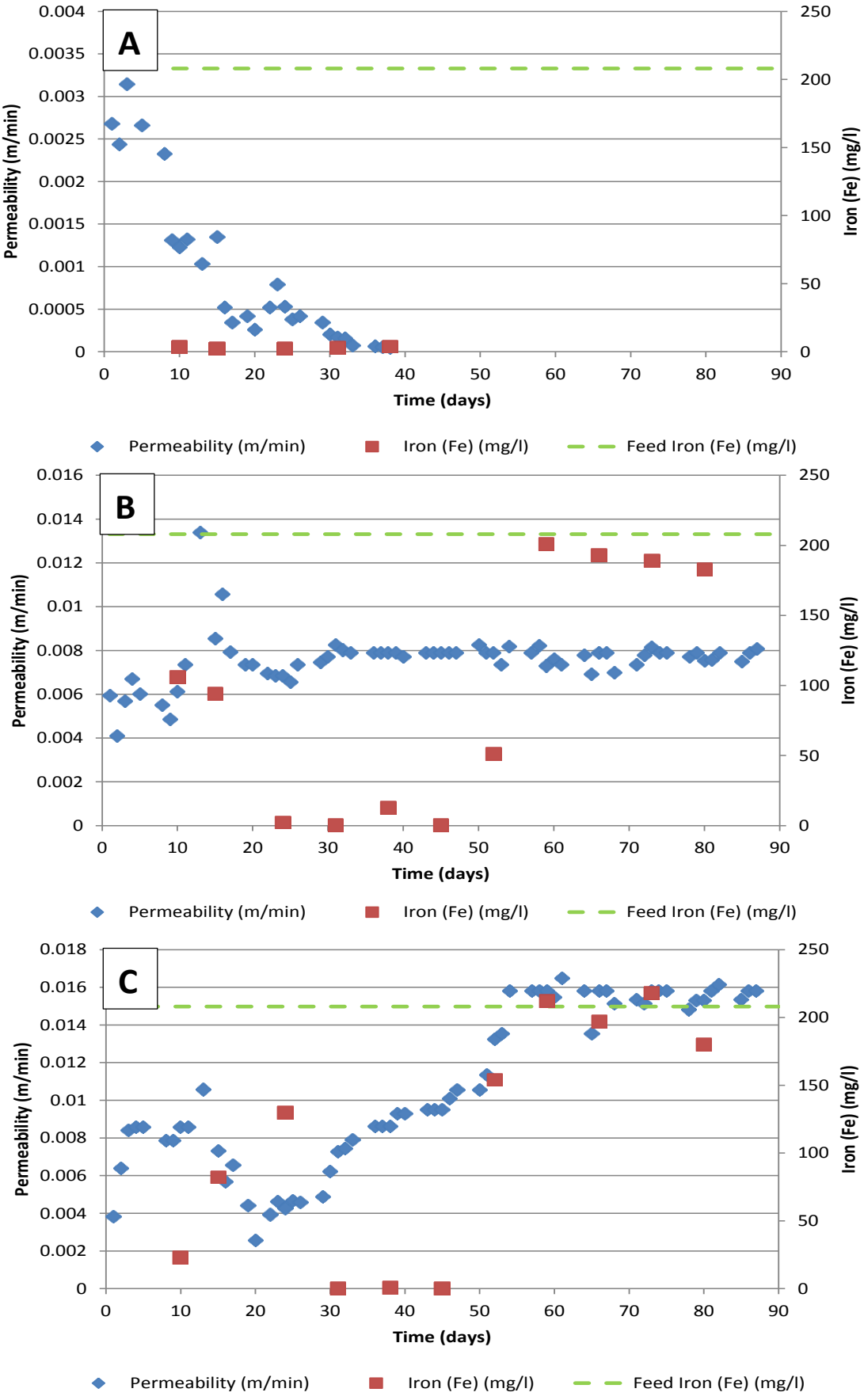

Figure 36: Permeability versus iron removal, for A-Manure, B-Straw and C-Compost

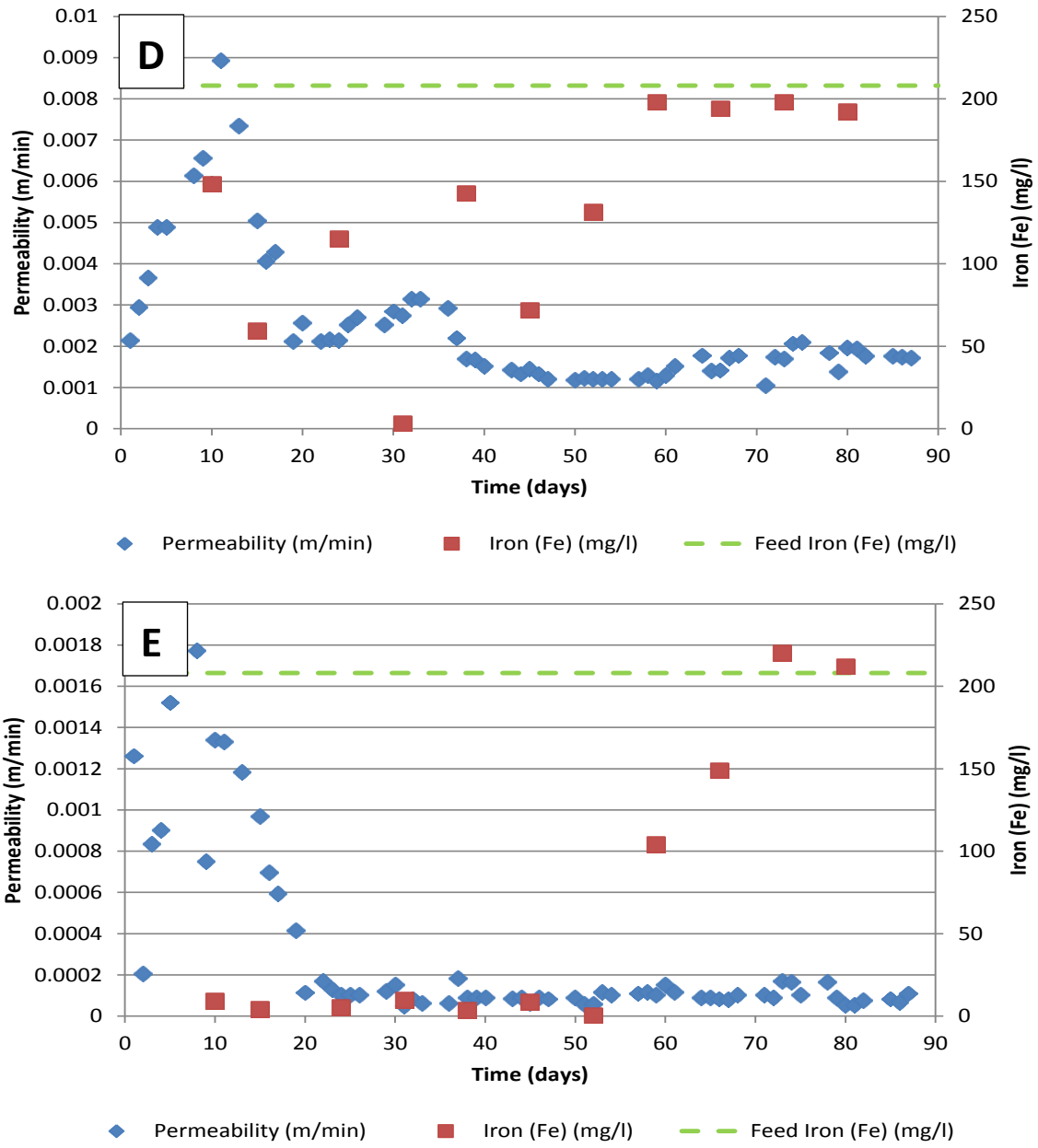

Figure 37: Permeability versus iron removal, for D-Wood shavings and E-Combined sample

The green dotted line in graphs A though E (Figure 36 and 37) indicates the initial level of iron in the fed synthetic AMD (210 *mg/l*). The blue points indicate the permeabilities of the carbon sources in (*m/min*) and the red points are the weekly iron samples in (*mg/l*) for each carbon source.

Two distinct points are highlighted in graphs A through E namely:

- Optimal iron removal point: This point indicates the time taken before the largest amount of iron to be removed from the fed AMD;

- Point at which iron is no longer removed: This is a point in time when the water exiting the bioreactor matches the AMD entering the bioreactor, thereby indicating no further iron removal.

Table 5: Optimal iron removal point and final iron removal point

Carbon Source	Optimal iron removal point	Point at which iron is no longer removed
Manure-A	Day 15	Clogged before reaching 210*mg/l*
Straw-B	Day 31	Day 59
Compost-C	Day 31	Day 59
Wood shavings-D	Day 31	Day 59
Combination-E	Day 15	Day 73

The manure (graph A) only has data up to day 38, because at this point the bioreactor was completely clogged. The manure bioreactor removed iron virtually from the start of the experiment. Day 15 was the manure's optimal iron removal point, as 98 % of the iron in the fed AMD was removed. The bioreactor clogged before further samples were taken. At the optimal iron removal point, on day 15, the permeability of the bioreactor was 0.0013 *m/min* for the manure. After this optimal point, the bioreactor started to clog and the iron removal remained constant until the bioreactor clogged.

The straw (graph B) did not fully clog over the life span of the experiment. The straw bioreactor, at day 24, started showing iron removal rates in excess of 98.8% of the sample feed. Day 31 was the straw's optimal iron removal point as 99 % of the iron in the fed AMD was removed. Thereafter, the outlet concentration of iron started to trend towards the initial feed of 210 *mg/l*. The straw sample exiting the bioreactor was the same as the fed AMD entering the bioreactor at day 59. Minimal iron was removed thereafter. Subsequent, samples plotted just below the 210 *mg/l* feed AMD mark. At the optimal iron removal point on day 31, the permeability of the bioreactor was at the straw's stabilised permeability of 0.0076 *m/min*. The straw bioreactor never clogged over the experimental lifespan but reached a stabilised permeability.

The compost (graph C) also did not fully clog over the life span of the experiment but increased in permeability up to its stabilisation point. The compost bioreactor, at day 31, had lowered the

iron by 99%. Day 31 was the compost's optimal iron removal point as 99% of the iron in the fed AMD was removed. At day 52, the iron load started to trend towards the initial feed of 210 *mg/l*. Subsequent samples plotted around the 210 *mg/l* feed AMD mark. At the optimal iron removal point on day 31, the permeability of the bioreactor was increased towards its stabilisation point.

The wood shavings (graph D) did not fully clog over the life span of the experiment. The wood shavings' iron graph was highly variable, with a wide spread of exit iron readings plotted on the graph. The wood shavings bioreactor, at day 31, had lowered the iron by 98% (this was the best of the plotted data points), therefore making day 31 the wood shavings optimal iron removal point. Thereafter, the outlet concentration of iron started to trend towards the initial feed of 3100 *mg/l*. At day 59, the wood shaving samples exiting the bioreactor was the same as the AMD entering the bioreactor. Minimal iron was removed. Subsequent samples plotted just below the 210 *mg/l* feed AMD mark. At the optimal iron removal point on day 31, the permeability of the bioreactor was decreasing toward its stabilisation permeability. The wood shavings bioreactor never clogged over the experimental lifespan but reached a stabilised permeability.

The combination bioreactor (graph E) did not fully clog over the life span of the experiment. The combination bioreactor, at day 15, had lowered the iron by 98%. Day 15 was the combination bioreactor's optimal iron removal point as 98 % of the iron in the feed AMD was removed. This high iron removal rate continued up to day 52. Thereafter the outlet concentration of iron started to trend towards the initial feed of 3100 *mg/l*. At day 73, the combination reactor's sample exiting the bioreactor was the same as the AMD entering the bioreactor. No further iron was removed. The subsequent sample plotted around the 210 *mg/l* feed AMD mark. At the optimal iron removal point on day 15, the permeability of the bioreactor was decreasing toward its stabilisation permeability. The combination bioreactor never clogged over the experimental lifespan but reached a stabilised permeability. The overall stabilisation permeability for the combination bioreactor was quite low.

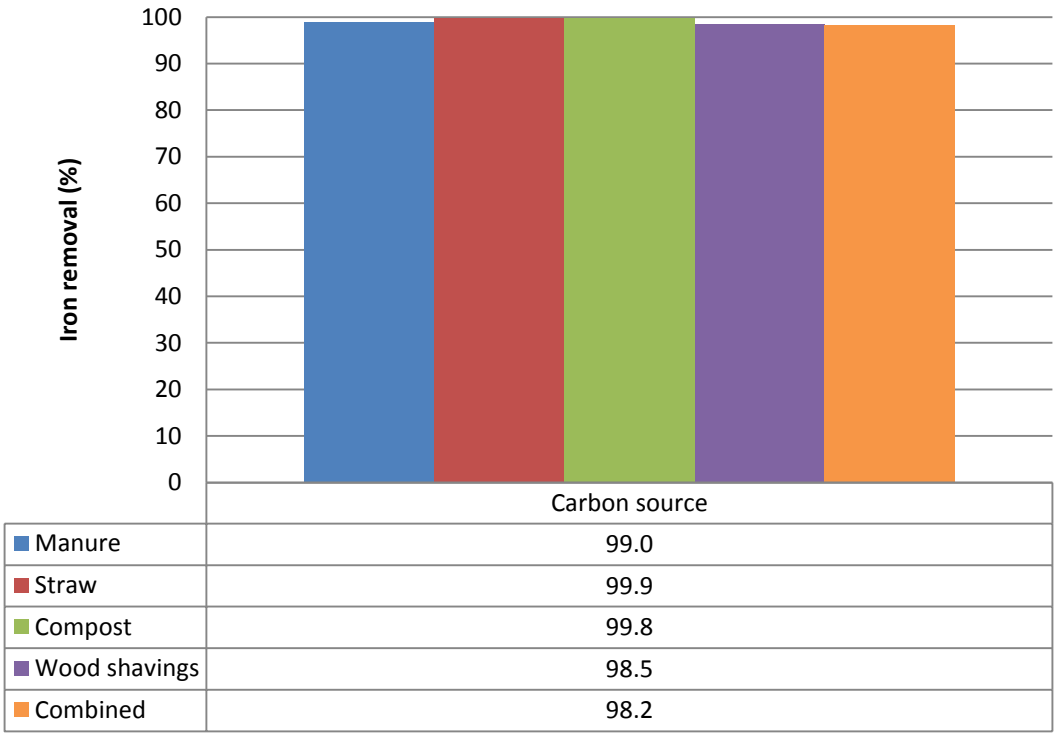

	Carbon source
Manure	99.0
Straw	99.9
Compost	99.8
Wood shavings	98.5
Combined	98.2

Figure 38: The percentage of iron removed at the optimal iron removal points for all the carbon sources

As seen in Figure 38, all of the carbon sources removed between 98 and 100 % of the iron from the AMD. Straw and compost removed the highest percentage of iron with 99.9%, and the combined bioreactor the least iron, with 98.2% iron removal. The point in time at which these optimal iron removal points accrued, varied between the carbon sources, with manure and the combined bioreactor being approximately 15 days after initiation of the experiment and the rest of the bioreactors after 31 days from the start of the experiment. All of the carbon sources did well at removing iron from the AMD.

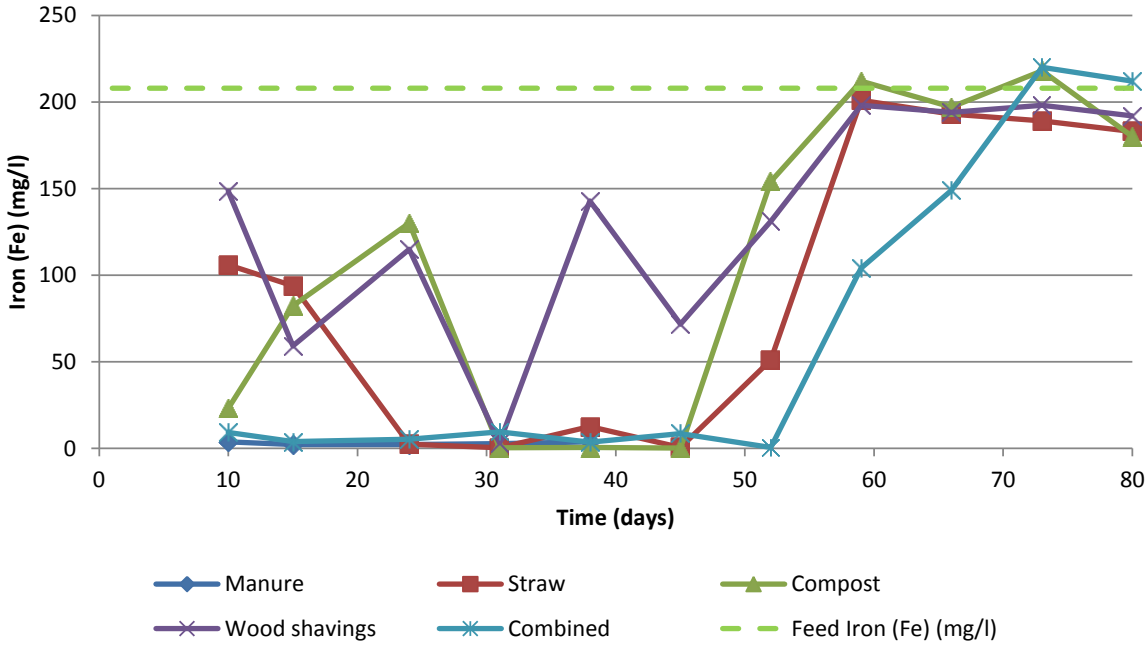

Figure 39: Iron break through curves for all carbon sources

As seen in Figure 39, manure and the combined bioreactor continuously removed large quantities of iron from the fed AMD (they had the longest periods of high iron removal). Straw and compost also removed iron effectively but only for a short period of time before it moved back to the initial feed value of 210 *mg/l*. The wood chips bioreactor values were scattered on the graph but an identifiable trend could be observed. The combined carbon sources' breakthrough point on the graph was far superior to the other carbon sources at day 73 after initiation of the experiment.

5.5.6 Permeability versus iron removal of bioreactors discussion

From an iron removal perspective, manure and the combination bioreactor were the best materials to use within a DPBR, as they removed 98 and 100% of the iron from the feed AMD for a prolonged period of time (38 and 52 days respectively). All of the bioreactors fell within a narrow range of 98 and 100% iron removal rate. Therefore, the overall average iron removal of the carbon sources in the bioreactors was about 98%. The iron gets precipitated in the carbon source during the chemical reaction with the SRB. This precipitation of iron is one of the mechanisms which clog the bioreactors.

When one looks at permeability variables in addition to iron removal, manure is no longer the best carbon source to use, as it clogged the quickest out of the carbon sources. The combined bioreactor (which removed the lowest amount of iron) and the straw bioreactors allowed for a

longer period of iron removal as they only reached the point at which no further iron was removed on days 59 and 73 respectively.

Compost would be recommended for use in the DPBR due to its high permeability and close to 99.8% iron removal rate. However, compost's breakthrough curve showed that its optimal iron removal period was the quickest out of the carbon sources, starting on day 31 and ending at day 45.

Straw could be recommended for use in the DPBR, as it has high stabilisation permeabilities, as well as having iron removal of close to 99.9%. Straw's breakthrough curves were also more than 59 days. Therefore, straw allowed a high constant amount of AMD to flow through the carbon sources, without the carbon source completely clogging over the experimental lifespan.

The combined bioreactor had removal rates in excess of 99% of the sample feed as well as having a prolonged time span of 73 days. However, the very low permeabilities that were observed from the onset are not preferred.

5.5.7 Permeability versus pH adjustment of reactors results

Following previous comparisons between permeability and sulfate, as well as iron reduction results, the permeability of each bioreactor was plotted against the pH exiting in each bioreactor. Samples of AMD exiting the five bioreactors were taken on a weekly basis. No samples were taken for the chicken litter bioreactor as this bioreactor clogged before the first sample stage.

The results for the remaining carbon sources can be seen in (Figure 40 and 41) and are labeled as follows:

A) Manure;
B) Straw;
C) Compost;
D) Wood shavings; and
E) Combination of the other carbon sources.

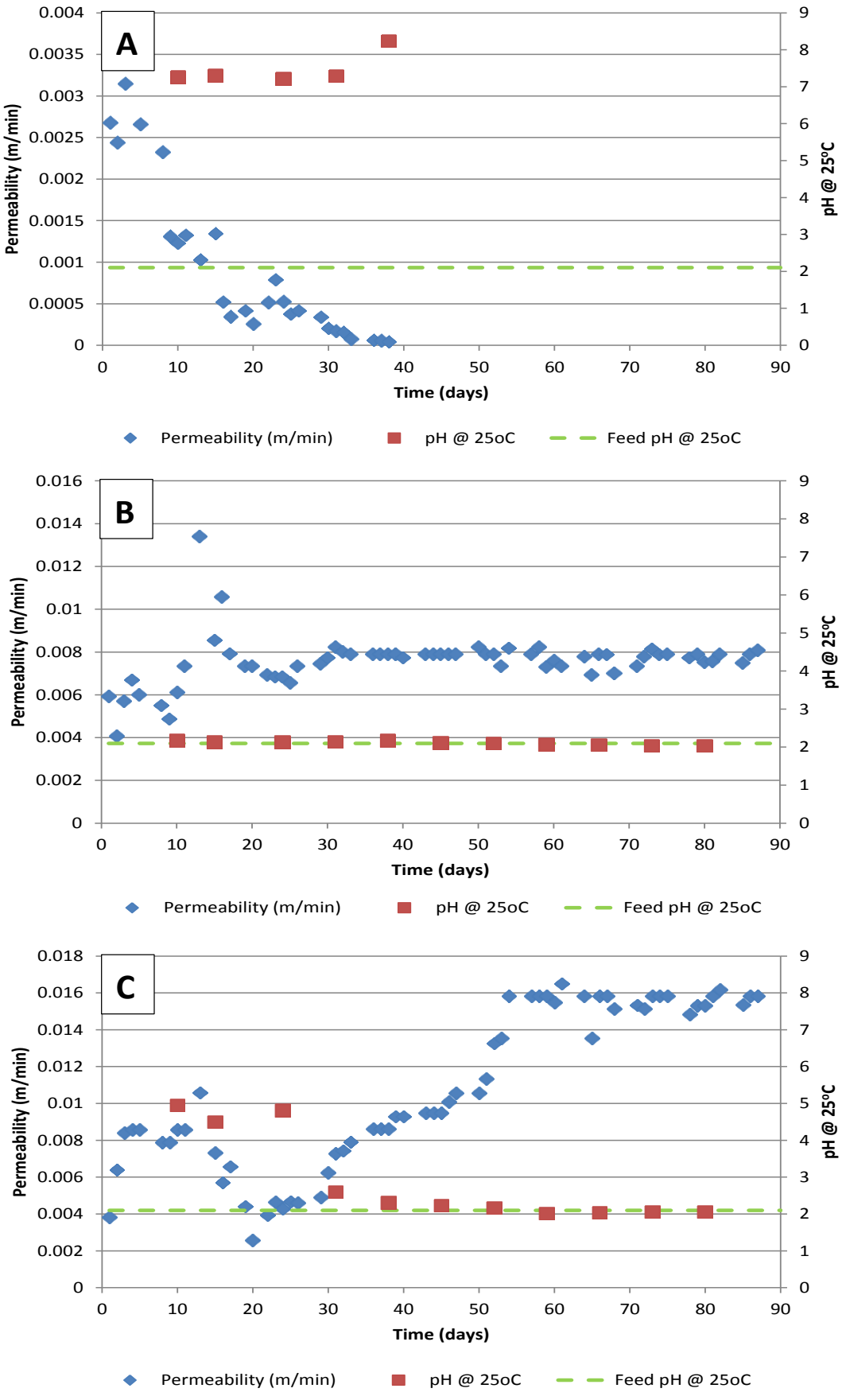

Figure 40: Permeability versus pH adjustment, for A-Manure, B-Straw and C-Compost

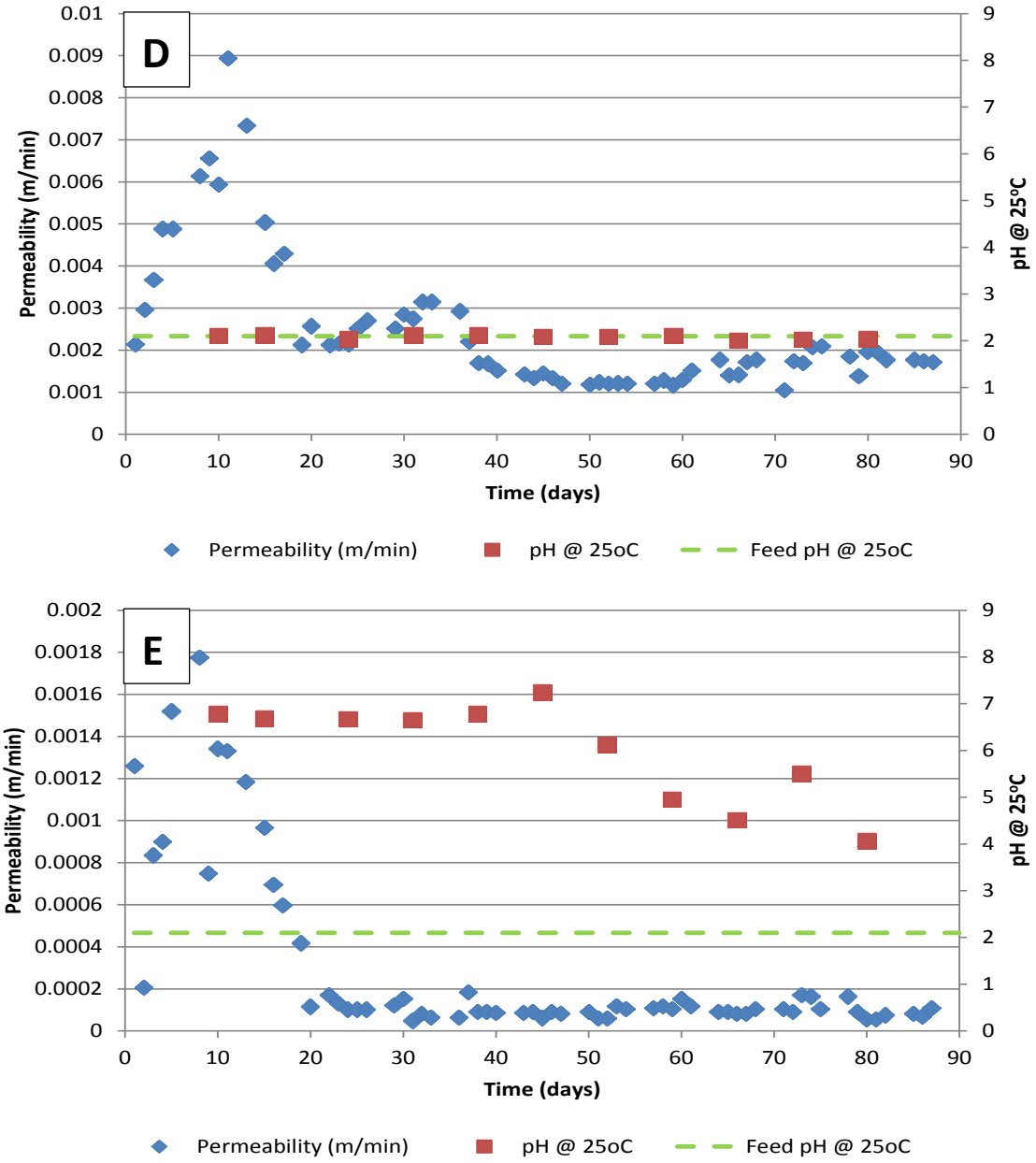

Figure 41: Permeability versus pH adjustment, for D-Wood shavings and E-Combined sample

The green dotted line in graphs A though E (Figure 40 and 41) indicates the initial pH level in the fed synthetic AMD (pH 2.1). The blue points in graphs A though E indicated the permeabilities in (*m/min*) and the red points are the weekly pH samples for each carbon source.

Two distinct points are highlighted in graphs A through E namely:

- Optimal pH point: This point indicates the time taken before the pH reached a natural condition from the original 2.1pH of the fed AMD;

- Point at which pH is no longer affected: This is a point in time when the pH exiting the bioreactor matches the fed AMD pH entering the bioreactor, thereby indicating no further change in the pH levels.

Table 6: Optimal pH point and the point at which pH is no longer affected

Carbon Source	Optimal pH point	Point at which pH is no longer affected
Manure-A	Day 10	Clogged before reaching a pH of 2.1
Straw-B	No effect on pH	Day 1
Compost-C	Day 10	Day 31
Wood shavings-D	No effect on pH	Day 1
Combination-E	Day 10	Day >80

The manure (graph A) only had data up to day 38 because at this point the bioreactor was completely clogged. The manure bioreactor increased the pH of the exit samples almost from the starting point of the experiment. The pH in the manure bioreactor remained around 7.3 until the bioreactor clogged.

The straw (graph B) did not fully clog over the life span of the experiment. The straw bioreactor had no influence on the pH of the AMD throughout the experiment, with most of the sample remaining at a feed pH of 2.1 throughout the experiment.

The compost (graph C) also did not fully clog over the life span of the experiment but increased in permeability until its stabilisation point. The compost bioreactor increased the pH from 2.1 to 4.8 at day 10. At day 31, the pH dropped back down to the feed pH of 2.1.

The wood shavings (graph D) did not fully clog over the life span of the experiment. The wood shavings bioreactor had no influence on the pH of the AMD throughout the experiment, with most of the sample remaining at a feed pH of 2.1.

The final combination bioreactor (graph E) did not fully clog over the life span of the experiment. The combination bioreactor increased the pH from 2.1 to 6.7 at day 10 (almost from the initiation of the experiment). Thereafter, the pH started trending towards the initial

fed AMD pH of 2.1. The exit AMD pH never reached the 2.1 initial feed pH mark in the 80 days of the experimental lifespan.

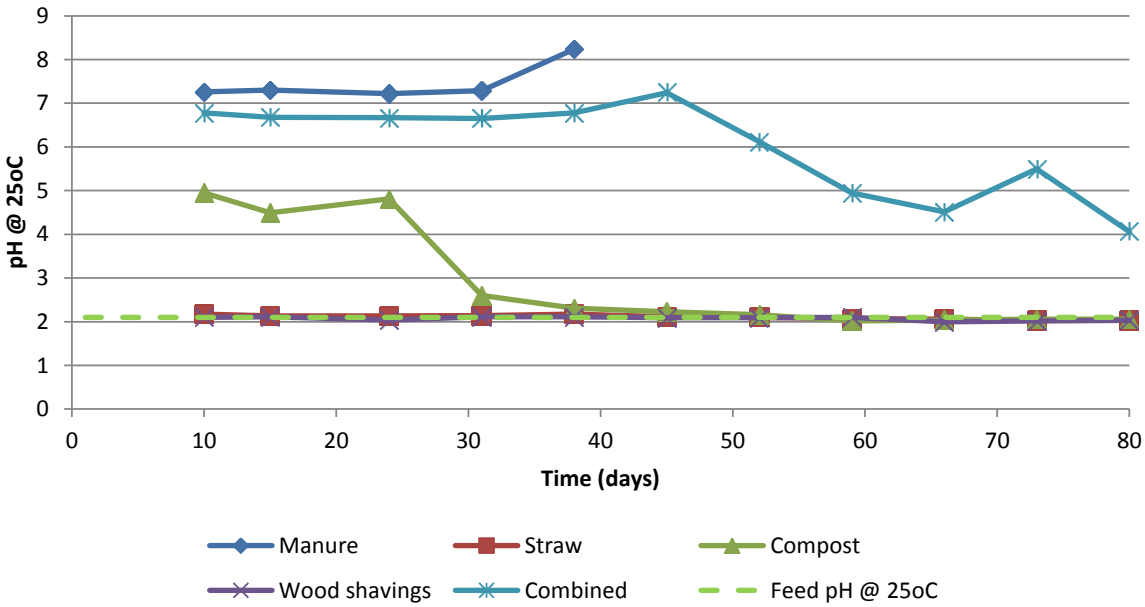

Figure 42: pH break through curves for all carbon sources

As seen in Figure 42, manure and the combined bioreactor increased the pH of the exiting AMD to values close to 7. Straw and wood shavings had no real effect on the pH, with compost increasing the pH for a period of one month before dropping back to the feed pH. Both the manure and the combined bioreactor increase the pH for the longest period of 40 and 50 days respectively. The combined bioreactor slowly started to lessen the pH from day 52 of the experiment.

5.5.8 Permeability versus pH adjustment of reactors discussion

When one looks at neutralizing the acidic AMD, manure is the best option to use in the DPBR. However, the fact that it clogged the quickest out of all the materials resulted in manure not being the ideal material to use. The combined bioreactor and the compost bioreactor allowed for increasing of the pH for a period of 52 days and 31 days respectively.

Compost is recommended for use in the DPBR, as it has high stabilisation permeabilities, as well as having a 56% increase in the AMD pH. The compost's breakthrough curve point was at day 31. Therefore, compost allowed a high constant amount of AMD to flow through the carbon sources, without the carbon source completely clogging over the experimental lifespan.

The combined bioreactor had superior neutralizing effects over a prolonged time span of 52 days and did not ever drop below the feed pH of 2.1. However, its very low permeabilities from the onset are not preferred.

5.6 Discussion

The findings presented in this work consistently demonstrate four things:

1. Manure is always highly effective in terms of pH improvement, sulfate removal and iron removal. However this is always at the expense of permeability, since the packing clogs very rapidly;
2. Compost and straw have excellent permeabilities which do not change significantly over very long timeframes. This is, however, at the expense of the remedial ability of the packing. In other words, compost and straw breakthrough too rapidly in terms of sulfate, iron and pH behaviour;
3. The combined reactor, in every instance, offered a good compromise between these different behaviours; and finally
4. The permeabilities of the carbon sources played a larger role in the efficacy of the bioreactor than their chemical treatment ability.

Manure has lots of Sulfure Reducing Bacteria (SRB) since it comes from ruminant guts. This means that SO_4^{2-} rapidly increases. Typically this is accompanied by a rise in pH as SO_4^{2-} is the conjugate base of H_2SO_4. This causes iron to precipitate; this system is thus a victim of its own success because a rapid pH increase leads to clogging. In other systems, SRB are not as prevalent and hence a rapid pH increase and subsequent iron precipitation and clogging are not observed to the same extent.

It would appear that the manure adds an inoculum of the correct bacteria for high chemical removal and pH improvement, especially into the combined based reactors. This information is very useful for design purposes.

6. CONCLUSION

In this dissertation, the permeabilities as well as the treatment potential (in terms of sulfate removal, iron removal and pH correction) of various carbon sources were determined over a period of three months. The different carbon sources were chosen as they would make up the typical packing in a DPBR. All of the carbon sources were typical waste products, thereby making them ideal in treating waste water.

Clogging in these carbon sources lessen the amount of AMD that came into contact with SRB in the DPBR, thereby reducing the efficiency of the bioreactor. In two bioreactors (manure and chicken litter), clogging prevented all of the AMD from moving through the bioreactor, rendering the process obsolete and a possible environmental hazard.

The various carbon sources showed no significant difference in terms of sulfate and iron removal. The range between the best performing carbon source and the poorest performing carbon source, in terms of sulfate removal, was 17%. For iron removal, the range between the best and poorest performing carbon sources was only 2%. It was found that the permeability of the carbon sources played a larger role in the efficiency of the DPBR than the type of carbon source used. It was also important to note how the sulfate and iron decreased in time, as well as the period of time at which the sulfate and iron removal rates were at their optimum.

The pH correction of the AMD by the DPBR was reliant on the specific carbon source used. Straw and wood shavings had no real effect on the pH. Compost showed some pH correction. The manure bioreactor, as well as the combined bioreactor (due to the fact the combined bioreactor had one layer of manure in it) had a good neutralizing effect on the AMD.

Taking into consideration the following factors:

- The permeability of the carbon source and how it drops with time;
- The period of time the sulfate and iron removal rates were at their optimum; and
- The pH correction abilities of each carbon source,

The carbon sources which performed the best were the combined bioreactor and the compost.

Table 7: Carbon sources comparison table

	Permeability	Sulfate removal	Iron removal	pH neutralisation
Manure	Poor	Good	Good	Good
Straw	Good	Good	Good	Poor
Compost	Average	Good	Good	Average
Wood shavings	Good	Good	Good	Poor
Chicken litter	Poor	N/A	N/A	N/A
Combined bioreactor	Average	Good	Good	Good

As seen in Table 7, the combined bioreactor's weakness lies in its permeability. The stabilisation permeability in the combined bioreactor was quite low; this was due to the manure and chicken litter layers that were constituents of the combined bioreactor. Fortunately, the combined bioreactor also harnessed the positive attributes of the other carbon sources. With some refining, the permeability of the combined bioreactor could be improved.

Compost did not remove the same amounts of iron and sulfate as the combined bioreactor. However, compost had good permeability which allowed a lot of AMD to flow through the bioreactor. However, this could be due to short circuiting. Chicken litter was a very poor carbon source in the DPBR, as it clogged almost immediately. The use of chicken litter within the DPBR should therefore be avoided.

As discussed, it would appear that the manure adds an inoculum of the correct bacteria for high chemical removal and pH improvement, especially in the combined bioreactor. The combined bioreactor has the happy medium of manure with the correct inoculum of bacteria and highly permeably carbon sources to increase the permeability of the bioreactor.

6.1 DPBR repacking schedule

Since the purpose of the DPBR is to remove sulfates and iron, as well as to improve pH, the carbon source used within the DPBR needs to perform these functions well. When looking at the breakthrough curves for sulfate and iron removal, as well as for pH correction (Figure 35,

Figure 39 and Figure 42) by the various carbon sources, a pattern can be seen. Sulfate removal for all carbon sources occurs quite early in the experimental lifespan (from days 10 to 30).

Thereafter they trend towards the feed AMD quality of 3100*mg/l*. Iron removal starts from day 10 up to day 50 of the experiment for the preferred carbon source (the combined bioreactor). The pH neutralisation occurred almost from day 1 until day 50 of the experimental life span for the combined bioreactor.

If one looks at the iron and sulfate removal rates, as well as when they occurred in the experimental lifespan, sulfate removal appeared to be the limiting factor, as the optimal sulfate removal band occurs early in the experimental lifespan. Sulfates also seem to diminish before the iron removal band. Its optimal sulfate removal point is between days 10 and 30, whereas iron and pH seem to have a longer optimal zone of just more than 50 days, for the best performing bioreactors.

From the main experiment, it was found that the carbon source within the reactor would need to be removed and repacked every 30 days. This would be needed for the bioreactor to function optimally and remove 50% of the sulfates and 98% of the iron, as well as for it to neutralize the pH to about seven.

6.2 Design guidelines

To design a hybrid passive water treatment chain, each link in the water treatment process must first be fully understood. In this dissertation, two key areas in the DPBR were quantified. The first area identified was to understand the permeabilities and porosities of combined organic layers within the DPBR. The second area was to understand when the DPBR has to be repacked. This was done by determining how long it took for the carbon sources to clog the bioreactor and whether this occurred before or after the carbon in the bioreactor had been depleted. In addition to these areas, this dissertation went one step further and determined the optimal time range for sulfate and iron removal, as well as for pH neutralisation. The permeabilities and porosities of the composite organic layers were determined and an indication on when the DPBR should be repacked was understood to compile this basic design guideline for the DPBR.

It must be noted that the results from this dissertation were obtained from small-scale bench tests and further pilot and full scale studies should be investigated. The following key guidelines should be followed in the preliminary design of the DPBR:

- Chicken litter should be avoided as a carbon source;
- Manure as a single carbon source should also be avoided;
- Single carbon sources should be avoided;
- A combination bioreactor would be the preferred design strategy as it displayed the best properties of all the different trials presented here;
- The DPBR should be packed in layers of different carbon sources, with varying effective porosities; and
- If the permeability of the combination bioreactor is not improved, the DPBR should be repacked 30 days after initiation of the water treatment.

6.3 Future work

The permeability of the combined bioreactor could improve. Attributes such as chemical removal and permeability could be designed into the system by varying the thickness, combinations and mixtures of the different carbon sources. Looking at the results of this dissertation, the researcher would start by investigating the different ratios of manure and compost to be used for optimization of the system.

Further literature topics could summarize the different passive water treatment technologies and rank there efficacy with which they treat certain pollutants. This would help both mining houses and designers with the first options analysis process, regarding the different water treatment options that can be utilized. The research could be expanded to determine the capital expenditure, as well as the operational expenditure of each treatment technology. In doing this research, designers and mining houses would gain an overview of the technologies that could be used, as well as the capital and operational expenditures involved in the implementation and running of specific treatment technologies.

7. REFERENCES

25 Years of Safe Drinking Water Act: History and Trends. (1999). Environmental Protection Agency.

2013 World Population Data Sheets. (2013, September/15/2014). Retrieved from http://www.prb.org/pdf13/2013-population-data-sheet_eng.pdf

Albright, L. F. (2009). *Albright's Chemical Engineering Handbook*: CRC Press.

Aspeling, B. (2015). Hybrid Water Treatment Chain: Golder Associates.

Ávila, C., Bayona, J. M., Martín, I., Salas, J. J., & García, J. (2015). Emerging organic contaminant removal in a full-scale hybrid constructed wetland system for wastewater treatment and reuse. *Ecological Engineering, 80*, 108-116.

Ávila, C., Garfí, M., & García, J. (2013). Three-stage hybrid constructed wetland system for wastewater treatment and reuse in warm climate regions. *Ecological Engineering, 61, Part A*, 43-49.

Baker, M. N. (1981). *The Quest for Pure Water*: American Water Works Association.

Blowes, D. W., Robertson, W. D., Ptacek, C. J., & Merkley, C. (1994). Removal of agricultural nitrate from tile-drainage effluent water using in-line bioreactors. *Journal of Contaminant Hydrology*(15), 207-221.

Blumberg, B., Cooper, D., & Schindler, P. (2005). *Business research methods*. Berkshire: McGraw-Hill Education.

Brix, H., Arias, C., & del Bubba, M. (2001). Media selection for sustainable phosphorus removal in subsurface flow constructed wetlands. *Water Science and Technology, 44*(11-12), 47-54.

Cameron, S. G., & Schipper, L. A. (2012). Hydraulic properties, hydraulic effiency and nitrate removal of organic carbon media for use in denitrification beds. *Ecological Engneering*(42), 1-7.

Chun, J. A., Cooke, R. A., J.W, E., & Kang, M. S. (2009). Estimation of flow and transport parameters for woodchip-based bioreactors: 1. Laboratory-scale bioreactor. *Biosystems Engineering*, *I*(04), 384-395.

Coetser, S. E., Molwantwa, J., Heath, R., & Pulles, W. (2004). *Implementing the integrated passive treatment system (IMPI) technology at the VCC passive treatment plant*, Cape Town.

CSIR. (2010). *A CSIR perspective on water in South Africa* (CSIR/NRE/PW/IR/2011/0012/A). Retrieved from CSIR Pretoria: www.csir.co.za/nre/.../CSIR%20Perspective%20on%20Water_2010.PDF

Fogler, H. (2005). *Elements of Chemical Reaction Engineering* USA: Prentice Hall.

Freedomina (Producer). (2015, 01/11/2015). World Water Treatment Products.

Gibb, J. P., Barcelona, M. J., Ritchey, J. D., & LeFaivre, M. H. (1984). *Effective Porosity of Geologic Materials*. Retrieved from State Water Survey Devision Illinois: www.isws.illinois.edu/pubdoc/cr/iswscr-351.pdf

Gibert, O., Lefevre, B., Fernandez, M., Bernat, X., Paraira, M., Calderer, M., & Martinez-Llado, X. (2013). Characterising biofilm development on granular activated carbon used for drinking water production. *Water Research*(47), 1101-1110.

Government Communication and Information System. (2011). Retrieved from Department of Water Affairs Pretoria: www.dwa.gov.za/nwrs/LinkClick.aspx?fileticket=d-cvjKg1IJI%3D&tabid=72&mid=435

Greenan, D. M., Moorman, T. B., Kaspar, T. C., Parkin, T. B., & Jaynes, D. B. (2006). Comparing carbon substrates for denitrification of subsurface drainage water. *Journal of Environmental Quality*(35), 824-829.

Guiping, F., Zhang, J., Chen, W., & Chen, Z. (2013). Medium clogging and dynamics of organic matter accumulation in constructed wetlands. *Ecological Engineering*(60), 393-398.

Gusek, J. J. (2008). *Passive Treatment 101: An Overview of Technologies*. Paper presented at the U.S. EPA/National Groundwater Association's Remediation of Abandoned Mine Lands Conference, Denver.

Heimbuch, J. (Producer). (2010). Treehugger. Retrieved from www.treehugger.com

Hengen, T. J., Squillace, M. K., O'Sullivan, A. D., & Stone, J. J. (2014). Life cycle assessment analysis of active and passive acid mine drainage treatment technologies. *Resources, Conservation and Recycling, 86*, 160-167.

Hiscock, K. (2005). *Hydrogeology Principles and Practice*. Australia: Blackwell Publishing.

Hobbs, P., & Kennedy, K. (2010). *Acid mine drainage: addressing the problem in South Africa* (CSIR/NRE/WR/IR/2011/0029/A.). Retrieved from CSIR Pretoria: www.csir.co.za/nre/.../CSIR%20Perspective%20on%20Water_2010.PDF

Iliuta, I., & Larachi, F. (2005). Modelling simultaneous bilogical clogging and physical plugging in trickel-bed bioreactors for wastewater treatment. *Chemical Engineering Science*(60), 1477-1489.

Johnson, B. D., & Hallberg, K. B. (2002). Pitfalls of passive mine water treatment. *Environmental Science and Bio Technology*(1), 335-343.

Knowles, P. R., Griffin, P., & Davies, P. A. (2010). Complementary methods to investigate the development of clogging within a horizontal sub-surface flow tertiary treatment wetland. *Water Research*(44), 320-330.

Langergraber, G. (2005). The role of plant uptake on the removal of organic matter and nutrients in subsurface flow constructed wetlands: a simulation studey. *Water Science Technology, 9*(51), 213-224.

Leedy, P. D., & Ormrod, J. E. (2014). *Practical Research Planning and Design*. Essex: Pearson Education Limited.

Lightbody, A. F., Nepf, H. M., & Bays, J. S. (2009). Modeling the hydraulic effect of transverse deep zones on the performance of short-circuiting constructed treatment wetlands. *Ecological Engineering, 35*(5), 754-768.

Lynch, S. (2004). *Development of a Raster Database of Annual, Monthly and Daily Rainfall for Southern Africa* (1156/1/04). Retrieved from Water Research Council, South Africa: www.wrc.org.za/knowledge%20hub%20documents/research%20reports/1156-1-04.pdf.

McCarthy, T. S. (2011). The impact of acid mine drainage in South Africa. S Afr J Sci. 107(5/6), Art. #712, 7 pages.

McCauley, C. A., O'Sullivan, A. D., Milke, M. W., Weber, P. A., & Trumm, D. A. (2009). Sulfate and metal removal in bioreactors treating acid mine drainage dominated with iron and aluminum. *Water Research, 43*(4), 961-970.

Mitsch, W. J., & Gosselink, J. G. (2007) *Wetlands*. New Jersey: John Wiley & sons, Inc.

Muller, B. (2013). Water Treatment Active vs Passive: Golder Associates.

Muller, B. (2014). Water Treatment Decision Tree: Golder Associates.

National Water Resource Strategy 2. (2013). Retrieved from Department of Water Affairs Pretoria: www.dwa.gov.za/nwrs/NWRS2013.aspx

Neculita, C.-M., Zagury, G. J., & Bussière, B. (2008). Effectiveness of sulfate-reducing passive bioreactors for treating highly contaminated acid mine drainage: I. Effect of hydraulic retention time. *Applied Geochemistry, 23*(12), 3442-3451.

Nemec, D., & Levec, J. (2005). Flow through packed bed reactors: 1 Single-phase flow. *Chemical Engineering*(60), 6947-6957.

Overview of the South African Water Sector. (n.d.). Retrieved from Department of Water Affairs Pretoria: www.dwa.gov.za/io/Docs/CMA/CMA%20GB%20Training%20Manuals /gbtrainingmanualchapter1.pdf.

Clog. (2015). In *Oxford Dictionaries*. Retrieved from: www.oxforddictionaries.com /definition/english/clog

Pinetown, K. L., Ward, C. R., & van der Westhuizen, W. A. (2007). Quantitative evaluation of minerals in coal deposits in the Witbank and Highveld Coalfields, and the potential impact on acid mine drainage. *International Journal of Coal Geology, 70*(1–3), 166-183.

Pozo-Morales, L., Franco, M., Garvi, D., & Lebrato, J. (2014). Experimental basis for the design of horizontal subsurface-flow treatment wetlands in naturally aerated channels with an anti-clogging stone layout. *Ecological Engineering, 70*, 68-81.

Pulles, W., Coetser, L., Heath, R., & Muhlbauer, R. (2004). *Development of high-rate passive sulphate reduction technology for mine waters*, Newcastle.

Pulles, W., & Meyer, D. (2012). *Vryheid Coronation Colliery: Passive Mine Water Treatment*. Retrieved from Golder Associates Library: www.golder.com

Pulles, W., & Rose, P. D. (2002). South Africa Patent No. US 7306732 B2.

Scheidegger, A. E. (1974). *The Physics of Flow Through Porous Media*. University of Toronto Press

Shaw, S. P., & Fredine, C. G. (1956). Wetlands of the United States-Their extent and their value to waterfowl and other wildlife. *Fish and Wildlife Services Circular, 39*, 67.

Sheridan, C. M. (2012). Chemical Enginering Modelling of a vegitated submerged reeded bed for winery effluent treatment.

Tukac, V., & Hanika, J. (1992). Influence of catalyst particles orientation on the pressure drop and the liquid dispersion in the trickle bed reactor. *Chemical Engineering Science*(47), 2227-2232.

UNEP. (2002). *Global Environment Outlook 3*. London: Earthscan Publications Ltd.

UNEP. (2010). *Africa Water Atlas*. Division of Early Warning and Assessment (DEWA). United Nations Environment Programme (UNEP). Nairobi, Kenya.

Van Loosdrecht, M. C. M., & Heijnen, S. J. (1993). Biofilm bioreactors for waste-water treatment. *Trends in Biotechnology, 11*(4), 117-121.

Velten, S., Boller, M., Koster, O., Helbing, J., Weilenmann, H., & Hammes, F. (2011). Development of biomass in a drinking water granular active. *Water Research*(45), 6347-6354.

Villholth, K. G., & Jensen, K. H. (1998). Flow and transport processes in a macroporous subsurface-drained. *Journal of Hydrology*(207), 121-135.

Vymazal, J. (2014). Constructed wetlands for treatment of industrial wastewaters: A review. *Ecological Engineering, 73*, 724-751.

Wang, Y., Song, X., Liao, W., Niu, R., Wang, W., Ding, Y., Yan, D. (2014). Impacts of inlet–outlet configuration, flow rate and filter size on hydraulic behavior of quasi-2-dimensional horizontal constructed wetland: NaCl and dye tracer test. *Ecological Engineering, 69*, 177-185.

Water Quotes and Facts. (1999). Retrieved from www.jperret.tripod.com

Wichern, M., Lindenblatt, C., Lubken, M., & Horn, H. (2008). Experimental results and mathematical modelling of an autotrophic and hetrotrophic biofilm in a sand filter treating landfill leachate and municipal wastewater. *Water Research*(42), 3899-3909.

Wildman, T. A. (2002). *Design of field-scale bioreactor for bioremediation of nitrate-N in tile drainage effluent*. University of Illinois at Urbana-Champaign

Younger, P. C., Banwart, S. A., & Hedin, R. S. (2002). *Mine Water: Hydraulogy, Pollution, Remediation*: Kluwer Academic Publishers.

Yu, T., Wu, Z. B., & Xu, D. (2006). Clogging characteristicsof the subsurface flow wetland. *Environmental Science Technology*(29), 74-76 (in chinese).

Zhang, C., Chen, R., Liao, Q., & Zhu, X. (2013). Simulation of bacterial locomotion and attachment in the interspaces of packed bed reactors. *International Journal of Hydrogen Energy, 38*(35), 15680-15685.

Zhao, L., Zhu, W., & Tong, W. (2009). Clogging processes caused by biofilm growth and organic particle accumulation in lab-scale vertical flow constructed wetlands. *Journal of Environmental Sciences, 21*(6), 750-757.

Zheng, Y., Wang, X., Xiong, J., Liu, Y., & Zhao, Y. (2014). Hybrid constructed wetlands for highly polluted river water treatment and comparison of surface- and subsurface-flow cells. *Journal of Environmental Sciences, 26*(4), 749-756.

Zidan, A. R. A., El-Gamal, M. M., Rashed, A. A., & El-Hady Eid, M. A. A. (2015). Wastewater treatment in horizontal subsurface flow constructed wetlands using different media (setup stage). *Water Science, 29*(1), 26-35.

8. APPENDICES

Appendix A WISA Bicentennial conference paper 2016

EFFICIENCY OF DEGRADING PACKED BED REACTORS

A. Botes[1,2], C. James[3] and C. Sheridan[1*]

[1]Industrial and Mining Water Research Unit (IMWaRU), School of Chemical and Metallurgical Engineering, University of the Witwatersrand, Johannesburg, South Africa

[2]Rehabilitation and Closure Division, Golder Associates

[3]School of Civil and Environmental Engineering, University of the Witwatersrand, Johannesburg, South Africa

*To whom all correspondence should be addressed craig.sheridan@wits.ac.za

In South Africa, the need for water treatment is increasing, especially in the mining sector. As active water treatment technologies are expensive, the mining sector has an increasing need for passive water treatment technology, with low maintenance and operating costs, yet efficient water treatment ability. Literature on passive water treatment suggests that these systems only offer a narrow range of treatment capabilities. Therefore, hybrid water treatment systems could be a solution to low-cost water treatment in South Africa. The Degrading Packed Bed Reactor (DPBR) is one of the units comprising the hybrid treatment group. The DPBR's main action is to convert sulfates into sulfides and alkalinity.

In this study, six small-scale DPBRs were constructed. Each was classified according to its unique organic source (manure, straw, vegetable food processing waste, wood shavings, chicken litter and a combined sample with layers of all the carbon sources). Synthetic Acid Mine Drainage (AMD) was fed through the six bioreactors for a period of three months. Permeabilities, leachate samples and effective void volumes were measured from the DPBRs.

From the experiments conducted, it was found that the manure and combination bioreactors (with equal layers of manure, straw, compost, wood shavings and chicken litter) had the lowest overall permeabilities, with straw and compost having the highest permeabilities. Linked to this, the experiments showed that the manure and combination bioreactors had the largest decreases in effective porosity with straw and compost having the least. Hydraulically, the combination bioreactor performed the best by incorporating the best attributes from each carbon source. Wood shavings preformed almost as well. Chicken litter clogged within 18 days after the initiation of the experiment and thus was the least effective substrate.

1) INTRODUCTION

In South Africa, the need for water treatment is increasing, especially in the mining sector. As active water treatment technologies are expensive, the mining sector is in need of a passive water treatment technology, with low maintenance and operating costs, yet efficient water treatment ability (1). Literature on passive water treatment suggests that these systems only offer a narrow range of treatment capabilities. Hybrid water treatment systems could therefore be the solution to low cost water treatment in South Africa (2).

Hybrid systems combine treatment processes from both active and passive water treatment systems, utilising the most suitable and cost effective processes from each (3). Hybrid systems use a segmented approach to treat water and are tailor-made to treat a specific pollution cocktail by targeting a specific pollutant at a specific position in the treatment chain. Although such systems have high initial Capital Expenditure (CAPEX) costs to set up the treatment chain, they can save money on long-term operation and maintenance costs (2, 3).

In order for hybrid systems to become a widely used and trusted water treatment technology, existing knowledge gaps must be addressed by research. Hybrid systems also need to be tested in pilot- and full-scale experiments (4) before they system can be fully understood. There are numerous areas within the hybrid treatment system with very little or no information about them. These areas need to be studied and optimized.

A promising hybrid treatment technology is the Degrading Packed Bed Reactor (DPBR) (5). The DPBR's main action is to convert sulfates into sulfides and alkalinity. It achieves this by allowing sulfate rich water to trickle through layers of different types of organic matter as shown in **Figure 1**. The organic matter donates electrons to the Sulfate Reducing Bacteria (SRB), and thus the sulfates are reduced to sulfides. This chemical process is well documented in journal articles (6, 7) and is summarized in Equation 1 (8, 9).

$$2CH_2O + {SO_4}^{2-} \leftrightarrow 2CHO_3{}^{-} + H_2S\ (\text{g or aq}) \qquad [1]$$

Although the chemical process is well understood, the hydraulics of such a system remains unclear. The hydraulic processes occurring within a DPBR (or indeed any other reactor) are important to understand as they dictate the time available for reaction.

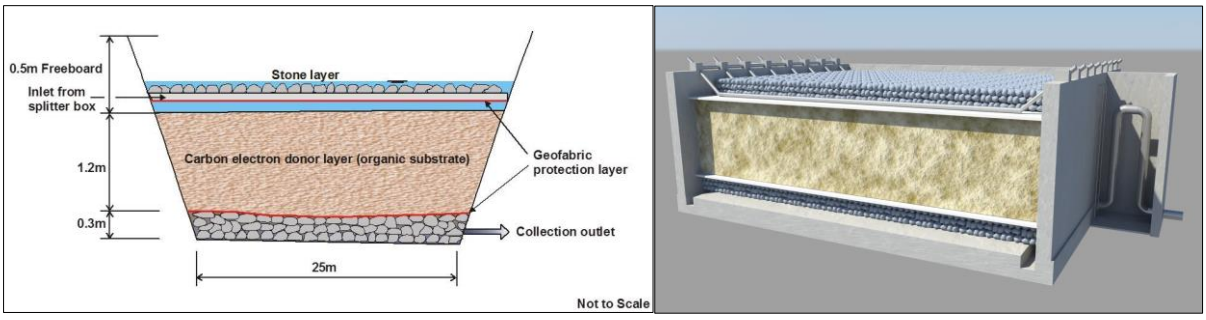

Figure 1: DPBR render

In order to maximise the remediation potential of the DPBR to treat polluted water, engineers and scientists need to understand the hydraulics behind the system. Polluted water is fed through a trickle system, onto the organic matter. The polluted water needs to remain in contact with organic matter long enough for the reaction to take place, yet not too long for it to have cost implications. Porosity is one of the key drivers in DPBR hydraulic performance. Porosity is the space around the organic media which allows the water to move through the organic matter. As the porosity drops, the amount of possible space around the organic matter is reduced; this in turn reduces the hydraulic performance.

A key term in understanding porosity is effective porosity (ϕ) [2]. "*Effective porosity is defined as the ratio of the interconnecting pore volume to the total volume of the medium" (10)*. Another less technical definition from Gibb et al is that effective porosity is the number of pore spaces which allow water to move freely through the organic material (11). Over time in the DPBR, biofilm growth as well as metal precipitation starts reducing the effective porosity of the bioreactor as the biofilm grows into the void and similarly, metals precipitate into the void.

Although there are numerous publications on the topic of porosity and various mathematical models aiming to predict the porosity of several materials, there is very little information on the porosities of organic materials. The limited research that has been done on the porosities and permeabilites of organic materials looks at flow and transport parameters in a woodchip based bioreactor (12). Chun and colleagues' research mainly focuses on a single, uniformly graded organic material. Very little is known about the general permeability and porosity values of organic materials such as kraal manure, straw, vegetable food processing waste (compost), wood shavings, chicken litter and a composite sample consisting of equal layers of all of the above carbon sources (5), all of which can be used as packing within a DPBR.

The true value of the DPBR lies in its utilisation of waste material (the organic sources described above) to treat waste water. The DPBR has numerous layers of these materials, placed on top of one another.

For design purposes, it is important to understand the flow rate through the DPBR; clogging of the bed could have significant impacts downstream, of the process. It would be incorrect to design a DPBR for the initial flow through the multiple layers of organic materials because the multiple layers are of varying size, shape, packing and porosity (13). One of the biggest parameters that influence the flow of water through constructed wetlands is clogging (14) as cited in Guiping and colleagues (15) and this effect all so occurs in DPBRs. In recent years there has been more investigation into clogging in published research as a result of the importance of this phenomenon (16).

Guiping et al (15) as well as Zhao et al (17) describe clogging as an extremely intricate process which is not yet well understood. The clogging phenomenon therefore contains large gaps of knowledge for future research.

Clogging can occur through two broad methods: clogging by mechanical mechanisms and clogging through biological mechanisms. During clogging by mechanical mechanisms, solid particles in the treated water get lodged between the organic materials, reducing the organic materials' effective porosity. This process is also known as plugging (18). Biological clogging occurs through the growth of

biofilms. Biofilms grow naturally in most ecosystems where micro-organisms are found on solid surfaces. In unfavourable systems, biofilms tend to consist of a single layer of attached cells. However, in favourable, high nutrient environments such as constructed wetlands and bioreactors, biofilm growth tends to be more extensive (19). The biofilm grows in and around the organic media in the DPBR, and thereby reduces its effective porosity and hydraulic efficiency.

To design a hybrid water treatment process, each step in the water treatment process must be fully understood. The DPBR has two clear knowledge gaps. The first gap that needs to be understood includes the permeabilities and porosities of combined organic layers. The second gap that needs to be understood is at what point the DPBR has to be repacked. This can be done by determining the length of time it takes for the carbon sources to clog the reactor and whether this occurs before or after the carbon in the bioreactor has been depleted.

In this study, the permeabilities and porosities of the composite organic layers within the DPBR were determined and an indication of how quickly certain carbon sources clog was also obtained. This was done to compile basic design guiding principles which will guide future designs of the DPBR.

2) METHODOLOGY

The aim of this study was to determine how the permeability of the bioreactor changed with time due to clogging. To achieve the aim of the experiment, the following steps were followed: The experiment was set up as described in Section 2.1, the synthetic AMD was created, the effective porosity for the different carbon sources was then determined and finally, the falling head permeability experiments were conducted.

2.1) Experimental setup

In the manufacture of the simulated DPBR, a variety of materials and apparatus were utilized. Six 2*L* measuring cylinders were utilized to act as the bioreactor's outer skeleton. Two Watson Marlow 120DM3 three-channel laboratory peristaltic pumps were used to feed the AMD into the bioreactors. PVC tubing was used to transport the AMD from the parent drum to the bioreactors. Special, Marprene tubing was used within the peristaltic pumps as normal PVC hardens over time due to continual deformation in the peristaltic pump. A schematic of the experimental layout can be seen in Figure 2 and a rendered image of the experimental setup is shown in Figure 3.

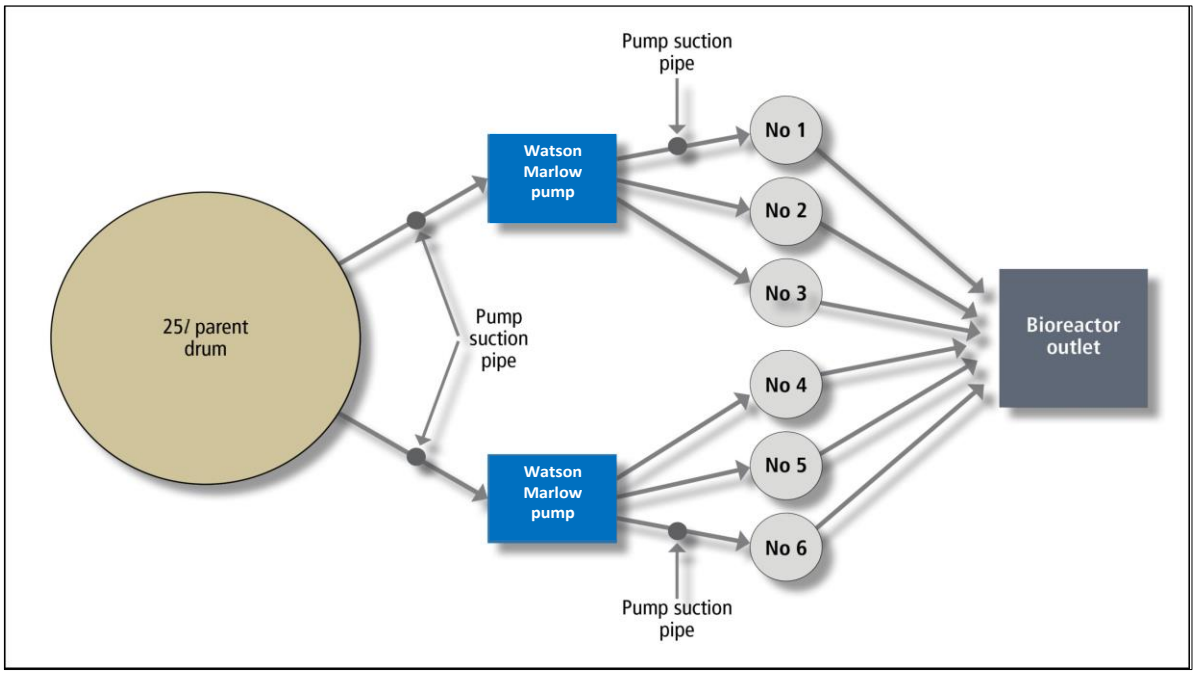

Figure 2: Experimental Setup

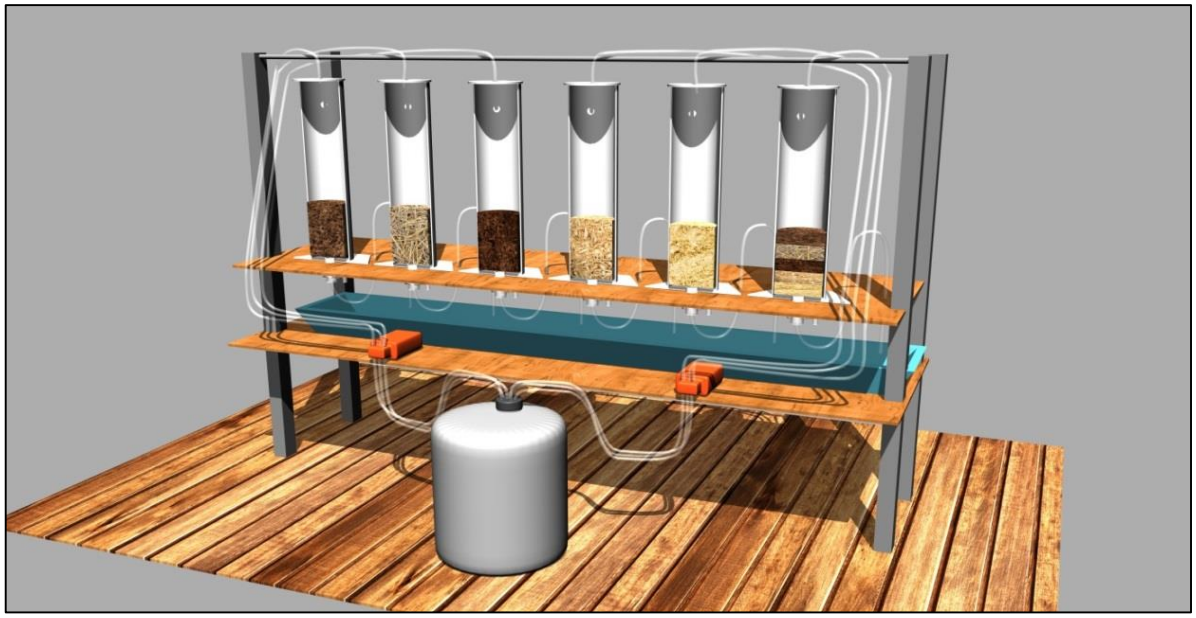

Figure 3: Rendered image of the experimental setup

In the experiment, five bioreactors, each with their own carbon sources, were filled to the 1200*ml* mark. The sixth bioreactor was filled with alternating layers of the first five carbon sources to the same total mark of 1200*ml*. The bioreactors were then filled with synthetic AMD to the same water level mark. The five carbon sources used were kraal manure, straw, vegetable food processing waste (compost), wood shavings and chicken litter.

2.2) Synthetic AMD

A 25*L* parent drum was filled with synthetic AMD. The synthetic AMD was based upon samples of actual AMD taken from the eMalahleni region, in the Mpumalanga

coal fields. These samples were analyzed and their chemical compositions were found to be:

- 3100 mg/*l sulfate*;
- 208 mg/*l iron*; and
- *pH* of 2.6

The synthetic AMD replicated the eMalahleni region AMD.

2.3) Effective porosity

The effective porosity of each carbon source was determined before the falling head permeability test experiment was started and once the falling head permeability test experiment was concluded. This was done to determine the effective porosity drop over the experimental lifespan. The effective porosity was determined by using the effective porosity equation [2].

$$\emptyset = \frac{V_p}{V_b} \quad [2]$$

$\emptyset = effective\ porosity\ (dimensionless)$
$V_p = total\ volume\ of\ interconnected\ voids\ (cm^3)$
$V_b = bulk\ volume\ (cm^3)$

At the beginning of each experiment, the total volume of water up to the 1200*ml* mark was recorded as the bulk volume. Thereafter, the carbon sources were placed in the bioreactors up to the same 1200*ml* mark. Synthetic AMD was then poured from a 1500*ml* beaker into the bioreactor up to the 1200*ml* mark. The total interconnected voids were deduced from the amount of AMD which fit into the bioreactor with the organic matter, to the marker point of 1200*ml.*

2.4) Falling head permeability tests

Once the experiments were setup and the initial effective porosities were determined, synthetic AMD was fed into the six bioreactors to a level of approximately 1600*ml* and the stopwatches were started. When the water level reached the sample level of 1200*ml,* the stopwatches were stopped and the time was recorded (*Falling head permeability test*).

$$k = \frac{al}{At} \times ln\frac{h_0}{h_1} \quad [3]$$

$k = permeability\ (m/min)$
$a = internal\ cross\ sectional\ area\ standpipe\ (m^2)$
$l = length\ of\ the\ sample\ (m)$
$A = cross\ sectional\ area\ (m^2)$
$t = time\ it\ takes\ for\ water\ level\ to\ drop\ from\ h_0\ to\ h_1\ (min)$
$h_o = starting\ height\ of\ water\ above\ sample\ (m)$
$h_1 = final\ height\ of\ water\ above\ sample\ (m)$

This process was repeated daily for three months or until the reactor was fully clogged.

3) RESULTS AND DISCUSSIONS

During the experimental life span, six different experiments were conducted on the different carbon sources. The results are shown in Figure 4. Manure and chicken litter were seen to clog the most rapidly as seen in graphs A and E respectively. None of the other experiments clogged fully over the study period.

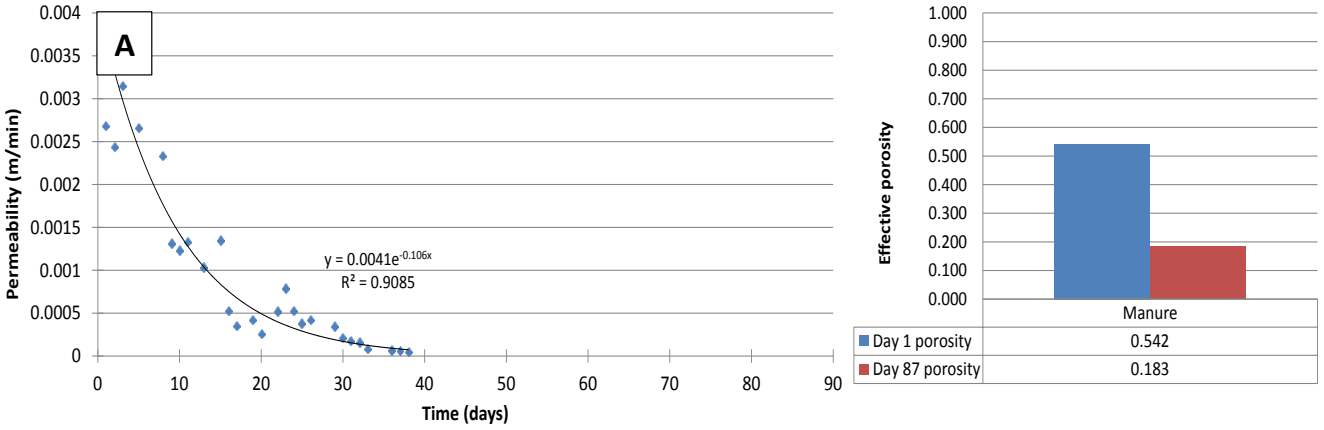
A
Permeability (m/min)
Time (days)
y = 0.0041e-0.106x
R² = 0.9085
Effective porosity
Manure
Day 1 porosity 0.542
Day 87 porosity 0.183

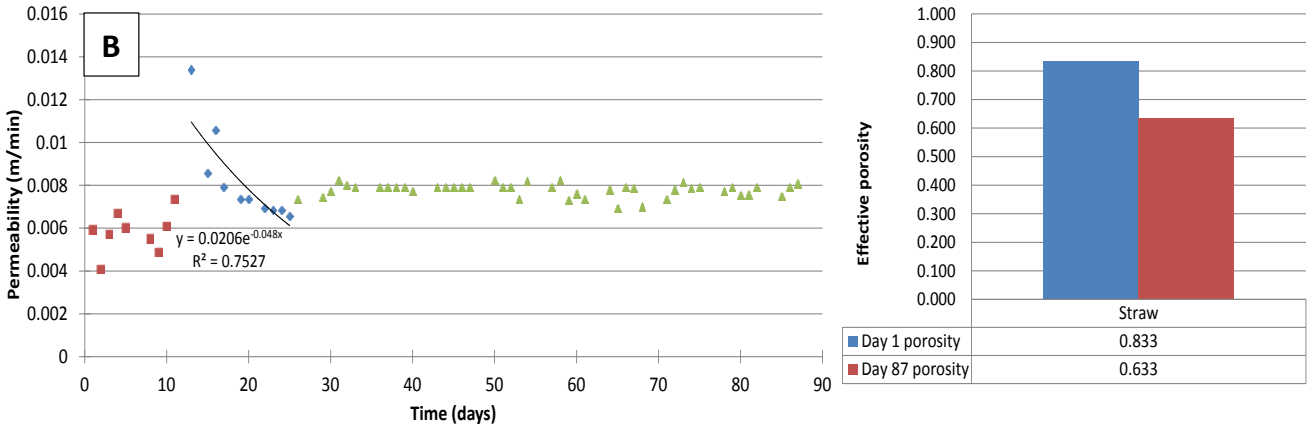
B
Permeability (m/min)
Time (days)
y = 0.0206e-0.048x
R² = 0.7527
Effective porosity
Straw
Day 1 porosity 0.833
Day 87 porosity 0.633

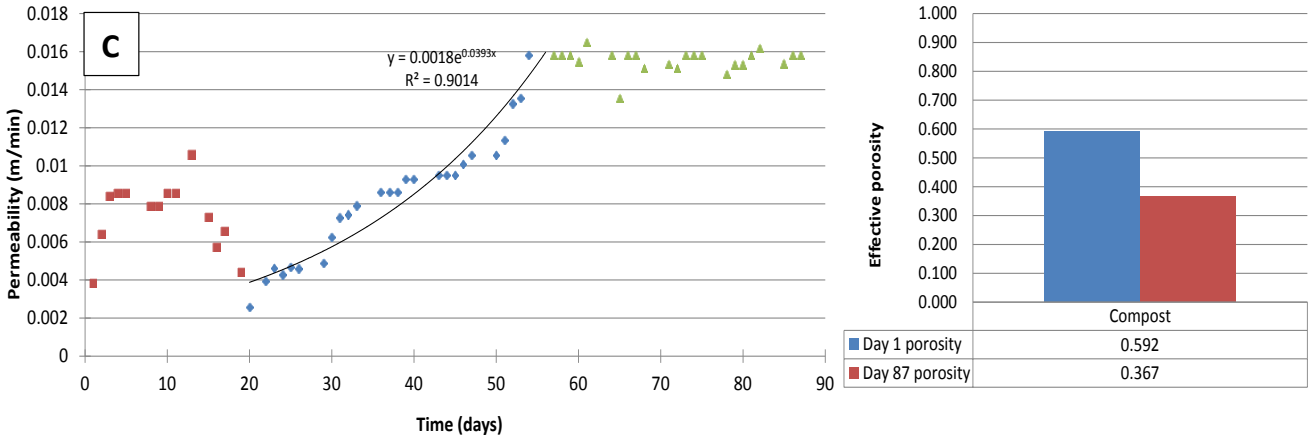
C
Permeability (m/min)
Time (days)
y = 0.0018e0.0393x
R² = 0.9014
Effective porosity
Compost
Day 1 porosity 0.592
Day 87 porosity 0.367

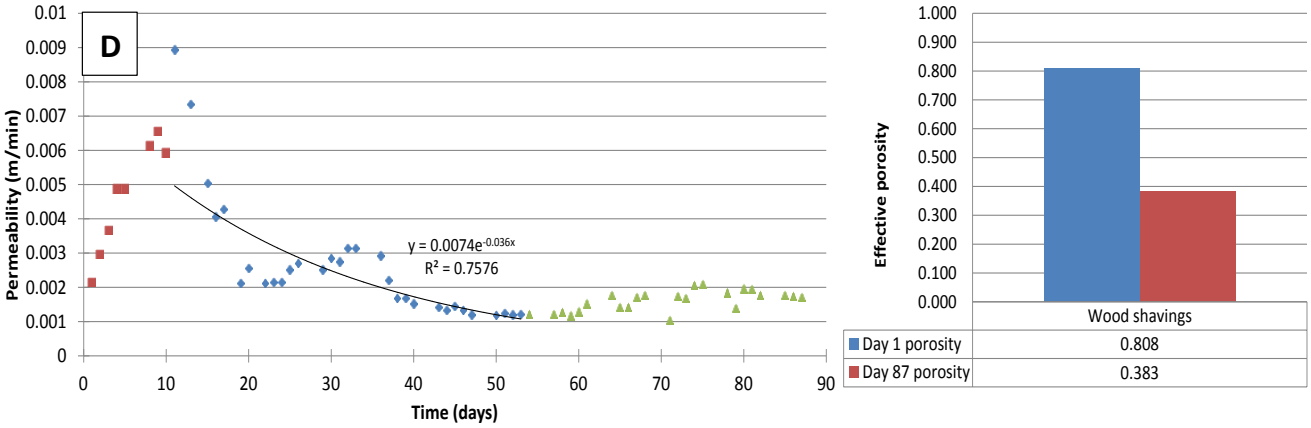
D
Permeability (m/min)
Time (days)
y = 0.0074e-0.036x
R² = 0.7576
Effective porosity
Wood shavings
Day 1 porosity 0.808
Day 87 porosity 0.383

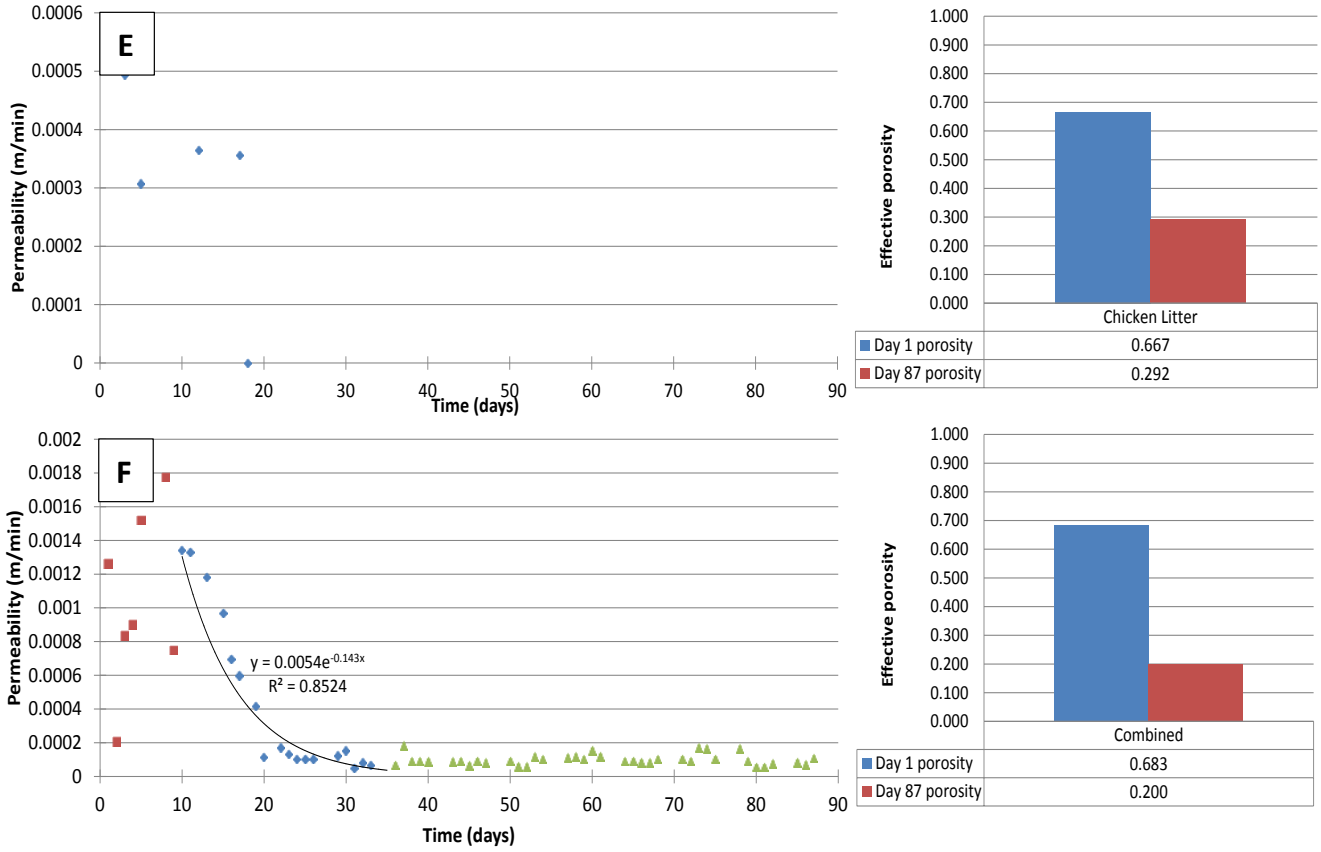

Figure 4: Permeability of the six different bioreactors over the three month period as well as the decrease in effective porosity from the start of the experiment to the end. A-Manure; B-Straw; C-Compost; D-Wood shavings; E-Chicken litter and F-Combined sample

As seen in Figure 4, all of the carbon sources, with the exception of the manure and chicken litter, had an establishment phase (shown by the red data points in Figure 4), where the initial reading of permeability varied with no obvious trend or pattern in the data. After the establishment phase, exponential trends started developing (shown by the blue data points in Figure 4). These trends started to develop as the bioreactor started to clog. These exponential trends were mainly in the negative direction (clogging of the bioreactor), with the exception of the compost bioreactor. The final phase which was identified was the stabilisation phase (shown by the green data points in Figure 4). Four of the carbon sources (straw, compost, wood shavings and combination bioreactor) showed a clear stabilisation phase, whereby the permeability values continued to decrease but at a vastly reduced rate for the remainder of the experimental lifespan. This is key as a relatively constant permeability is reached in the bioreactor; this stabilisation value would be the true permeability design value for the specific carbon source.

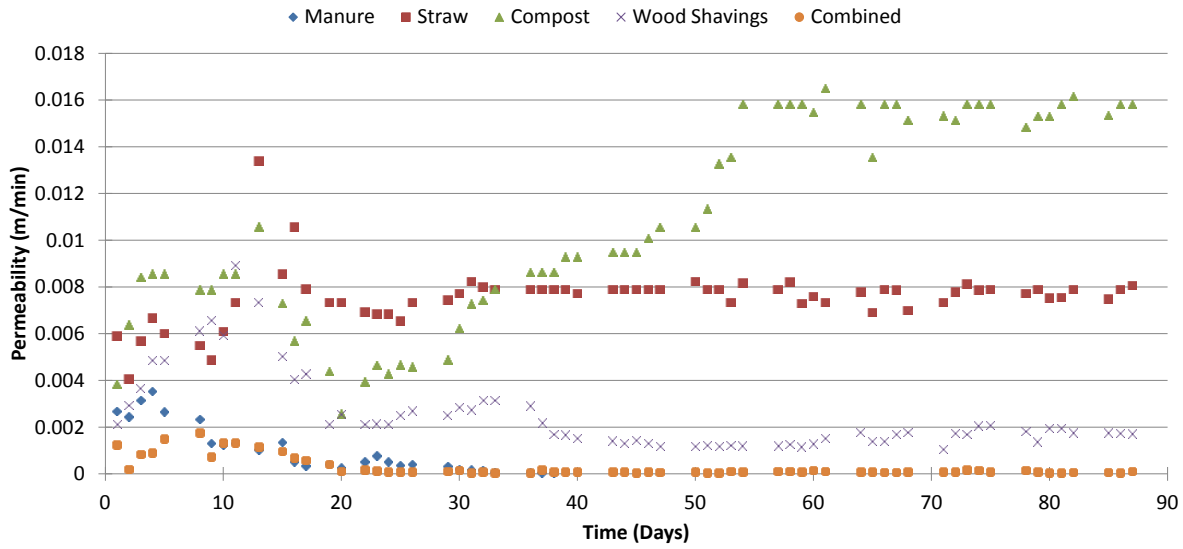

Figure 5: Permeability of different carbon sources

As seen in Figure 5, compost and straw had the overall highest permeabilities. Manure and the combined sample had the lowest. Although the combination bioreactor never fully clogged, it was only as permeable as its least permeable layer, manure.

With the help of the SRB in the biofilm, the carbon source precipitated the metals within the AMD in the bioreactors, thereby reducing the effective porosities of the bioreactors. This can be seen in Table 1.

Table 1: Effective porosities of carbon sources

	Manure	Straw	Compost	Wood shavings	Chicken litter	Combined sample
Day 1 effective porosity	0.542	0.833	0.592	0.808	0.667	0.683
Day 87 effective porosity	0.183	0.633	0.367	0.383	0.292	0.2
% decrease in effective porosity	66.24	24.01	38.01	52.60	56.22	70.72

Also seen in Table 1, the manure and the combined sample had the largest reduction in effective porosity, with straw and compost having the least. The effective porosities obtained followed the carbon sources' permeabilities, as manure and the combined samples had the lowest permeabilities while straw and compost had the highest.

The average permeabilities of the stabilisation phase for the bioreactor, which did not clog, was determined and can be seen in Figure 6.

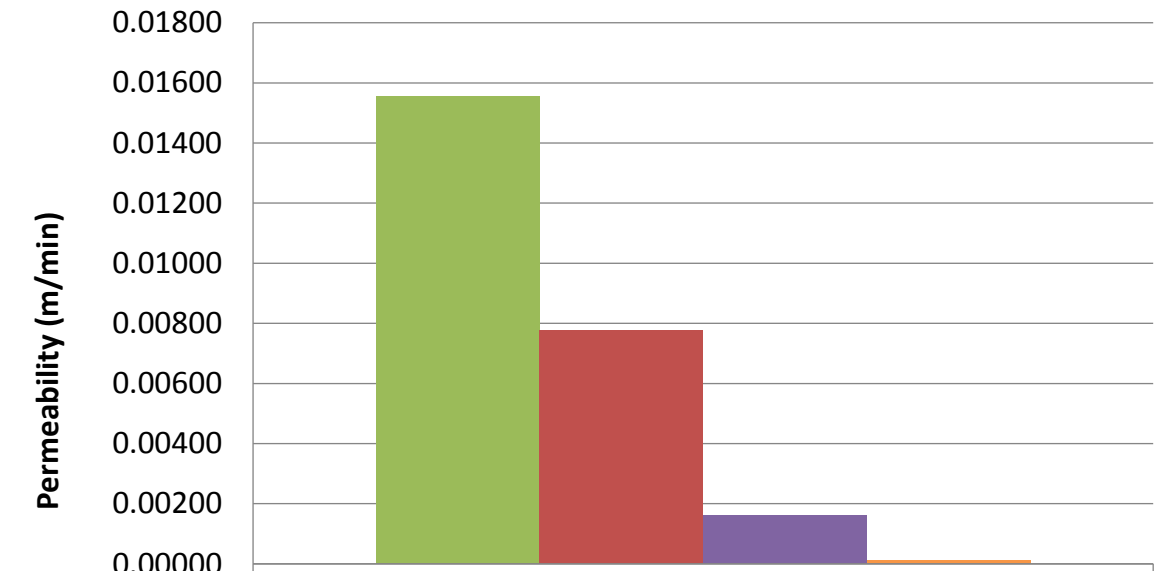

	Carbon sources
Compost	0.01557
Straw	0.00776
Wood Shavings	0.00161
Combined	0.000099

Figure 6: Average permeabilities of the stabilisation phase

The compost bioreactor had the highest stabilisation permeability and the combination bioreactor had the lowest. The stabilisation phase is of significance because it impacts the steady flow of AMD passing through the bioreactors. The polluted water needs to remain in and amongst the organic matter long enough for this reaction to take place, yet not too long as this increases the costs (a larger bioreactor will be needed to treat larger volumes of AMD). This stabilisation permeability can be used as the hydraulic design permeability of the bioreactor.

4) CONCLUSION

The chicken litter carbon source had the lowest permeability from the start of the experiment. The chicken litter held large air bubbles in-between the larger clumps of litter. The air bubbles blocked the bioreactor, not allowing any flow of AMD through the bioreactor. The chicken litter completely clogged within 18 days after the initiation of the experiment. It is therefore recommended not to be used as a carbon source in the DPBR.

Manure showed the quickest establishment and started clogging from day 2 of the experiment. This could be seen as both an advantage and disadvantage. The advantage lies in the fact that the bioreactor very rapidly establishes operating conditions and begins to precipitate metals. The disadvantage is the fact that the fast precipitation of metals clogs up the pores in the bioreactor, as can be seen by a 66%

decrease in effective porosity. The manure was also one of two carbon sources which fully clogged on day 38 of the experiment.

The straw, compost, wood shavings and combination bioreactors all seemed to stabilise at a certain point in time and further reduction in permeability occurred at a slow rate thereafter. All four stabilisation points occurred at different times during the experiment, with the straw bioreactor stabilising the quickest and the wood shavings and compost bioreactors taking the longest. This stabilisation permeability can be used as the hydraulic design permeability of the bioreactor.

The combination bioreactor seemed to have a dilution effect. All of the five constituent carbon sources found in equal layers within the bioreactor seemed to average out the different phases of the bioreactors. The overall permeability of the combination bioreactor was only as permeable as its lowest permeable layer, manure. The combination bioreactor's permeability closely followed the manure's permeability graph, with a decrease in effective porosity of 70%. However, the combination bioreactor did not clog over the experimental lifespan. Hydraulically, the combination bioreactor seemed to be the best performing reactor; it never fully clogged and the AMD moved through the bioreactor at a constant rate.

Further research could explore different thickness, combinations and mixtures of specific carbon sources to attain the desired hydraulic parameters within the bioreactor. By varying the thickness, combinations and mixtures, hydraulic attributes could be designed into the system.

The hydraulic parameters explained in this paper need to be balanced up against the chemical parameters. It still needs to be determined at what point the bioreactor starts to convert sulfates into sulfides and precipitate metals in the bioreactor. The main function of the DPBR is to treat sulfates and precipitate metals within AMD. Therefore, the operating range of the DPBR, which takes into consideration the permeabilities as well as the chemical treatment potential of the bioreactor, is currently being determined and this information will be available in a follow-up paper.

5) REFERENCES

1. Coetser SE, Molwantwa J, Heath R, Pulles W, editors. Implementing the integrated passive treatment system (IMPI) technology at the VCC passive treatment plant 2004; Cape Town: Document Transformation Technologies.

2. Johnson BD, Hallberg KB. Pitfalls of passive mine water treatment. Environmental Science and Bio Technology. 2002(1):335-43.
3. Ávila C, Bayona JM, Martín I, Salas JJ, García J. Emerging organic contaminant removal in a full-scale hybrid constructed wetland system for wastewater treatment and reuse. Ecological Engineering. 2015;80:108-16.
4. Gusek JJ. Passive Treatment 101: An Overview of Technologies. US EPA/National Groundwater Association's Remediation of Abandoned Mine Lands Conference; Denver 2008.

5. Pulles W, Rose PD, inventors Treatment of water. South Africa patent US 7306732 B2. 2002.
6. Blowes DW, Robertson WD, Ptacek CJ, Merkley C. Removal of agricultural nitrate from tile-drainage effluent water using in-line bioreactors. Journal of Contaminant Hydrology. 1994(15):207-21.
7. Greenan DM, Moorman TB, Kaspar TC, Parkin TB, Jaynes DB. Comparing carbon substrates for denitrification of subsurface drainage water. Journal of Environmental Quality. 2006(35):824-9.
8. Lee D-J, Liu X, Weng H-L. Sulphate and organic carbon removal by microbial fuel cell with sulphate-reducing bacteria and sulphate-oxidising bacteria anodic biofilm. Bioresource Technology. 2014(156):14-9.
9. Wu S, Kuschk P, Wiessner A, Muller J, Saad R, Dong R. Sulphur transformations in constructed wetlands fro wastewater treatment: A review. Ecological Engineering. 2013(52):278-89.
10. Bear J. Dynamic of Fluids in Porous Media. New York: Dover Publications Inc; 1988.
11. Gibb JP, Barcelona MJ, Ritchey JD, LeFaivre MH. Effective Porosity of Geologic Materials. Illinois: Champaign, 1984.
12. Chun JA, Cooke RA, J.W E, Kang MS. Estimation of flow and transport parameters for woodchip-based bioreactors: 1. laboratory-scale bioreactor. Biosystems Engineering. 2009;I(04):384-95.
13. Cameron SG, Schipper LA. Hydraulic properties, hydraulic effiency and nitrate removal f organic carbon media for use in denitrification beds. Ecological Engneering. 2012(42):1-7.
14. Yu T, Wu ZB, Xu D. Clogging characteristicsof the subsurface flow wetland. Environmental Science Technology. 2006(29):74-6 (in chinese).
15. Guiping F, Zhang J, Chen W, Chen Z. Medium clogging and dinamics of organic matter accumulation in constructed wetlands. Ecological Engineering. 2013(60):393-8.
16. Knowles PR, Griffin P, Davies PA. Complementary methods to investigate the development of clogging within a horizontal sub-surface flow tertiary treatment wetland. Water Research. 2010(44):320-30.
17. Zhao L, Zhu W, Tong W. Clogging processes caused by biofilm growth and organic particle accumulation in lab-scale vertical flow constructed wetlands. Journal of Environmental Sciences. 2009;21(6):750-7.
18. Iliuta I, Larachi F. Modelling simultaneous bilogical clogging and physical plugging in trickel-bed bioreactors for wastewater treatment. Chemical Engineering Science. 2005(60):1477-89.
19. Van Loosdrecht MCM, Heijnen SJ. Biofilm bioreactors for waste-water treatment. Trends in Biotechnology. 1993;11(4):117-21.

Appendix B Pilot experiment, constant head permeability data

Days	Manometer readings (cm)	Manometer total (cm)	Tempreture (°C)	Flow rate (l/min)	Constant water head (ml)	Area of sample (m2)	Length of sample (m)	Constant Head permeability (m/min)
1	7	14	12	0.00031	1200	0.00636172	0.165	0.057430562
1	7	14	15	0.00031	1200	0.00636172	0.165	0.057430562
2	7	14	12	0.00031	1200	0.00636172	0.165	0.057430562
2	7	14	15	0.00031	1200	0.00636172	0.165	0.057430562
3	9	18	12	0.00031	1200	0.00636172	0.165	0.044668215
3	10	20	15	0.00031	1200	0.00636172	0.165	0.040201394
4	9	18	12	0.00031	1200	0.00636172	0.165	0.044668215
4	9	18	15	0.00031	1200	0.00636172	0.165	0.044668215
5	10	20	12	0.00031	1200	0.00636172	0.165	0.040201394
5	10	20	15	0.00031	1200	0.00636172	0.165	0.040201394
6	10	20	12	0.00031	1200	0.00636172	0.165	0.040201394
6	10	20	15	0.00031	1200	0.00636172	0.165	0.040201394
7	10	20	12	0.00031	1200	0.00636172	0.165	0.040201394
7	10	20	15	0.00031	1200	0.00636172	0.165	0.040201394
8	10	20	12	0.00031	1200	0.00636172	0.165	0.040201394
8	10	20	15	0.00031	1200	0.00636172	0.165	0.040201394
9	10	20	12	0.00031	1200	0.00636172	0.165	0.040201394
9	10	20	15	0.00031	1200	0.00636172	0.165	0.040201394
10	11	22	12	0.00031	1200	0.00636172	0.165	0.036546722
10	12	24	15	0.00031	1200	0.00636172	0.165	0.033501161
11	12	24	12	0.00031	1200	0.00636172	0.165	0.033501161
11	13	26	15	0.00031	1200	0.00636172	0.165	0.030924149
12	13	26	12	0.00031	1200	0.00636172	0.165	0.030924149
12	14	28	15	0.00031	1200	0.00636172	0.165	0.028715281
13	14	28	12	0.00031	1200	0.00636172	0.165	0.028715281
13	14	28	15	0.00031	1200	0.00636172	0.165	0.028715281
14	13	26	12	0.00031	1200	0.00636172	0.165	0.030924149
14	12	24	15	0.00031	1200	0.00636172	0.165	0.033501161
15	12	24	12	0.00031	1200	0.00636172	0.165	0.033501161
15	12	24	15	0.00031	1200	0.00636172	0.165	0.033501161
16	12	24	12	0.00031	1200	0.00636172	0.165	0.033501161
16	13	26	15	0.00031	1200	0.00636172	0.165	0.030924149
17	13	26	12	0.00031	1200	0.00636172	0.165	0.030924149
17	14	28	15	0.00031	1200	0.00636172	0.165	0.028715281
18	15	30	12	0.00031	1200	0.00636172	0.165	0.026800929
18	14	28	15	0.00031	1200	0.00636172	0.165	0.028715281
19	14	28	12	0.00031	1200	0.00636172	0.165	0.028715281
19	15	30	15	0.00031	1200	0.00636172	0.165	0.026800929
20	16	32	13	0.00031	1200	0.00636172	0.165	0.025125871
20	12	24	16	0.00031	1200	0.00636172	0.165	0.033501161
21	12	24	13	0.00031	1200	0.00636172	0.165	0.033501161
21	13	26	16	0.00031	1200	0.00636172	0.165	0.030924149
22	14	28	15	0.00031	1200	0.00636172	0.165	0.028715281
22	14	28	17	0.00031	1200	0.00636172	0.165	0.028715281
23	13	26	15	0.00031	1200	0.00636172	0.165	0.030924149
23	13	26	12	0.00031	1200	0.00636172	0.165	0.030924149
24	14	28	14	0.00031	1200	0.00636172	0.165	0.028715281
24	14	28	15	0.00031	1200	0.00636172	0.165	0.028715281
25	14	28	15	0.00031	1200	0.00636172	0.165	0.028715281
25	15	30	16	0.00031	1200	0.00636172	0.165	0.026800929
26	15	30	12	0.00031	1200	0.00636172	0.165	0.026800929
26	16	32	15	0.00031	1200	0.00636172	0.165	0.025125871
27	13	26	13	0.00031	1200	0.00636172	0.165	0.030924149
27	13	26	15	0.00031	1200	0.00636172	0.165	0.030924149
28	13	26	12	0.00031	1200	0.00636172	0.165	0.030924149
28	13	26	15	0.00031	1200	0.00636172	0.165	0.030924149
29	13	26	12	0.00031	1200	0.00636172	0.165	0.030924149
29	13	26	15	0.00031	1200	0.00636172	0.165	0.030924149
30	14	28	12	0.00031	1200	0.00636172	0.165	0.028715281
30	14	28	15	0.00031	1200	0.00636172	0.165	0.028715281
31	15	30	13	0.00031	1200	0.00636172	0.165	0.026800929
31	15	30	16	0.00031	1200	0.00636172	0.165	0.026800929
32	16	32	14	0.00031	1200	0.00636172	0.165	0.025125871
32	13	26	16	0.00031	1200	0.00636172	0.165	0.030924149
33	13	26	12	0.00031	1200	0.00636172	0.165	0.030924149
33	14	28	15	0.00031	1200	0.00636172	0.165	0.028715281
34	14	28	11	0.00031	1200	0.00636172	0.165	0.028715281
34	14	28	15	0.00031	1200	0.00636172	0.165	0.028715281
35	14	28	11	0.00031	1200	0.00636172	0.165	0.028715281

Appendix C Main experiment, manure permeability data

Days	Time (min)	Top bioreactor reading (ml)	Bottom bioreactor reading (ml)	Height ho(m)	Height h1(m)	Tempreture (°C)	Flow rate (l/min)	Area of sample (m2)	Length of sample (m)	Falling head permeability (m/min)
1	10	1600	1360	0.28	0.238	15	0.00031	0.00636172	0.165	0.002681562
2	10	1600	1380	0.28	0.2415	16	0.00031	0.00636172	0.165	0.002440682
3	7	1600	1400	0.28	0.245	18	0.00031	0.00636172	0.165	0.003147526
4	3	1600	1500	0.28	0.2625	19	0.00031	0.00636172	0.165	0.003549619
5	4	1600	1500	0.28	0.2625	20	0.00031	0.00636172	0.165	0.002662214
8	4	1640	1550	0.287	0.27125	17	0.00031	0.00636172	0.165	0.002328204
9	5	1540	1480	0.2695	0.259	18	0.00031	0.00636172	0.165	0.001311431
10	6	1600	1530	0.28	0.26775	20	0.00031	0.00636172	0.165	0.001230237
11	6	1700	1620	0.2975	0.2835	20	0.00031	0.00636172	0.165	0.001325558
13	4	1620	1580	0.2835	0.2765	22	0.00031	0.00636172	0.165	0.001031304
15	7	1620	1530	0.2835	0.26775	18	0.00031	0.00636172	0.165	0.001347305
16	8	1600	1560	0.28	0.273	20	0.00031	0.00636172	0.165	0.00052218
17	6	1600	1580	0.28	0.2765	23	0.00031	0.00636172	0.165	0.000345917
19	10	1600	1560	0.28	0.273	23	0.00031	0.00636172	0.165	0.000417744
20	8	1600	1580	0.28	0.2765	25	0.00031	0.00636172	0.165	0.000259437
22	4	1600	1580	0.28	0.2765	26	0.00031	0.00636172	0.165	0.000518875
23	8	1600	1540	0.28	0.2695	24	0.00031	0.00636172	0.165	0.000788313
24	16	1600	1520	0.28	0.266	25	0.00031	0.00636172	0.165	0.000528962
25	11	1600	1560	0.28	0.273	26	0.00031	0.00636172	0.165	0.000379767
26	10	1600	1560	0.28	0.273	23	0.00031	0.00636172	0.165	0.000417744
29	12	1620	1580	0.2835	0.2765	25	0.00031	0.00636172	0.165	0.000343768
30	10	1610	1590	0.28175	0.27825	24	0.00031	0.00636172	0.165	0.000206253
31	36	1620	1560	0.2835	0.273	26	0.00031	0.00636172	0.165	0.000172977
32	13	1610	1590	0.28175	0.27825	26	0.00031	0.00636172	0.165	0.000158656
33	13	1620	1610	0.2835	0.28175	27	0.00031	0.00636172	0.165	7.85904E-05
36	15	1710	1700	0.29925	0.2975	26	0.00031	0.00636172	0.165	6.45163E-05
37	16	1810	1800	0.31675	0.315	25	0.00031	0.00636172	0.165	5.71331E-05
38	18	2000	1990	0.35	0.34825	30	0.00031	0.00636172	0.165	4.59483E-05

Appendix D Main experiment, straw permeability data

Days	Time (min)	Top bioreactor reading (ml)	Bottom bioreactor reading (ml)	Height ho(m)	Height h1(m)	Tempreture (°C)	Flow rate (l/min)	Area of sample (m2)	Length of sample (m)	Falling head permeability (m/min)
1	8	1600	1200	0.28	0.21	15	0.00031	0.00636172	0.165	0.005933443
2	9	1600	1280	0.28	0.224	16	0.00031	0.00636172	0.165	0.004090965
3	6	1600	1300	0.28	0.2275	18	0.00031	0.00636172	0.165	0.005710083
4	4	1600	1360	0.28	0.238	19	0.00031	0.00636172	0.165	0.006703906
5	4	1620	1400	0.2835	0.245	20	0.00031	0.00636172	0.165	0.006020599
8	4	1600	1400	0.28	0.245	17	0.00031	0.00636172	0.165	0.00550817
9	5	1600	1380	0.28	0.2415	18	0.00031	0.00636172	0.165	0.004881364
10	2	1400	1300	0.245	0.2275	20	0.00031	0.00636172	0.165	0.006113908
11	5	1600	1280	0.28	0.224	20	0.00031	0.00636172	0.165	0.007363737
13	2	1600	1360	0.28	0.238	22	0.00031	0.00636172	0.165	0.013407812
15	4	1600	1300	0.28	0.2275	18	0.00031	0.00636172	0.165	0.008565124
16	3	1600	1320	0.28	0.231	20	0.00031	0.00636172	0.165	0.010580454
17	4	1600	1320	0.28	0.231	23	0.00031	0.00636172	0.165	0.007935341
19	5	1600	1280	0.28	0.224	23	0.00031	0.00636172	0.165	0.007363737
20	5	1600	1280	0.28	0.224	25	0.00031	0.00636172	0.165	0.007363737
22	5	1580	1280	0.2765	0.224		0.00031	0.00636172	0.165	0.006948637
23	5	1600	1300	0.28	0.2275	24	0.00031	0.00636172	0.165	0.006852099
24	5	1600	1300	0.28	0.2275	25	0.00031	0.00636172	0.165	0.006852099
25	6	1600	1260	0.28	0.2205	26	0.00031	0.00636172	0.165	0.006569527
26	5	1600	1280	0.28	0.224	23	0.00031	0.00636172	0.165	0.007363737
29	6	1600	1220	0.28	0.2135	25	0.00031	0.00636172	0.165	0.007456701
30	6	1590	1200	0.27825	0.21	24	0.00031	0.00636172	0.165	0.007738843
31	6	1620	1200	0.2835	0.21	26	0.00031	0.00636172	0.165	0.008252876
32	6	1580	1180	0.2765	0.2065	26	0.00031	0.00636172	0.165	0.008027536
33	6	1600	1200	0.28	0.21	27	0.00031	0.00636172	0.165	0.007911257
36	6	1600	1200	0.28	0.21	26	0.00031	0.00636172	0.165	0.007911257
37	6	1600	1200	0.28	0.21	25	0.00031	0.00636172	0.165	0.007911257
38	6	1600	1200	0.28	0.21	30	0.00031	0.00636172	0.165	0.007911257
39	6	1600	1200	0.28	0.21	24	0.00031	0.00636172	0.165	0.007911257
40	6	1590	1200	0.27825	0.21	25	0.00031	0.00636172	0.165	0.007738843
43	6	1600	1200	0.28	0.21	23	0.00031	0.00636172	0.165	0.007911257
44	6	1600	1200	0.28	0.21	24	0.00031	0.00636172	0.165	0.007911257
45	6	1600	1200	0.28	0.21	24	0.00031	0.00636172	0.165	0.007911257
46	6	1600	1200	0.28	0.21	24	0.00031	0.00636172	0.165	0.007911257
47	6	1600	1200	0.28	0.21	23	0.00031	0.00636172	0.165	0.007911257
50	6	1580	1200	0.2765	0.21	24	0.00031	0.00636172	0.165	0.008253099
51	6	1600	1200	0.28	0.21	24	0.00031	0.00636172	0.165	0.007911257
52	6	1600	1200	0.28	0.21	23	0.00031	0.00636172	0.165	0.007911257
53	5	1500	1200	0.2625	0.21	24	0.00031	0.00636172	0.165	0.007363737
54	6	1600	1200	0.28	0.21	23	0.00031	0.00636172	0.165	0.008184059
57	6	1600	1200	0.28	0.21	24	0.00031	0.00636172	0.165	0.007911257
58	5	1540	1200	0.2695	0.21	22	0.00031	0.00636172	0.165	0.008232208
59	7	1600	1200	0.28	0.21	21	0.00031	0.00636172	0.165	0.007302699
60	5	1600	1300	0.28	0.2275	21	0.00031	0.00636172	0.165	0.007613443
61	5	1600	1280	0.28	0.224	21	0.00031	0.00636172	0.165	0.007363737
64	6	1620	1220	0.2835	0.2135	24	0.00031	0.00636172	0.165	0.00779832
65	7	1610	1200	0.28175	0.21	25	0.00031	0.00636172	0.165	0.00692794
66	6	1600	1200	0.28	0.21	26	0.00031	0.00636172	0.165	0.007911257
67	5	1600	1260	0.28	0.2205	27	0.00031	0.00636172	0.165	0.007883433
68	6	1600	1240	0.28	0.217	27	0.00031	0.00636172	0.165	0.007009537
71	5	1500	1200	0.2625	0.21	26	0.00031	0.00636172	0.165	0.007363737
72	5	1520	1200	0.266	0.21	23	0.00031	0.00636172	0.165	0.00780083
73	5	1600	1250	0.28	0.21875	23	0.00031	0.00636172	0.165	0.008146383
74	5	1600	1260	0.28	0.2205	24	0.00031	0.00636172	0.165	0.007883433
75	6	1600	1200	0.28	0.21	23	0.00031	0.00636172	0.165	0.007911257
78	6	1590	1200	0.27825	0.21	22	0.00031	0.00636172	0.165	0.007738843
79	6	1600	1200	0.28	0.21	23	0.00031	0.00636172	0.165	0.007911257
80	6	1600	1200	0.28	0.21	24	0.00031	0.00636172	0.165	0.00753453
81	6	1580	1200	0.2765	0.21	25	0.00031	0.00636172	0.165	0.00756534
82	6	1600	1200	0.28	0.21	25	0.00031	0.00636172	0.165	0.007911257
85	6	1590	1210	0.27825	0.21175	23	0.00031	0.00636172	0.165	0.007510626
86	6	1600	1200	0.28	0.21	23	0.00031	0.00636172	0.165	0.007911257
87	6	1610	1200	0.28175	0.21	24	0.00031	0.00636172	0.165	0.008082597

Appendix E Main experiment, compost permeability data

Days	Time (min)	Top bioreactor reading (ml)	Bottom bioreactor reading (ml)	Height ho(m)	Height h1(m)	Tempreture (°C)	Flow rate (l/min)	Area of sample (m2)	Length of sample (m)	Falling head permeability (m/min)
1	7	1600	1360	0.28	0.238	15	0.00031	0.00636172	0.165	0.003830803
2	7	1600	1220	0.28	0.2135	16	0.00031	0.00636172	0.165	0.006391458
3	5	1600	1240	0.28	0.217	18	0.00031	0.00636172	0.165	0.008411444
4	4	1600	1300	0.28	0.2275	19	0.00031	0.00636172	0.165	0.008565124
5	4	1600	1300	0.28	0.2275	20	0.00031	0.00636172	0.165	0.008565124
8	5	1600	1260	0.28	0.2205	17	0.00031	0.00636172	0.165	0.007883433
9	5	1600	1260	0.28	0.2205	18	0.00031	0.00636172	0.165	0.007883433
10	4	1600	1300	0.28	0.2275	20	0.00031	0.00636172	0.165	0.008565124
11	4	1600	1300	0.28	0.2275	20	0.00031	0.00636172	0.165	0.008565124
13	3	1600	1320	0.28	0.231	22	0.00031	0.00636172	0.165	0.010580454
15	4	1600	1340	0.28	0.2345	18	0.00031	0.00636172	0.165	0.007315028
16	6	1600	1300	0.28	0.2275	20	0.00031	0.00636172	0.165	0.005710083
17	3	1600	1420	0.28	0.2485	23	0.00031	0.00636172	0.165	0.006564072
19	5	1600	1400	0.28	0.245	23	0.00031	0.00636172	0.165	0.004406536
20	5	1600	1480	0.28	0.259	25	0.00031	0.00636172	0.165	0.002572731
22	5	1600	1420	0.28	0.2485	26	0.00031	0.00636172	0.165	0.003938443
23	5	1600	1390	0.28	0.24325	24	0.00031	0.00636172	0.165	0.004643096
24	8	1600	1300	0.28	0.2275	25	0.00031	0.00636172	0.165	0.004282562
25	6	1600	1350	0.28	0.23625	26	0.00031	0.00636172	0.165	0.004672224
26	6	1560	1320	0.273	0.231	23	0.00031	0.00636172	0.165	0.004593987
29	7	1600	1300	0.28	0.2275	25	0.00031	0.00636172	0.165	0.004894356
30	7	1590	1220	0.27825	0.2135	24	0.00031	0.00636172	0.165	0.006243674
31	6	1590	1220	0.27825	0.2135	26	0.00031	0.00636172	0.165	0.007284287
32	7	1590	1160	0.27825	0.203	26	0.00031	0.00636172	0.165	0.007432402
33	6	1600	1200	0.28	0.21	27	0.00031	0.00636172	0.165	0.007911257
36	6	1600	1200	0.28	0.21	26	0.00031	0.00636172	0.165	0.008630462
37	6	1600	1200	0.28	0.21	25	0.00031	0.00636172	0.165	0.008630462
38	6	1600	1200	0.28	0.21	30	0.00031	0.00636172	0.165	0.008630462
39	5	1590	1200	0.27825	0.21	24	0.00031	0.00636172	0.165	0.009286611
40	5	1590	1200	0.27825	0.21	25	0.00031	0.00636172	0.165	0.009286611
43	5	1600	1200	0.28	0.21	23	0.00031	0.00636172	0.165	0.009493508
44	5	1600	1200	0.28	0.21	24	0.00031	0.00636172	0.165	0.009493508
45	5	1600	1200	0.28	0.21	24	0.00031	0.00636172	0.165	0.009493508
46	5	1580	1200	0.2765	0.21	24	0.00031	0.00636172	0.165	0.010087121
47	5	1600	1200	0.28	0.21	23	0.00031	0.00636172	0.165	0.010548343
50	5	1600	1200	0.28	0.21	24	0.00031	0.00636172	0.165	0.010548343
51	4	1580	1200	0.2765	0.21	24	0.00031	0.00636172	0.165	0.011348011
52	4	1590	1200	0.27825	0.21	23	0.00031	0.00636172	0.165	0.013266587
53	4	1600	1200	0.28	0.21	24	0.00031	0.00636172	0.165	0.013562155
54	3	1600	1200	0.28	0.21	23	0.00031	0.00636172	0.165	0.015822514
57	3	1600	1200	0.28	0.21	24	0.00031	0.00636172	0.165	0.015822514
58	3	1600	1200	0.28	0.21	22	0.00031	0.00636172	0.165	0.015822514
59	3	1600	1200	0.28	0.21	21	0.00031	0.00636172	0.165	0.015822514
60	3	1590	1200	0.27825	0.21	21	0.00031	0.00636172	0.165	0.015477685
61	3	1620	1200	0.2835	0.21	21	0.00031	0.00636172	0.165	0.016505753
64	3	1600	1200	0.28	0.21	24	0.00031	0.00636172	0.165	0.015822514
65	4	1600	1200	0.28	0.21	24	0.00031	0.00636172	0.165	0.013562155
66	3	1600	1200	0.28	0.21	26	0.00031	0.00636172	0.165	0.015822514
67	3	1600	1200	0.28	0.21	27	0.00031	0.00636172	0.165	0.015822514
68	3	1580	1200	0.2765	0.21	27	0.00031	0.00636172	0.165	0.015130681
71	2	1500	1200	0.2625	0.21	26	0.00031	0.00636172	0.165	0.015341119
72	3	1580	1200	0.2765	0.21	23	0.00031	0.00636172	0.165	0.015130681
73	3	1600	1200	0.28	0.21	23	0.00031	0.00636172	0.165	0.015822514
74	3	1600	1200	0.28	0.21	24	0.00031	0.00636172	0.165	0.015822514
75	3	1600	1200	0.28	0.21	23	0.00031	0.00636172	0.165	0.015822514
78	3	1600	1200	0.28	0.21	22	0.00031	0.00636172	0.165	0.014833607
79	3	1600	1200	0.28	0.21	23	0.00031	0.00636172	0.165	0.01531211
80	3	1600	1200	0.28	0.21	24	0.00031	0.00636172	0.165	0.01531211
81	3	1600	1200	0.28	0.21	25	0.00031	0.00636172	0.165	0.015822514
82	3	1610	1200	0.28175	0.21	25	0.00031	0.00636172	0.165	0.016165194
85	3	1600	1210	0.28	0.21175	23	0.00031	0.00636172	0.165	0.01536608
86	3	1600	1200	0.28	0.21	23	0.00031	0.00636172	0.165	0.015822514
87	3	1600	1200	0.28	0.21	24	0.00031	0.00636172	0.165	0.015822514

Appendix F Main experiment, wood shavings permeability data

Days	Time (min)	Top bioreactor reading (ml)	Bottom bioreactor reading (ml)	Height ho(m)	Height h1(m)	Tempreture (^{o}C)	Flow rate (l/min)	Area of sample (m2)	Length of sample (m)	Falling head permeability (m/min)
1	6	1600	1480	0.28	0.259	15	0.00031	0.00636172	0.165	0.002143942
2	7	1610	1420	0.28175	0.2485	16	0.00031	0.00636172	0.165	0.002960037
3	6	1600	1400	0.28	0.245	18	0.00031	0.00636172	0.165	0.003672113
4	5	1600	1380	0.28	0.2415	19	0.00031	0.00636172	0.165	0.004881364
5	5	1600	1380	0.28	0.2415	20	0.00031	0.00636172	0.165	0.004881364
8	6	1600	1280	0.28	0.224	17	0.00031	0.00636172	0.165	0.006136448
9	6	1600	1260	0.28	0.2205	18	0.00031	0.00636172	0.165	0.006569527
10	5	1580	1320	0.2765	0.231	20	0.00031	0.00636172	0.165	0.005933173
11	3	1600	1360	0.28	0.238	20	0.00031	0.00636172	0.165	0.008938541
13	3	1600	1400	0.28	0.245	22	0.00031	0.00636172	0.165	0.007344227
15	3	1600	1460	0.28	0.2555	18	0.00031	0.00636172	0.165	0.005036196
16	4	1600	1450	0.28	0.25375	20	0.00031	0.00636172	0.165	0.004060653
17	3	1600	1480	0.28	0.259	23	0.00031	0.00636172	0.165	0.004287885
19	5	1600	1500	0.28	0.2625	23	0.00031	0.00636172	0.165	0.002129771
20	5	1600	1480	0.28	0.259	25	0.00031	0.00636172	0.165	0.002572731
22	5	1600	1500	0.28	0.2625	26	0.00031	0.00636172	0.165	0.002129771
23	7	1600	1460	0.28	0.2555	24	0.00031	0.00636172	0.165	0.00215837
24	6	1600	1480	0.28	0.259	25	0.00031	0.00636172	0.165	0.002143942
25	6	1600	1460	0.28	0.2555	26	0.00031	0.00636172	0.165	0.002518098
26	6	1600	1450	0.28	0.25375	23	0.00031	0.00636172	0.165	0.002707102
29	6	1600	1460	0.28	0.2555	25	0.00031	0.00636172	0.165	0.002518098
30	7	1580	1400	0.2765	0.245	24	0.00031	0.00636172	0.165	0.002851026
31	8	1600	1400	0.28	0.245	26	0.00031	0.00636172	0.165	0.002754085
32	7	1600	1400	0.28	0.245	26	0.00031	0.00636172	0.165	0.003147526
33	7	1600	1400	0.28	0.245	27	0.00031	0.00636172	0.165	0.003147526
36	10	1600	1340	0.28	0.2345	26	0.00031	0.00636172	0.165	0.002926011
37	10	1600	1400	0.28	0.245	25	0.00031	0.00636172	0.165	0.002203268
38	11	1590	1420	0.27825	0.2485	30	0.00031	0.00636172	0.165	0.001696157
39	7	1600	1490	0.28	0.26075	24	0.00031	0.00636172	0.165	0.001678934
40	7	1600	1500	0.28	0.2625	25	0.00031	0.00636172	0.165	0.001521265
43	9	1600	1480	0.28	0.259	23	0.00031	0.00636172	0.165	0.001429295
44	8	1600	1500	0.28	0.2625	24	0.00031	0.00636172	0.165	0.001331107
45	12	1600	1440	0.28	0.252	24	0.00031	0.00636172	0.165	0.001448707
46	8	1600	1500	0.28	0.2625	24	0.00031	0.00636172	0.165	0.001331107
47	8	1590	1500	0.27825	0.2625	23	0.00031	0.00636172	0.165	0.001201796
50	9	1600	1500	0.28	0.2625	24	0.00031	0.00636172	0.165	0.001183206
51	6	1590	1520	0.27825	0.266	24	0.00031	0.00636172	0.165	0.001238151
52	8	1590	1500	0.27825	0.2625	23	0.00031	0.00636172	0.165	0.001201796
53	7	1590	1510	0.27825	0.26425	24	0.00031	0.00636172	0.165	0.00121686
54	7	1600	1520	0.28	0.266	23	0.00031	0.00636172	0.165	0.001209056
57	7	1600	1520	0.28	0.266	24	0.00031	0.00636172	0.165	0.001209056
58	7	1620	1540	0.2835	0.2695	22	0.00031	0.00636172	0.165	0.001285572
59	10	1600	1490	0.28	0.26075	21	0.00031	0.00636172	0.165	0.001175254
60	7	1500	1420	0.2625	0.2485	21	0.00031	0.00636172	0.165	0.001291908
61	7	1600	1500	0.28	0.2625	21	0.00031	0.00636172	0.165	0.001521265
64	6	1600	1500	0.28	0.2625	24	0.00031	0.00636172	0.165	0.001774809
65	6	1600	1520	0.28	0.266	25	0.00031	0.00636172	0.165	0.001410566
66	8	1600	1500	0.28	0.2625	26	0.00031	0.00636172	0.165	0.001419847
67	8	1600	1480	0.28	0.259	27	0.00031	0.00636172	0.165	0.001715154
68	6	1600	1500	0.28	0.2625	27	0.00031	0.00636172	0.165	0.001774809
71	10	1620	1520	0.2835	0.266	26	0.00031	0.00636172	0.165	0.001051311
72	10	1600	1440	0.28	0.252	23	0.00031	0.00636172	0.165	0.001738449
73	10	1640	1480	0.287	0.259	23	0.00031	0.00636172	0.165	0.001693794
74	10	1700	1500	0.2975	0.2625	24	0.00031	0.00636172	0.165	0.002065192
75	10	1680	1480	0.294	0.259	23	0.00031	0.00636172	0.165	0.002091403
78	10	1700	1520	0.2975	0.266	22	0.00031	0.00636172	0.165	0.001846646
79	11	1700	1550	0.2975	0.27125	23	0.00031	0.00636172	0.165	0.0013856
80	11	1760	1550	0.308	0.27125	24	0.00031	0.00636172	0.165	0.001959319
81	10	1800	1600	0.315	0.28	25	0.00031	0.00636172	0.165	0.00194342
82	11	1800	1600	0.315	0.28	25	0.00031	0.00636172	0.165	0.001766746
85	11	1800	1600	0.315	0.28	23	0.00031	0.00636172	0.165	0.001766746
86	11	1800	1600	0.315	0.28	23	0.00031	0.00636172	0.165	0.001735197
87	11	1800	1600	0.315	0.28	24	0.00031	0.00636172	0.165	0.001719841

Appendix G Main experiment, chicken litter permeability data

Days	Time (min)	Manometer readings (cm)	Top bioreactor reading (ml)	Bottom bioreactor reading (ml)	Height ho(m)	Height h1(m)	Tempreture (^{o}C)	Flow rate (l/min)	Area of sample (m2)	Length of sample (m)	Falling head permeability (m/min)
3	4		1680	1660	0.294	0.2905	18	0.00031	0.00636172	0.165	0.000494018
4	8		1660	1660	0.2905	0.2905	18	0.00031	0.00636172	0.165	0
5	6		1800	1780	0.315	0.3115	19	0.00031	0.00636172	0.165	0.000307266
6					0	0		0.00031	0.00636172	0.165	0
7					0	0		0.00031	0.00636172	0.165	0
8					0	0		0.00031	0.00636172	0.165	0
9					0	0		0.00031	0.00636172	0.165	0
10					0	0		0.00031	0.00636172	0.165	0
11					0	0		0.00031	0.00636172	0.165	0
12	5		1820	1800	0.3185	0.315	20	0.00031	0.00636172	0.165	0.000364645
13					0	0		0.00031	0.00636172	0.165	0
14					0	0		0.00031	0.00636172	0.165	0
15					0	0		0.00031	0.00636172	0.165	0
16					0	0		0.00031	0.00636172	0.165	0
17	5		1860	1840	0.3255	0.322	20	0.00031	0.00636172	0.165	0.00035676
18	7		1880	1880	0.329	0.329		0.00031	0.00636172	0.165	0

Appendix H Main experiment, combination permeability data

Days	Time (min)	Manometer readings (cm)	Top bioreactor reading (ml)	Bottom bioreactor reading (ml)	Height ho(m)	Height h1(m)	Tempreture (°C)	Flow rate (l/min)	Area of sample (m2)	Length of sample (m)	Falling head permeability (m/min)
1	5		1600	1540	0.28	0.2695	15	0.00031	0.00636172	0.165	0.0012613
2	10		1600	1580	0.28	0.2765	16	0.00031	0.00636172	0.165	0.00020755
3	5		1600	1560	0.28	0.273	18	0.00031	0.00636172	0.165	0.000835488
4	7		1600	1540	0.28	0.2695	19	0.00031	0.00636172	0.165	0.000900929
5	7		1600	1500	0.28	0.2625	20	0.00031	0.00636172	0.165	0.001521265
8	6		1600	1500	0.28	0.2625	17	0.00031	0.00636172	0.165	0.001774809
9	7		1600	1550	0.28	0.27125	18	0.00031	0.00636172	0.165	0.000748362
10	6		1470	1400	0.25725	0.245	20	0.00031	0.00636172	0.165	0.00134173
11	8		1600	1500	0.28	0.2625	20	0.00031	0.00636172	0.165	0.001331107
13	9		1600	1500	0.28	0.2625	22	0.00031	0.00636172	0.165	0.001183206
15	11		1600	1500	0.28	0.2625	18	0.00031	0.00636172	0.165	0.000968078
16	6		1600	1560	0.28	0.273	20	0.00031	0.00636172	0.165	0.00069624
17	7		1600	1560	0.28	0.273	23	0.00031	0.00636172	0.165	0.000596777
19	10		1600	1560	0.28	0.273	23	0.00031	0.00636172	0.165	0.000417744
20	9		1600	1590	0.28	0.27825	25	0.00031	0.00636172	0.165	0.000114943
22	6		1620	1610	0.2835	0.28175	26	0.00031	0.00636172	0.165	0.000170279
23	7		1790	1780	0.31325	0.3115	24	0.00031	0.00636172	0.165	0.000132053
24	9		1800	1790	0.315	0.31325	23	0.00031	0.00636172	0.165	0.000102136
29	15		1800	1780	0.315	0.3115	25	0.00031	0.00636172	0.165	0.000122906
30	12		1800	1780	0.315	0.3115	24	0.00031	0.00636172	0.165	0.000153633
31	19		1800	1790	0.315	0.31325	26	0.00031	0.00636172	0.165	4.83801E-05
32	11		1800	1790	0.315	0.31325	26	0.00031	0.00636172	0.165	8.35657E-05
33	14		1800	1790	0.315	0.31325	27	0.00031	0.00636172	0.165	6.56587E-05
36	14		1800	1790	0.315	0.31325	26	0.00031	0.00636172	0.165	6.56587E-05
37	15		1810	1780	0.31675	0.3115	25	0.00031	0.00636172	0.165	0.000183848
38	20		1800	1780	0.315	0.3115	30	0.00031	0.00636172	0.165	9.21797E-05
39	10		1800	1790	0.315	0.31325	24	0.00031	0.00636172	0.165	9.19222E-05
40	10		1890	1880	0.33075	0.329	25	0.00031	0.00636172	0.165	8.75334E-05
43	10		1900	1890	0.3325	0.33075	23	0.00031	0.00636172	0.165	8.70714E-05
44	9		2000	1990	0.35	0.34825	24	0.00031	0.00636172	0.165	9.18966E-05
45	13		2010	2000	0.35175	0.35	24	0.00031	0.00636172	0.165	6.33034E-05
46	9		2000	1990	0.35	0.34825	24	0.00031	0.00636172	0.165	9.18966E-05
47	10		2000	1990	0.35	0.34825	23	0.00031	0.00636172	0.165	8.27069E-05
50	9		2000	1990	0.35	0.34825	24	0.00031	0.00636172	0.165	9.18966E-05
51	7		2000	1995	0.35	0.349125	24	0.00031	0.00636172	0.165	5.90024E-05
52	14		2000	1990	0.35	0.34825	23	0.00031	0.00636172	0.165	5.90764E-05
53	7		2000	1990	0.35	0.34825	24	0.00031	0.00636172	0.165	0.000118153
54	8		1990	1980	0.34825	0.3465	23	0.00031	0.00636172	0.165	0.000103905
57	8		2010	2000	0.35175	0.35	24	0.00031	0.00636172	0.165	0.000109726
58	7		2000	1990	0.35	0.34825	22	0.00031	0.00636172	0.165	0.000118153
59	12		2000	1985	0.35	0.347375	21	0.00031	0.00636172	0.165	0.000103514
60	6		1800	1790	0.315	0.31325	21	0.00031	0.00636172	0.165	0.000153204
61	7		2000	1990	0.35	0.34825	21	0.00031	0.00636172	0.165	0.000118153
64	9		2000	1990	0.35	0.34825	24	0.00031	0.00636172	0.165	9.18966E-05
65	9		2000	1990	0.35	0.34825	25	0.00031	0.00636172	0.165	9.18966E-05
66	10		2000	1990	0.35	0.34825	26	0.00031	0.00636172	0.165	8.27069E-05
67	5		2000	1995	0.35	0.349125	27	0.00031	0.00636172	0.165	8.26033E-05
68	8		2000	1990	0.35	0.34825	27	0.00031	0.00636172	0.165	0.000103384
71	16		2000	1980	0.35	0.3465	26	0.00031	0.00636172	0.165	0.000103644
72	9		2000	1990	0.35	0.34825	23	0.00031	0.00636172	0.165	9.18966E-05
73	12		2025	2000	0.354375	0.35	23	0.00031	0.00636172	0.165	0.00017081
74	10		2000	1980	0.35	0.3465	24	0.00031	0.00636172	0.165	0.000165831
75	8		2000	1990	0.35	0.34825	23	0.00031	0.00636172	0.165	0.000103384
78	10		2020	2000	0.3535	0.35	22	0.00031	0.00636172	0.165	0.00016418
79	9		2000	1990	0.35	0.34825	23	0.00031	0.00636172	0.165	9.18966E-05
80	15		2000	1990	0.35	0.34825	24	0.00031	0.00636172	0.165	5.5138E-05
81	15		2000	1990	0.35	0.34825	25	0.00031	0.00636172	0.165	5.5138E-05
82	11		2000	1990	0.35	0.34825	25	0.00031	0.00636172	0.165	7.51881E-05
85	10		2000	1990	0.35	0.34825	23	0.00031	0.00636172	0.165	8.27069E-05
86	12		2000	1990	0.35	0.34825	23	0.00031	0.00636172	0.165	6.89225E-05
87	15		2020	2000	0.3535	0.35	24	0.00031	0.00636172	0.165	0.000109454

Appendix I Main experiment, all carbon sources permeability data

Days	Manure	Straw	Compost	Wood Shavings	Combined
1	0.002681562	0.005933443	0.003830803	0.002143942	0.0012613
2	0.002440682	0.004090965	0.006391458	0.002960037	0.00020755
3	0.003147526	0.005710083	0.008411444	0.003672113	0.000835488
4	0.003549619	0.006703906	0.008565124	0.004881364	0.000900929
5	0.002662214	0.006020599	0.008565124	0.004881364	0.001521265
8	0.002328204	0.00550817	0.007883433	0.006136448	0.001774809
9	0.001311431	0.004881364	0.007883433	0.006569527	0.000748362
10	0.001230237	0.006113908	0.008565124	0.005933173	0.00134173
11	0.001325558	0.007363737	0.008565124	0.008938541	0.001331107
13	0.001031304	0.013407812	0.010580454	0.007344227	0.001183206
15	0.001347305	0.008565124	0.007315028	0.005036196	0.000968078
16	0.00052218	0.010580454	0.005710083	0.004060653	0.00069624
17	0.000345917	0.007935341	0.006564072	0.004287885	0.000596777
19	0.000417744	0.007363737	0.004406536	0.002129771	0.000417744
20	0.000259437	0.007363737	0.002572731	0.002572731	0.000114943
22	0.000518875	0.006948637	0.003938443	0.002129771	0.000170279
23	0.000788313	0.006852099	0.004643096	0.00215837	0.000132053
24	0.000528962	0.006852099	0.004282562	0.002143942	0.000102136
25	0.000379767	0.006569527	0.004672224	0.002518098	0.00010212
26	0.000417744	0.007363737	0.004593987	0.002707102	0.00010211
29	0.000343768	0.007456701	0.004894356	0.002518098	0.000122906
30	0.000206253	0.007738843	0.006243674	0.002851026	0.000153633
31	0.000172977	0.008252876	0.007284287	0.002754085	4.83801E-05
32	0.000158656	0.008027536	0.007432402	0.003147526	8.35657E-05
33	7.85904E-05	0.007911257	0.007911257	0.003147526	6.56587E-05
36	6.45163E-05	0.007911257	0.008630462	0.002926011	6.56587E-05
37	5.71331E-05	0.007911257	0.008630462	0.002203268	0.000183848
38	4.59483E-05	0.007911257	0.008630462	0.001696157	9.21797E-05
39		0.007911257	0.009286611	0.001678934	9.19222E-05
40		0.007738843	0.009286611	0.001521265	8.75334E-05
43		0.007911257	0.009493508	0.001429295	8.70714E-05
44		0.007911257	0.009493508	0.001331107	9.18966E-05
45		0.007911257	0.009493508	0.001448707	6.33034E-05
46		0.007911257	0.010087121	0.001331107	9.18966E-05
47		0.007911257	0.010548343	0.001201796	8.27069E-05
50		0.008253099	0.010548343	0.001183206	9.18966E-05
51		0.007911257	0.011348011	0.001238151	5.90024E-05
52		0.007911257	0.013266587	0.001201796	5.90764E-05
53		0.007363737	0.013562155	0.00121686	0.000118153
54		0.008184059	0.015822514	0.001209056	0.000103905
57		0.007911257	0.015822514	0.001209056	0.000109726
58		0.008232208	0.015822514	0.001285572	0.000118153
59		0.007302699	0.015822514	0.001175254	0.000103514
60		0.007613443	0.015477685	0.001291908	0.000153204
61		0.007363737	0.016505753	0.001521265	0.000118153
64		0.00779832	0.015822514	0.001774809	9.18966E-05
65		0.00692794	0.013562155	0.001410566	9.18966E-05
66		0.007911257	0.015822514	0.001419847	8.27069E-05
67		0.007883433	0.015822514	0.001715154	8.26033E-05
68		0.007009537	0.015130681	0.001774809	0.000103384
71		0.007363737	0.015341119	0.001051311	0.000103644
72		0.00780083	0.015130681	0.001738449	9.18966E-05
73		0.008146383	0.015822514	0.001693794	0.00017081
74		0.007883433	0.015822514	0.002065192	0.000165831
75		0.007911257	0.015822514	0.002091403	0.000103384
78		0.007738843	0.014833607	0.001846646	0.00016418
79		0.007911257	0.01531211	0.0013856	9.18966E-05
80		0.00753453	0.01531211	0.001959319	5.5138E-05
81		0.00756534	0.015822514	0.00194342	5.5138E-05
82		0.007911257	0.016165194	0.001766746	7.51881E-05
85		0.007510626	0.01536608	0.001766746	8.27069E-05
86		0.007911257	0.015822514	0.001735197	6.89225E-05
87		0.008082597	0.015822514	0.001719841	0.000109454

Appendix J Main experiment, sulfate sample analysis

Sulfate (SO_4) (mg/l)							
Ion Chromatography							
Days	Dates	Manure	Straw	Compost	Wood sha	Chicken Litter	Combined
10	2015/09/16	1686.17	1622.42	1687.63	1635.9		1723.29
15	2015/09/21	1194.82	1573.35	1698.77	1601.1		1694.4
24	2015/09/30	1625.78	1550.07	1622.39	1581.33		2300
31	2015/10/07	2272.35	2089.54	2510.43	2731.89		2839.79
38	2015/10/14	2274.95	2798.57	2338.75	3105		2700.73
45	2015/10/21		2756.67	3171.62	3155.87		2676.61
52	2015/10/28		3161.74	3217.22	3301.32		3335.56
59	2015/11/04		2303.56	2806.22	2876.19		2806.66
66	2015/11/11		2775.83	2860.99	2927.79		2866.16
73	2015/11/18		2745.06	2368.63	2879.55		2541.15
80	2015/11/25		2317.71	2700.8	2742.83		2625.58

Appendix K Main experiment, iron sample analysis

Iron (Fe) (mg/l)							
Spectrophotometer							
Days	Dates	Manure	Straw	Compost	Wood sha	Chicken Litter	Combined
10	2015/09/16	3.68	105.96	23.19	148.4		9.27
15	2015/09/21	2.18	93.93	82.31	59.23		3.87
24	2015/09/30	2.19	2.41	130.09	115		5.24
31	2015/10/07	2.77	0.29	0.41	3.19		9.62
38	2015/10/14	3.8	12.6	0.52	142.75		3.6
45	2015/10/21		0.6	0.17	71.77		8.59
52	2015/10/28		51.01	154.12	131.12		0.46
59	2015/11/04		201	212	198		104
66	2015/11/11		193	197	194		149
73	2015/11/18		189	218	198		220
80	2015/11/25		183	180	192		212

Appendix L Main experiment, pH sample analysis

pH @ 25°C							
M09							
Days	Dates	Manure	Straw	Compost	Wood shav	Chicken Litter	Combined
10	2015/09/16	7.26	2.17	4.95	2.1		6.78
15	2015/09/21	7.3	2.13	4.49	2.11		6.68
24	2015/09/30	7.22	2.13	4.81	2.04		6.67
31	2015/10/07	7.29	2.14	2.6	2.11		6.65
38	2015/10/14	8.24	2.17	2.31	2.11		6.78
45	2015/10/21		2.11	2.23	2.09		7.24
52	2015/10/28		2.1	2.16	2.09		6.12
59	2015/11/04		2.07	2.02	2.1		4.95
66	2015/11/11		2.06	2.04	2		4.51
73	2015/11/18		2.03	2.06	2.02		5.5
80	2015/11/25		2.03	2.06	2.03		4.06